

BAKER

RUSKINN

低氧 / 厌氧

论文选集

TOGETHER

WE CAN MAKE

MORE THAN

A DIFFERENCE

WE CAN
MAKE HISTORY

北京隆福佳生物科技有限公司

RUSKINN

论文选集

北京隆福佳生物科技有限公司

Contents

序言.....	1
Ruskinn & The Nobel Prize	2
Cell	
HIF.....	5
VEGF	12
Stem Cell.....	18
Cancer Stem Cell.....	20
Cancer.....	28
Cardiovascular.....	33
Metabolic diseases	38
Neural/Brain references	48
Drug Testing.....	55
Microorganism	
Gut microbiota.....	64
<i>Clostridium difficile</i>	71
<i>Bifidobacterium</i>	74
Laboratory Microorganisms	76
Oral Microorganisms	81
Food Microorganisms.....	83
Bactericidal references	85
Anaerobic Microorganism Degradation.....	86

序言

随着科学研究的发展,越来越多的科学家开始注重研究环境的真实性,模拟生物体内严格的生理氧、病理氧等实验条件。来自霍华德-休斯医学研究所的 **William G. Kaelin Jr**、弗朗西斯-克里克研究所的 **Sir Peter J. Ratcliffe** 和约翰斯霍普金斯的 **Gregg L. Semenza** 也因揭示细胞感知和适应氧气供应的机制而获得 **2019** 年诺贝尔生理学或医学奖。

北京隆福佳生物科技有限公司携手英国 **RUSKINN** 公司致力于低氧/厌氧领域相关科研推广工作。北京隆福佳生物科技有限公司的宗旨以科研服务为主,以利益为辅,立志为国家科研工作做贡献。英国 **RUSKINN** 公司作为低氧/厌氧领域领域的带头人,在全球拥有 **30** 多个相关的科研工作者作为应用顾问,每年都根据一线科研的实际需求更新产品并增加新功能,确保能够更贴心的服务于所有科研工作者和更专业的满足所有实验需求。

本论文搜集了近百篇论文,涉及到微生物研究、细胞研究相关的多个领域,希望该论文集能够给广大科研工作者提供一些借鉴。也希望能够得到广大科研工作者的支持、认可与建议。

英国 BAKER RUSKINN	销售总监	Samir Patel
英国 BAKER RUSKINN	亚太地区销售经理	Kalucia Tsai
北京隆福佳生物科技有限公司	CEO	袁宇霞
北京隆福佳生物科技有限公司	产品经理	王超

Mechanisms of hypoxia signalling: new implications for nephrology

*Johannes Schödel*¹ and *Peter J. Ratcliffe*^{2,3*}

¹Department of Nephrology and Hypertension, Universitätsklinikum Erlangen, Friedrich-AlexanderUniversität ErlangenNürnberg, Erlangen, Germany.

²Ludwig Institute for Cancer Research and Target Discovery Institute, Nuffield Department of Medicine, University of Oxford, Oxford, UK.

³The Francis Crick Institute, London, UK

Abstract

Studies of the regulation of erythropoietin (EPO) production by the liver and kidneys, one of the classical physiological responses to hypoxia, led to the discovery of human oxygen-sensing mechanisms, which are now being targeted therapeutically. The oxygen-sensitive signal is generated by 2-oxoglutarate-dependent dioxygenases that deploy molecular oxygen as a co-substrate to catalyse the post-translational hydroxylation of specific prolyl and asparaginyl residues in hypoxia-inducible factor (HIF), a key transcription factor that regulates transcriptional responses to hypoxia. Hydroxylation of HIF at different sites promotes both its degradation and inactivation. Under hypoxic conditions, these processes are suppressed, enabling HIF to escape destruction and form active transcriptional complexes at thousands of loci across the human genome. Accordingly, HIF prolyl hydroxylase inhibitors stabilize HIF and stimulate expression of HIF target genes, including the EPO gene. These molecules activate endogenous EPO gene expression in diseased kidneys and are being developed, or are already in clinical use, for the treatment of renal anaemia. In this Review, we summarize information on the molecular circuitry of hypoxia signalling pathways underlying these new treatments and highlight some of the outstanding questions relevant to their clinical use.

Striking Oxygen Sensitivity of the Peptidylglycine α -Amidating Monooxygenase (PAM) in Neuroendocrine Cells

Simpson PD¹, Eipper BA², Katz MJ³, Gandara L³, Wappner P³, Fischer R⁴, Hodson EJ¹, Ratcliffe PJ⁵, Masson N⁶

¹From the Centre for Cellular and Molecular Physiology, University of Oxford, Oxford OX3 7BN, United Kingdom.

²Department of Neuroscience, University of Connecticut Health Center, Farmington, Connecticut 06030.

³Fundacion Instituto Leloir, C1405BWE Buenos Aires, Argentina, and.

⁴Target Discovery Institute, University of Oxford, Oxford OX3 7FZ, United Kingdom.

⁵From the Centre for Cellular and Molecular Physiology, University of Oxford, Oxford OX3 7BN, United Kingdom, pjr@well.ox.ac.uk.

⁶From the Centre for Cellular and Molecular Physiology, University of Oxford, Oxford OX3 7BN, United Kingdom, nmasson@well.ox.ac.uk.

Abstract

Interactions between biological pathways and molecular oxygen require robust mechanisms for detecting and responding to changes in cellular oxygen availability, to support oxygen homeostasis. Peptidylglycine α -amidating monooxygenase (PAM) catalyzes a two-step reaction resulting in the C-terminal amidation of peptides, a process important for their stability and biological activity. Here we show that in human, mouse, and insect cells, peptide amidation is exquisitely sensitive to hypoxia. Different amidation events on chromogranin A, and on peptides processed from proopiomelanocortin, manifest similar striking sensitivity to hypoxia in a range of neuroendocrine cells, being progressively inhibited from mild (7% O₂) to severe (1% O₂) hypoxia. In developing *Drosophila melanogaster* larvae, FMRF amidation in thoracic ventral (Tv) neurons is strikingly suppressed by hypoxia. Our findings have thus defined a novel monooxygenase-based oxygen sensing mechanism that has the capacity to signal changes in oxygen availability to peptidergic pathways.

Capture-C reveals preformed chromatin interactions between HIF-binding sites and distant promoters

Platt JL¹, Salama R¹, Smythies J¹, Choudhry H², Davies JO³, Hughes JR³, Ratcliffe PJ⁴, Mole DR⁵.

¹Henry Wellcome Building for Molecular Physiology, University of Oxford, Oxford, UK.

²Department of Biochemistry, Faculty of Science, Center of Innovation in Personalized Medicine King Fahd Center for Medical Research King Abdulaziz University, Jeddah, Saudi Arabia.

³Medical Research Council Molecular Haematology Unit, Weatherall Institute of Molecular Medicine University of Oxford, Oxford, UK.

⁴Target Discovery Institute, University of Oxford, Oxford, UK drmole@well.ox.ac.uk Peter.Ratcliffe@ndm.ox.ac.uk.

⁵Henry Wellcome Building for Molecular Physiology, University of Oxford, Oxford, UK drmole@well.ox.ac.uk Peter.Ratcliffe@ndm.ox.ac.uk.

Abstract

Hypoxia-inducible factor (HIF) directs an extensive transcriptional cascade that transduces numerous adaptive responses to hypoxia. Pan-genomic analyses, using chromatin immunoprecipitation and transcript profiling, have revealed large numbers of HIF-binding sites that are generally associated with hypoxia-inducible transcripts, even over long chromosomal distances. However, these studies do not define the specific targets of HIF-binding sites and do not reveal how induction of HIF affects chromatin conformation over distantly connected functional elements. To address these questions, we deployed a recently developed chromosome conformation assay that enables simultaneous high-resolution analyses from multiple viewpoints. These assays defined specific long-range interactions between intergenic HIF-binding regions and one or more promoters of hypoxia-inducible genes, revealing the existence of multiple enhancer-promoter, promoter-enhancer, and enhancer-enhancer interactions. However, neither short-term activation of HIF by hypoxia, nor long-term stabilization of HIF in von Hippel-Lindau (VHL)-defective cells greatly alters these interactions, indicating that at least under these conditions, HIF can operate on preexisting patterns of chromatin-chromatin interactions that define potential transcriptional targets and permit rapid gene activation by hypoxic stress.

The Factor Inhibiting HIF Asparaginyl Hydroxylase Regulates Oxidative Metabolism and Accelerates Metabolic Adaptation to Hypoxia

Sim J¹, Cowburn AS¹, Palazon A¹, Madhu B², Tyrakis PA³, Macías D¹, Bargiela DM¹, Pietsch S¹, Gralla M⁴, Evans CE¹, Kittipassorn T⁵, Chey YCJ⁶, Branco CM¹, Rundqvist H⁴, Peet DJ⁶, Johnson RS⁷.

¹Physiological Laboratory, Department of Physiology, Development and Neuroscience, University of Cambridge, Cambridge CB2 3EG, UK.

²Cancer Research UK Cambridge Institute, Cambridge CB2 0RE, UK.

³Physiological Laboratory, Department of Physiology, Development and Neuroscience, University of Cambridge, Cambridge CB2 3EG, UK; Cancer Research UK Cambridge Institute, Cambridge CB2 0RE, UK.

⁴Department of Cell and Molecular Biology, Karolinska Institute, Stockholm SE-171 77, Sweden.

⁵School of Biological Sciences, University of Adelaide, Adelaide, SA 5005, Australia; Department of Physiology, Faculty of Medicine, Siriraj Hospital, Mahidol University, Bangkok 73170, Thailand.

⁶School of Biological Sciences, University of Adelaide, Adelaide, SA 5005, Australia.

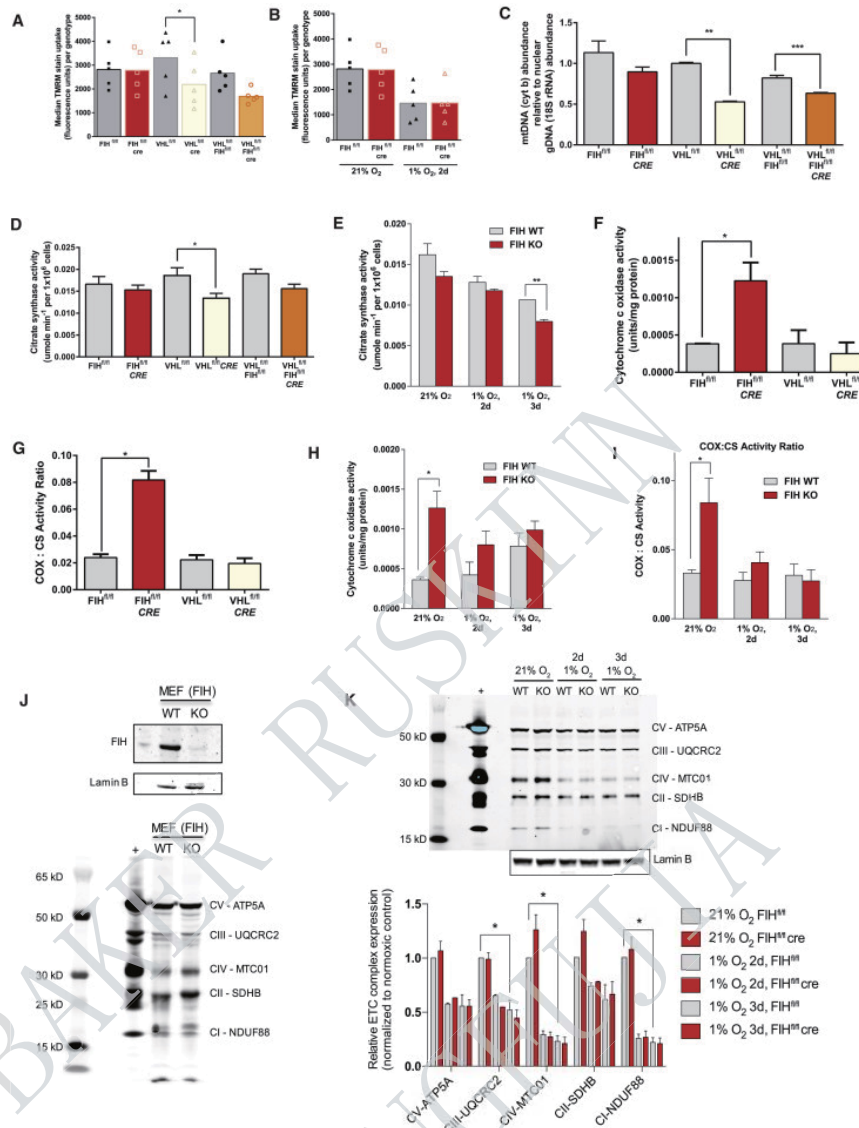
⁷Physiological Laboratory, Department of Physiology, Development and Neuroscience, University of Cambridge, Cambridge CB2 3EG, UK; Department of Cell and Molecular Biology, Karolinska Institute, Stockholm SE-171 77, Sweden. Electronic address: rsj33@cam.ac.uk.

出处: *Cell Metab.* 2018 Apr 3;27(4):898-913.e7. DOI: 10.1016/j.cmet.2018.02.020.

Ruskin 工作站使用情况: Sci-tive; O₂ 浓度:1%

Abstract

Animals require an immediate response to oxygen availability to allow rapid shifts between oxidative and glycolytic metabolism. These metabolic shifts are highly regulated by the HIF transcription factor. The factor inhibiting HIF (FIH) is an asparaginyl hydroxylase that controls HIF transcriptional activity in an oxygen-dependent manner. We show here that FIH loss increases oxidative metabolism, while also increasing glycolytic capacity, and that this gives rise to an increase in oxygen consumption. We further show that the loss of FIH acts to accelerate the cellular metabolic response to hypoxia. Skeletal muscle expresses 50-fold higher levels of FIH than other tissues: we analyzed skeletal muscle FIH mutants and found a decreased metabolic efficiency, correlated with an increased oxidative rate and an increased rate of hypoxic response. We find that FIH, through its regulation of oxidation, acts in concert with the PHD/vHL pathway to accelerate HIF-mediated metabolic responses to hypoxia.



Differential Regulation of HIF Leads to Differential Regulation of Mitochondrial Parameters

(A) Flow cytometry; histogram of cell count versus TMRM fluorescence, with shaded graph representing unstained controls. (B) Flow cytometry; histogram of cell count versus TMRM fluorescence, with shaded graph representing unstained controls. (C) mtDNA abundance in indicated cells. (D) Citrate synthase activity measured in indicated cells. (E) Citrate synthase activity in FIH KO compared with control MEFs over prolonged exposure to hypoxia. (F) FIH, but not vHL KO cell lysates show higher mitochondrial cytochrome c oxidase activity ($p = 0.049$) than control MEFs. (G) Cytochrome oxidase activity of FIH KO MEFs normalized to citrate synthase activity. (H) FIH KO MEFs have higher cytochrome oxidase activity than control cells in atmospheric oxygen, but this effect is blunted over hypoxic exposure. (I) The trends described in (H) persist even when the cytochrome oxidase activity of FIH KO and control MEFs is normalized to citrate synthase activity levels. (J) Western blot of control versus FIH KO MEFs with lamin B as a loading control and rat heart mitochondria as a positive control; demonstrates total electron transport chain complex content in MEF lysates. (K) Western blot of mitochondrial complex content in control versus FIH KO MEFs, with progressive hypoxic exposure.

HIF drives lipid deposition and cancer in ccRCC via repression of fatty acid metabolism

Weinan Du¹, Luchang Zhang¹, Adina Brett-Morris¹, Brittany Aguila¹, Janos Kerner², Charles L. Hoppel^{2,3}, Michelle Puchowicz⁴, Dolores Serra^{5,6}, Laura Herrero^{5,6}, Brian I. Rini⁷, Steven Campbell⁸ & Scott M. Welford¹

¹Department of Radiation Oncology, Case Western Reserve University School of Medicine, 10900 Euclid Avenue, Cleveland, OH 44106, USA. ²Department of Pharmacology, Case Western Reserve University School of Medicine, 10900 Euclid Avenue, Cleveland, OH 44106, USA.

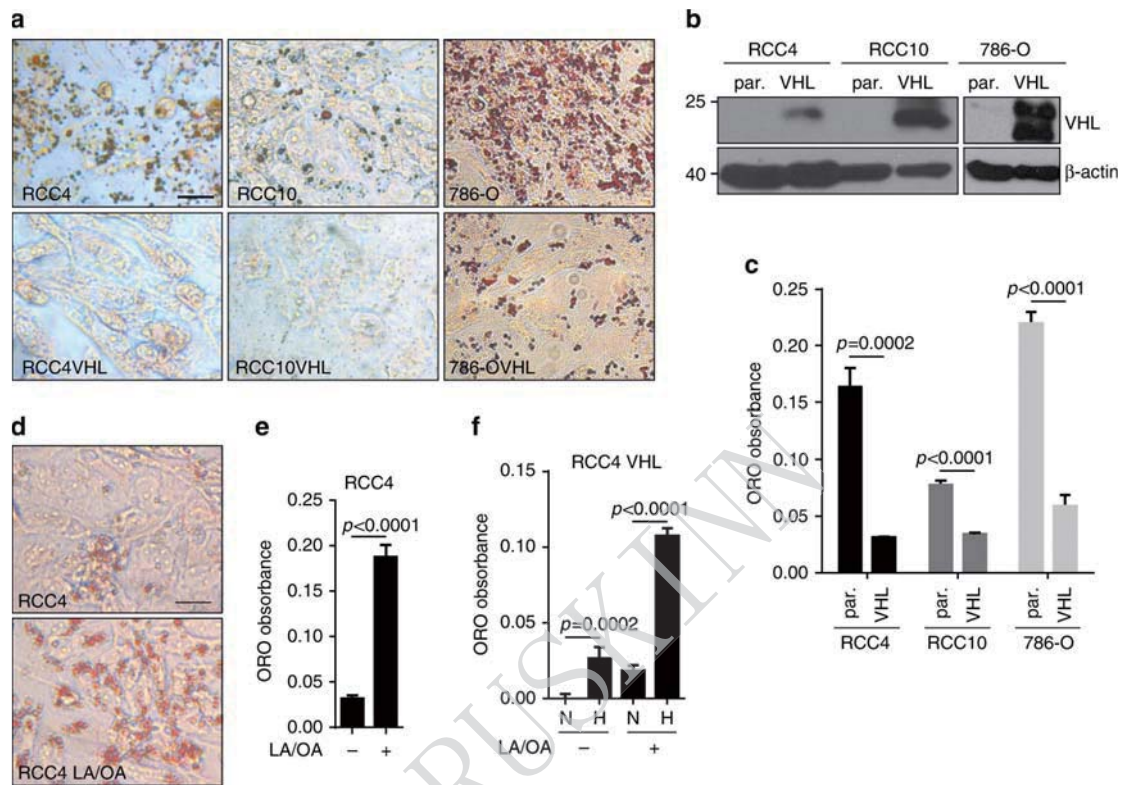
³Department of Medicine, Case Western Reserve University School of Medicine, 10900 Euclid Avenue, Cleveland, OH 44106, USA. ⁴Department of Nutrition, Case Western Reserve University School of Medicine, 10900 Euclid Avenue, Cleveland, OH 44106, USA. ⁵Department of Biochemistry and Physiology, Institut de Biomedicina de la Universitat de Barcelona (IBUB), Universitat de Barcelona, E-08028 Barcelona, Spain. ⁶Centro de Investigación Biomédica en Red de Fisiopatología de la Obesidad y la Nutrición (CIBEROBN), Instituto de Salud Carlos III, E-28029 Madrid, Spain. ⁷Department of Hematology and Oncology, Cleveland Clinic Foundation, 9500 Euclid Avenue, Cleveland, OH 44106, USA. ⁸Department of Urology, Cleveland Clinic Foundation, 9500 Euclid Avenue, Cleveland, OH 44106, USA.

出处: *Nat Commun.* 2017 11 24;8(1). DO:10.1038/s41467-017-01965-8

Ruskinn 工作站使用情况: Invivo₂; O₂ 浓度:1%

Abstract

Clear cell renal cell carcinoma (ccRCC) is histologically defined by its lipid and glycogen-rich cytoplasmic deposits. Alterations in the VHL tumor suppressor stabilizing the hypoxia-inducible factors (HIFs) are the most prevalent molecular features of clear cell tumors. The significance of lipid deposition remains undefined. We describe the mechanism of lipid deposition in ccRCC by identifying the rate-limiting component of mitochondrial fatty acid transport, carnitine palmitoyltransferase 1A (CPT1A), as a direct HIF target gene. CPT1A is repressed by HIF1 and HIF2, reducing fatty acid transport into the mitochondria, and forcing fatty acids to lipid droplets for storage. Droplet formation occurs independent of lipid source, but only when CPT1A is repressed. Functionally, repression of CPT1A is critical for tumor formation, as elevated CPT1A expression limits tumor growth. In human tumors, CPT1A expression and activity are decreased versus normal kidney; and poor patient outcome associates with lower expression of CPT1A in tumors in TCGA. Together, our studies identify HIF control of fatty acid metabolism as essential for ccRCC tumorigenesis.



Lipid accumulation in ccRCC cells is VHL dependent.

- a. Photomicrographs of RCC4, RCC10, and 786-O renal cell lines with or without VHL stained with Oil Red O 6 days after reaching confluence.
- b. Western blot demonstrating VHL expression in reconstituted lines. β -actin used as loading control.
- c. Quantification of Oil Red O extracted from cells shown in a.
- d. Oil Red O staining of RCC4 cells 2 days after treatment with linoleic/oleic acid (LA/OA).
- e. Quantification of Oil Red O staining of cells in d.
- f. Quantification of Oil Red O staining of RCC4 VHL cells treated with LA/OA cultured in either normoxia (N) or 1% oxygen (H).

Statistical tests for all panels were two-tailed Student's *t* tests. Scale bar = 10 μ m. Error bars represent standard deviations

Tet1 facilitates hypoxia tolerance by stabilizing the HIF- α proteins independent of its methylcytosine dioxygenase activity

Jing Wang,¹ Dawei Zhang,¹ Juan Du,¹ Chi Zhou,¹ Zhi Li,¹ Xing Liu,¹ Gang Ouyang,¹ and Wuhan Xiao^{1,2,3}

¹State Key Laboratory of Freshwater Ecology and Biotechnology, Institute of Hydrobiology, Chinese Academy of Sciences, Wuhan 430072, PR China,

²The Key Laboratory of Aquatic Biodiversity and Conservation, Institute of Hydrobiology, Chinese Academy of Science, Wuhan 430072, PR China and

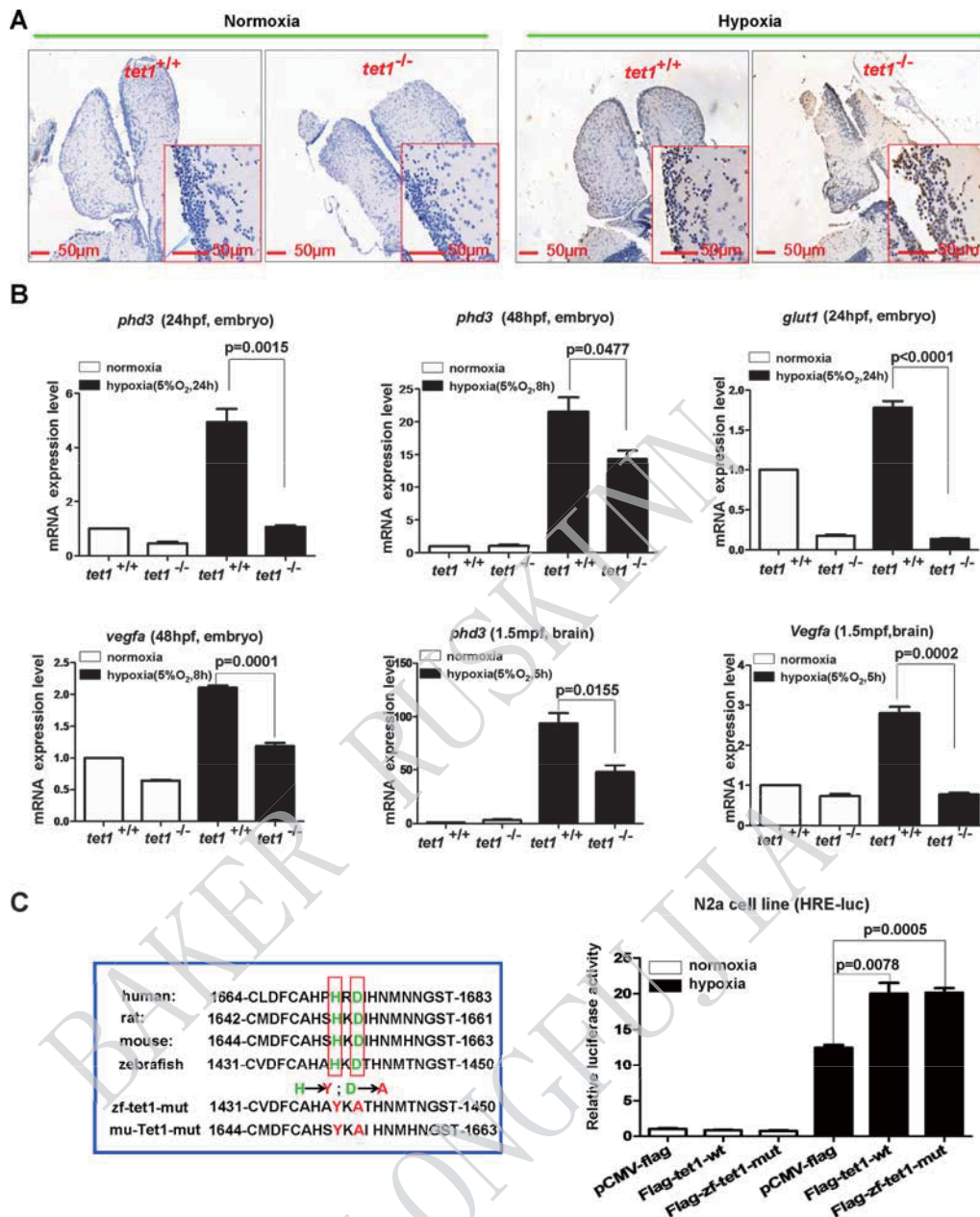
³The Key laboratory of Aquaculture Disease Control, Ministry of Agriculture, Wuhan, 430072, PR China

出处: *Nucleic Acids Res.* 2017 Dec 15;45(22). DOI:org/10.1093/nar/gkx869

Ruskinn 工作站使用情况: Invivo2 400; O₂ 浓度: 5%

Abstract

Because of the requirement of oxygen (O₂) to produce energy, aerobic organisms developed mechanisms to protect themselves against a shortage of oxygen in both acute status and chronic status. To date, how organisms tolerate acute hypoxia and the underlying mechanisms remain largely unknown. Here, we identify that *Tet1*, one member of the ten-eleven translocation (TET) family of methylcytosine dioxygenases, is required for hypoxia tolerance in zebrafish and mice. *Tet1*-null zebrafish and mice are more sensitive to hypoxic conditions compared with their wild-type siblings. We demonstrate that Tet1 stabilizes hypoxia-inducible factor α (HIF- α) and enhances HIF- α transcription activity independent of its enzymatic activity. In addition, we show that Tet1 modulates HIF-2 α and HIF-1 α through different mechanisms. Tet1 competes with prolyl hydroxylase protein 2 (PHD2) to bind to HIF-2 α , resulting in a reduction of HIF-2 α hydroxylation by PHD2. For HIF-1 α , however, Tet1 has no effect on HIF-1 α hydroxylation, but rather it appears to stabilize the C-terminus of HIF-1 α by affecting lysine site modification. Furthermore, we found that Tet1 enhances rather than prevents poly-ubiquitination on HIF- α . Our results reveal a previously unrecognized function of *Tet1* independent of its methylcytosine dioxygenase activity in hypoxia signaling.



Knockout of *tet1* in zebrafish causes more apoptotic cells in the brain and reduction of hypoxia-inducible gene expression under hypoxia.

(A) Compared with those in the brain of wild-type siblings, more apoptotic cells were detected in the brain of *tet1*-null zebrafish by TUNEL assays under hypoxia (5% O₂, 5 h). (B) Expressions of hypoxia-inducible genes including *phd3*, *glut1*, *vegfa* were reduced significantly in the brain of *tet1*-null zebrafish embryos and adults compared with those of their wild-type siblings under hypoxia. (C) Overexpression of both zebrafish *tet1* and its enzymatic inactive form (zf-tet1-mut) could activate the hypoxia response element luciferase (HRE-luc.) reporter in the N2a cell line under hypoxia. N2a cells were transfected with the indicated plasmids and luciferase activity was measured 20–24 h after transfection. The left red box indicates the alignment of partial Tet1 sequences surrounding Tet1 enzymatic activity region and the enzymatic inactive mutant (mut) with histidine mutated to tyrosine and aspartic acid mutated to alanine. zf-tet1-mut, zebrafish *tet1* mutant; mu-Tet1-mut, mouse Tet1 mutant.

其他文章:

1. Systemic inactivation of hypoxia-inducible factor prolyl 4-hydroxylase 2 in mice protects from

- alcohol-induced fatty liver disease.
 期刊: Redox Biology; Ruskinn 工作站使用情况: Invivo₂ 400
- 2.A long hypoxia-inducible factor 3 isoform 2 is a transcription activator that regulates erythropoietin.
 期刊: Cell. Mol. Life Sci.; Ruskinn 工作站使用情况: Sci-tive N
- 3.Lactate Efflux From Intervertebral Disc Cells Is Required for Maintenance of Spine Health.
 期刊: J. Bone Miner. Res. ; Ruskinn 工作站使用情况: Invivo₂ 300
- 4.HIF hydroxylase inhibitors decrease cellular oxygen consumption depending on their selectivity
 期刊: FASEB J.; Ruskinn 工作站使用情况: Invivo₂ 400
- 5.The neuronal oxygen-sensing pathway controls postnatal vascularization of the murine brain.
 期刊: FASEB J.; Ruskinn 工作站使用情况: Invivo₂ 400
- 6.The Bacterial Chromatin Protein HupA Can Remodel DNA and Associates with the Nucleoid in Clostridium difficile.
 期刊: J. Mol. Biol.; Ruskinn 工作站使用情况: Concept 1000
- 7.Blocking OLFM4/HIF - 1 α axis alleviates hypoxia - induced invasion, epithelial–mesenchymal transition, and chemotherapy resistance in non - small - cell lung cancer
 期刊: J. Cell. Physiol. ; Ruskinn 工作站使用情况: Ruskinn Workstation
- 8.Co-occurrence of RCC-susceptibility polymorphisms with HIF cis-acting sequences supports a pathway tuning model of cancer
 期刊: Sci Rep; Ruskinn 工作站使用情况: Invivo₂ 400
- 9.Mechanism and Consequences of The Impaired Hif-1 α Response to Hypoxia in Human Proximal Tubular HK-2 Cells Exposed to High Glucose.
 期刊: Sci Rep; Ruskinn 工作站使用情况: Invivo₂ 400
- 10.Elevated expression of hypoxia-inducible factor-2 α regulated catabolic factors during intervertebral disc degeneration
 期刊: Life Sci. ; Ruskinn 工作站使用情况: Invivo₂ 300
- 10.Inherent DNA-binding specificities of the HIF-1 α and HIF-2 α transcription factors in chromatin
 期刊: EMBO Rep.; Ruskinn 工作站使用情况: Invivo₂ 400
- 11.Defective Mitochondrial Cardiolipin Remodeling Dampens HIF-1 α Expression in Hypoxia
 期刊: Cell Rep; Ruskinn 工作站使用情况: Invivo₂
- 12.Protein kinase C binding protein 1 inhibits hypoxia-inducible factor-1 in the heart.
 期刊: Cardiovasc. Res.; Ruskinn 工作站使用情况: Invivo₂ 400
- 13.Bicarbonate Recycling by HIF-1-Dependent Carbonic Anhydrase Isoforms 9 and 12 Is Critical in Maintaining Intracellular pH and Viability of Nucleus Pulposus Cells.
 期刊: J. Bone Miner. Res. ; Ruskinn 工作站使用情况: Invivo₂ 300
- 14.AG311, a small molecule inhibitor of complex I and hypoxia-induced HIF-1 α stabilization.
 期刊: Cancer Lett. ; Ruskinn 工作站使用情况: Invivo₂ 400
- 15.Hypoxia Enhances Immunosuppression by Inhibiting CD4⁺ Effector T Cell Function and Promoting Treg Activity.
 期刊: Cell. Physiol. Biochem. ; Ruskinn 工作站使用情况: Invivo₂ 400
- 16.PHD3 is a transcriptional coactivator of HIF-1 α in nucleus pulposus cells independent of the PKM2-JMJD5 axis.
 期刊: FASEB J.; Ruskinn 工作站使用情况: Invivo₂ 300

An HIF-1 α /VEGF-A Axis in Cytotoxic T Cells Regulates Tumor Progression.

*Asis Palazon,¹ Petros A. Tyrakis,^{1,2} David Macias,² Pedro Veliça,³ Helene Rundqvist,³ Susan Fitzpatrick,² Nikola Vojnovic,³ Anthony T. Phan,⁴ Niklas Loman,⁶ Ingrid Hedenfalk,⁶ Thomas Hatschek,⁵ John Lövrot,⁵ Theodoros Foukakis,⁵ Ananda W. Goldrath,⁴ Jonas Bergh,⁵ and Randall S. Johnson^{1,3}, **

¹Department of Physiology, Development and Neuroscience, University of Cambridge, Cambridge CB2 3EG, UK

²Cancer Research UK, Cambridge Institute, Cambridge CB2 0RE, UK

³Department of Cell and Molecular Biology, Karolinska Institute, 171 77 Stockholm, Sweden

⁴Molecular Biology Section, Division of Biological Sciences, University of California San Diego, La Jolla, CA 92161, USA

⁵Karolinska Oncology, Karolinska Institute and University Hospital, 171 76 Stockholm, Sweden

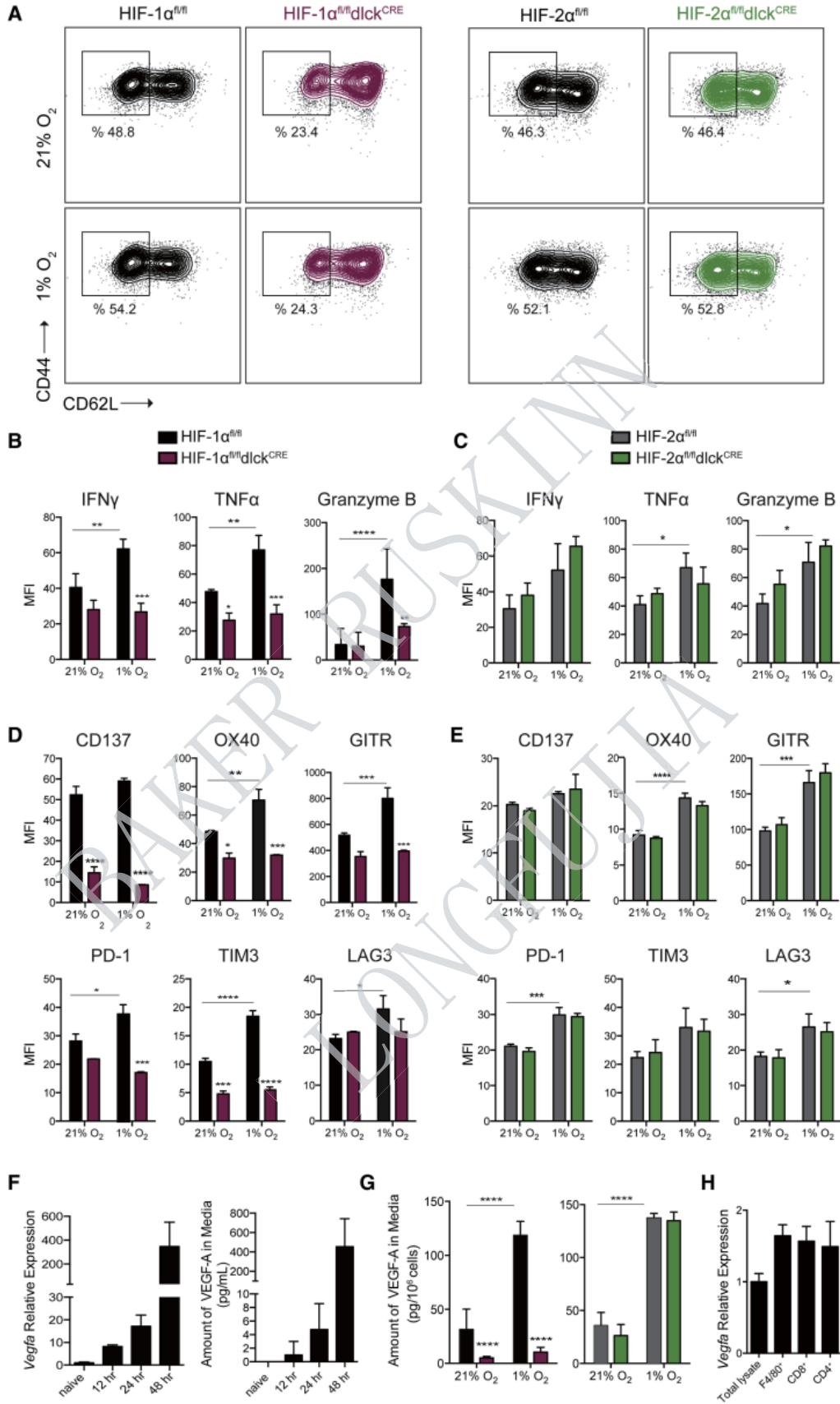
⁶Department of Clinical Sciences, Division of Oncology and Pathology, Lund University, 223 81 Lund, Sweden

出处: **Cancer Cell**, 2017, 32(5):669-683. DOI:org/10.1016/j.ccell.2017.10.003

Ruskinn 工作站使用情况: Invivo₂400; O₂ 浓度:1%

Abstract

Cytotoxic T cells infiltrating tumors are thought to utilize HIF transcription factors during adaptation to the hypoxic tumor microenvironment. Deletion analyses of the two key HIF isoforms found that HIF-1 α , but not HIF-2 α , was essential for the effector state in CD8⁺ T cells. Furthermore, loss of HIF-1 α in CD8⁺ T cells reduced tumor infiltration and tumor cell killing, and altered tumor vascularization. Deletion of VEGF-A, an HIF target gene, in CD8⁺ T cells accelerated tumorigenesis while also altering vascularization. Analyses of human breast cancer showed inverse correlations between VEGF-A expression and CD8⁺ T cell infiltration, and a link between T cell infiltration and vascularization. These data demonstrate that the HIF-1 α /VEGF-A axis is an essential aspect of tumor immunity.



Hypoxia and HIF-1 α , but Not HIF-2 α , Support CD8⁺ T Cell Acquisition of Effector Phenotype

(A) CD8⁺ T cells were isolated from spleens of HIF-1 α fl/fldlckCRE (maroon) or HIF-2 α fl/fldlckCRE (green) and littermate control (black) mice, and activated with α CD3/CD28 for 48 hr, then expanded for 5 days in IL-2 and subjected to 21% or 1% O₂ for 24 hr. Expression of CD44 and CD62L by flow cytometry is shown.

(B) Intracellular expression of IFN γ , TNF α , and granzyme B in HIF-1 α fl/fldlckCRE (maroon) and HIF-1 α fl/fl control littermates (black) by flow cytometry after restimulation (n = 3, error bars represent SD).

(C) Intracellular expression of IFN γ , TNF α , and granzyme B in HIF-2 α fl/fldlckCRE (green) and HIF-2 α fl/fl control littermates (gray) by flow cytometry after restimulation (n = 3, error bars represent SD).

(D) Surface expression of costimulatory molecules/checkpoint receptors CD137, OX40, GITR, PD-1, TIM-3, and LAG3 on CD8⁺ T cells isolated from HIF-1 α fl/fldlckCRE (maroon) HIF-1 α fl/fl control littermates (black), activated and expanded as in (A) (n = 3, error bars represent SD).

(E) Same as in (D) on CD8⁺ T cells isolated from HIF-2 α fl/fldlckCRE (green) or HIF-2 α fl/fl control littermate mice (gray) (n = 3, error bars represent SD).

(F) Relative mRNA levels of Vegfa (left, n = 3) and amount of VEGF-A in media (right, n = 4, error bars represent SD) on CD8⁺ T cells for the indicated time points after α CD3/CD28 activation.

(G) Amount of VEGF-A in media from CTLs expanded as in (A) and cultured under 21% O₂ or 1% O₂ for 24 hr (n = 4, error bars represent SD).

(H) Relative expression of Vegfa in total LLC tumor lysate and immune populations isolated from subcutaneous Lewis lung carcinoma (LLC) tumors 11 days after implantation (n = 10, error bars represent SD).

Grouped data were assessed by two-way ANOVA for multiple comparisons with Bonferroni correction. ****p < 0.00005, ***p < 0.0005, **p < 0.005, *p < 0.05. MFI, mean fluorescence intensity.

Rewiring of Lipid Metabolism and Storage in Ovarian Cancer Cells after Anti-VEGF Therapy

Matteo Curtarello ^{1,†}, Martina Tognon ^{1,†}, Carolina Venturoli ^{1,†}, Micol Silic-Benussi ¹, Angela Grassi ¹, Martina Verza ¹, Sonia Minuzzo ², Marica Pinazza ¹, Valentina Brillo ³, Giovanni Tosi ³, Ruggero Ferrazza ⁴, Graziano Guella ⁴, Egidio Iorio ⁵, Adrien Godfroid ⁶, Nor Eddine Sounni ⁶, Alberto Amadori ^{1,2} and Stefano Indraccolo ^{1,*}

¹ Veneto Institute of Oncology IOV-IRCCS, 35128 Padova, Italy; matteo.curtarello@iov.veneto.it (M.C.); martina.tognon@iov.veneto.it (M.T.); carolinaventuroli@live.it (C.V.); micol.silicbenussi@iov.veneto.it (M.S.-B.); angela.grassi@iov.veneto.it (A.G.); martina2.verza@gmail.com (M.V.); maricapinaz@alice.it (M.P.); albido@unipd.it (A.A.)

² Department of Surgery, Oncology and Gastroenterology, University of Padova, 35128 Padova, Italy; soniaanna.minuzzo@unipd.it

³ Department of Biology, University of Padova, 35128 Padova, Italy; valentina.brillo@studenti.unipd.it (V.B.); giovanni.tosi.1@studenti.unipd.it (G.T.)

⁴ Department of Physics, University of Trento, Via Sommarive 14, 38123 Trento, Italy; ruggero.ferrazza@yahoo.it (R.F.); graziano.guella@unitn.it (G.G.)

⁵ Core Facilities, NMR and MRI Unit, Istituto Superiore di Sanità, 00161 Roma, Italy; egidio.iorio@iss.it

⁶ Laboratory of Tumor and Development Biology, GIGA-Cancer, University of Liège, 4000 Liège, Belgium; adrien.godfroid@ulg.ac.be (A.G.); nesounni@ulg.ac.be (N.E.S.)

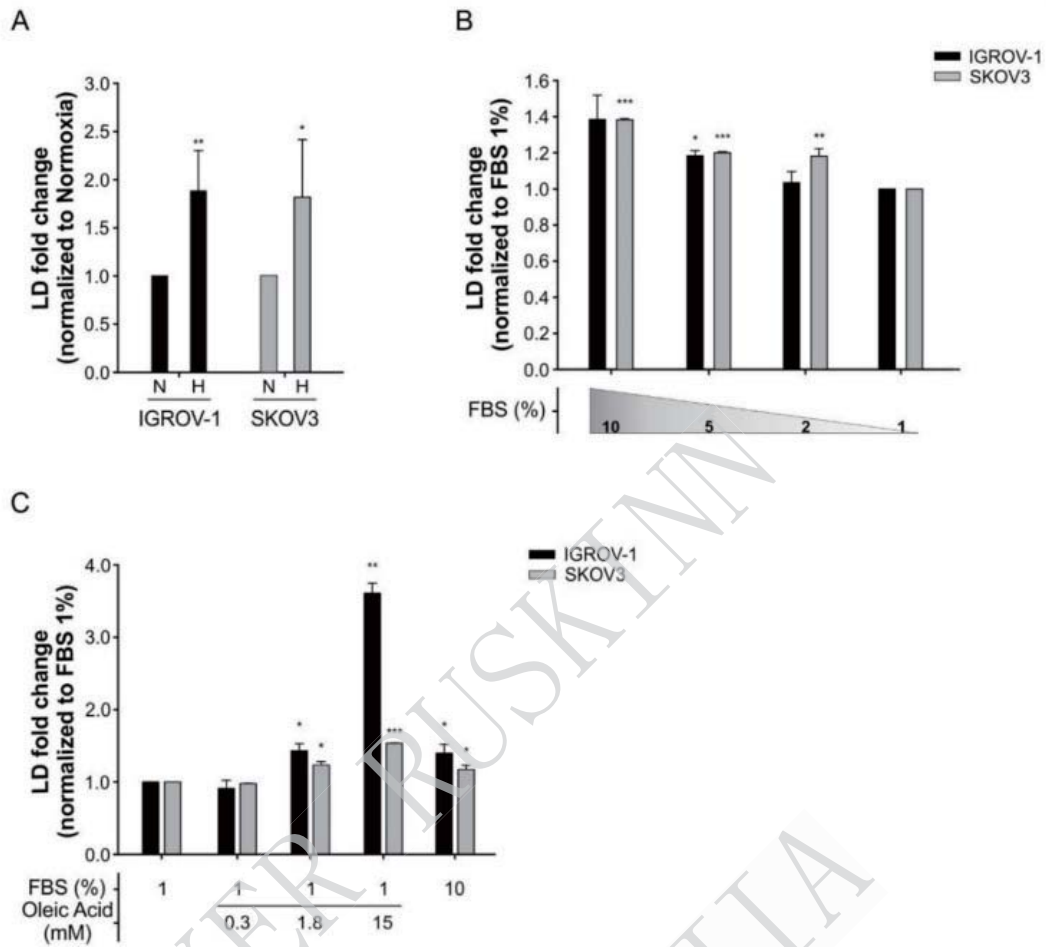
出处: **Cells** 2019 Dec 09;8(12). DOI: 10.3390/cells8121601

Ruskinn 工作站使用情况: Invivo₂ 300 O₂ 浓度: 0.5%

Abstract

Anti-angiogenic therapy triggers metabolic alterations in experimental and human tumors, the best characterized being exacerbated glycolysis and lactate production. By using both Liquid Chromatography-Mass Spectrometry (LC-MS) and Nuclear Magnetic Resonance (NMR) analysis, we found that treatment of ovarian cancer xenografts with the anti-Vascular Endothelial Growth Factor (VEGF) neutralizing antibody bevacizumab caused marked alterations of the tumor lipidomic profile, including increased levels of triacylglycerols and reduced saturation of lipid chains. Moreover, transcriptome analysis uncovered up-regulation of pathways involved in lipid metabolism. These alterations were accompanied by increased accumulation of lipid droplets in tumors. This phenomenon was reproduced under hypoxic conditions in vitro, where it mainly depended from uptake of exogenous lipids and was counteracted by treatment with the Liver X Receptor (LXR)-agonist GW3965, which inhibited cancer cell viability selectively under reduced serum conditions. This multi-level analysis indicates alterations of lipid metabolism following anti-VEGF therapy in ovarian cancer xenografts and suggests that LXR-agonists might empower anti-tumor effects of bevacizumab.

Keywords: ovarian cancer; bevacizumab; metabolism; lipid droplets; LXR agonist



LD accumulation under hypoxia condition and serum starvation in IGROV-1 and SKOV3 ovarian cancer cells.

(A) Quantification of LD in cancer cells, cultured under normoxia (N) or hypoxia (H) for 48 h, by flow cytometry analysis following staining with BODIPY 493/503 dye. X-mean values are normalized to normoxia condition. Columns show mean \pm SD values of three experimental replicates (* $p < 0.05$, ** $p < 0.01$, t-test)

(B) LD content in cancer cells cultured under normoxia and serum starvation for 24 h. X-mean values are normalized to 1% FBS condition. Columns show mean \pm SD values of three experimental replicates (* $p < 0.05$, ** $p < 0.01$, *** $p < 0.001$, t-test).

(C) LD content in cancer cells cultured under normoxia and 1% FBS condition with supplementation of oleic acid in three different concentrations (0.3 mM, 1.8 mM and 15 mM) for 24 h. Columns show mean \pm SD values of three experimental replicates (* $p < 0.05$, ** $p < 0.01$, *** $p < 0.001$, t-test)

其他文章:

1.The neuronal oxygen-sensing pathway controls postnatal vascularization of the murine brain

期刊: FASEB J.; 发表年份: 2019; Ruskinn 工作站使用情况: Invivo₂

2.Uric acid treatment after stroke modulates the Krüppel-like factor 2-VEGF-A axis to protect brain endothelial cell functions: Impact of hypertension.

期刊: Biochem. Pharmacol.; 发表年份: 2019; Ruskinn 工作站使用情况: Invivo₂

3.Hypoxia and inflammation in the release of VEGF and interleukins from human retinal pigment epithelial cells.

期刊: Graefes Arch. Clin. Exp. Ophthalmol.; 发表年份: 2017; Ruskinn 工作站使用情况: Invivo₂

4.VEGF121 and VEGF165 differentially promote vessel maturation and tumor growth in mice and humans.

期刊: Cancer Gene Ther.; 发表年份: 2016; Ruskinn 工作站使用情况: Invivo₂ 200

BAKER RUSKINN
LONGFUJIA

The Regulation of Mesenchymal Stem Cell Therapy Through Magnetic Resonance Imaging Agents-Based Cellular Condition and Oxygen Environment

Yuanting Lu^{1,3,†}, Lusheng Wei^{4,†}, Xiaodong Zhang³, Jiangli Cai², Yanchun Zhu⁵, Jijie Xiao³, Yuwen Duan³, Hong Liu², Zhiyong Wang^{2,□}, and Shaolin Li^{1,3,□}

¹Department of Medical Image, The Fifth Affiliated Hospital, Sun Yat-sen University, Zhuhai 519000, China

²Center for Functional Biomaterials, Key Laboratory for Polymeric Composite and Functional Materials of Ministry of Education, School of Materials Science and Engineering, Sun Yat-sen University, Guangzhou 510275, China

³Department of Medical Image, The Third Affiliated Hospital, Southern Medical University, Guangzhou 510515, China

⁴Department of Biliary-Pancreatic Surgery, Sun Yat-sen Memorial Hospital, Sun Yat-sen University, Guangzhou 510275, China

⁵Shenzhen Institutes of Advanced Technology, Chinese Academic of Sciences, ShenZhen 518055, China

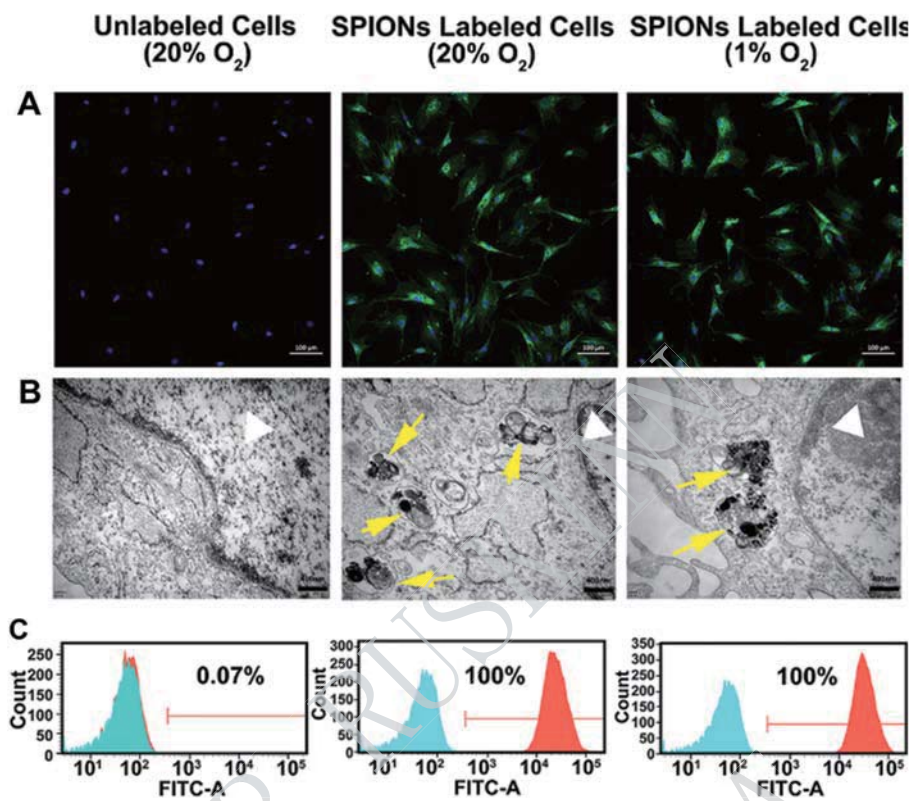
出处: *J Biomed Nanotechnol* 2018 Nov 01;14(11). DOI: 10.1166/jbn.2018.2639

Ruskinn 工作使用情况: Invivo₂ 300; O₂ 浓度: 1%, 20%

Abstract

Repairing articular cartilage defects is difficult due to the hypovascular biostructure and poor self-repairing capacity of articular cartilage. Currently, mesenchymal stem cells (MSCs) with excellent differentiation potential are considered as a promising biological approach for cartilage regeneration. The effect, however, remains far from satisfactory for clinical applications owing to the main drawbacks of tracking the retention of cells and a low differentiation efficiency. As known, the nanoparticles with superparamagnetic properties has been used to monitor the MSCs in vivo through magnetic resonance imaging (MRI) in clinical application. In this study, different external and internal bio-conditions were applied to regulate the biological behavior of cells. Here, intracellular MRI contrast agents, superparamagnetic iron oxide nanocrystals (SPIONs), and a hypoxic culture environment were found to exert synergistic effects on gene and protein expression, and the cell viability, cell cycle, apoptosis, reactive oxygen species and the stem cell differentiations were measured. The levels of chondrogenic and migrant markers (including collagen II, collagen X, aggrecan, SOX9, MMPs and CXCR4) increased, triggering directional differentiation and enhancing cell migration to the inflammatory site. Moreover, SPION-labeled hypoxia-preconditioned MSCs were found without reactive oxygen species generation and transplanted into rat models with articular cartilage disorders. Interestingly, MRI and histological identification confirmed that new cartilage-like tissue was regenerated and that defects were repaired, and this method is more efficient for cartilage regeneration than SPION-labeled normoxia MSCs. The synergistic effect of hypoxia-precondition and SPIONs based cellular iron source could improve the cell migration and facilitate chondrogenic differentiation.

Keywords: Mesenchymal Stem Cells, Superparamagnetic Iron Oxide Nanoparticles, Magnetic Resonance Imaging, Hypoxia-Preconditioned, Cartilage Defect.



Cellular uptake and distribution of SPIONs in BM-MSCs

(A) CLSM images of the SPION-labeled and unlabeled BMMSCs under normoxia or hypoxia conditions (scale bar = 100 μm). Herein, the nanocomplexes are conjugated with FITC (green); nuclei were stained via DAPI (blue). (B) TEM images of the SPION-labeled and unlabeled BM-MSCs (scale bar = 400 nm). The intracellular SPIONs are shown with yellow arrows in the cell, and the nucleus is indicated by white triangles. (C) Flow cytometry data indicated the labeling efficiency of the unlabeled and SPION-labeled BM-MSCs.

Intrabone transplant provides full stemness of cord blood stem cells with fast hematopoietic recovery and low GVHD rate: results from a prospective study

*Francesca Bonifazi*¹, *Elisa Dan*¹, *Myriam Labopin*, *Mariarosaria Sessa*¹, *Viviana Guadagnuolo*¹, *Martina Ferioli*¹, *Simonetta Rizzi*¹, *Sabrina De Carolis*³, *Barbara Sinigaglia*¹, *Maria Rosa Motta*¹, *Andrea Bontadini*⁴, *Valeria Giudice*⁵, *Giovanni Martinelli*⁶, *Mario Arpinati*¹, *Michele Cavo*^{1,3}, *Massimiliano Bonafè*^{3,6}, *Gianluca Storci*^{3,7}

¹ Institute of Hematology “L. and A. Seràgnoli”, University Hospital S. Orsola-Malpighi, Bologna, Italy

² Hôpital Saint-Antoine 184 rue du Faubourg Saint-Antoine, 75571 Paris Cedex 12, Paris, France ³ DIMES, Department of Experimental, Diagnostic and Specialty Medicine, University of Bologna, Bologna, Italy

⁴ Immunogenetics, University Hospital S. Orsola-Malpighi, Bologna, Italy

⁵ Apheresis Unit, University Hospital S. Orsola-Malpighi, Bologna, Italy

⁶ Biosciences Laboratory, Istituto Scientifico Romagnolo per lo Studio e la Cura dei Tumori (IRST) IRCCS, Meldola, Italy

⁷ Interdepartmental Center “Luigi Galvani”, CIG, University of Bologna, Bologna, Italy

出处: **Bone Marrow Transplant.** 2019 05;54(5). DOI: 10.1038/s41409-018-0335-x

Ruskin 工作使用情况: Invivo₂ 300, O₂ 浓度: 7%

Abstract

Umbilical Cord Blood (UCB) represents a valid option for patients with hematopoietic malignancies lacking an HLA matched donor. To overcome the limitation of the low stem cell dose of UCB, the intrabone (IB) route has been proposed. We report the results of a prospective study on a poor-prognosis cohort of 23 patients receiving intrabone single UCB transplant (Clinicaltrials.gov NCT00886522). Cumulative incidence of hematological recovery at day 90 was 82 ± 9% (ANC > 0.5 × 10⁹/L) and 70 ± 10% (platelet > 50 × 10⁹/L) and correlated with CD34+ cells in the graft. NRM was 20 ± 9%. No severe aGVHD and only one extensive cGVHD occurred, with fast immune reconstitution. To test the hypothesis that the direct IB injection could affect the expression of stem cells regulatory pathways, CD34+ cells from BM aspirates at day + 10, + 20, + 30, processed in hypoxic conditions mimicking the BM-microenvironment (7%pO₂), were studied for the expression of c-Mpl, Notch1 and CXCR4. We found that the expression of c-Mpl in CD34+ cells at day + 10 significantly correlated with hematological recovery. In conclusion, IB-UCB transplant success is associated with low incidence of GVHD and high-speed platelet recovery; intrabone route may preserve full hematopoietic stemness by direct delivery of UCB stem cells into the hypoxic HSC niche.

Changes of Metabolic Phenotype of Cardiac Progenitor Cells During Differentiation: Neutral Effect of Stimulation of Adenosine Monophosphate-Activated Protein Kinase

Emilie Andre',¹ Aure' lia De Pauw,¹ Roxane Verdoy,¹ Davide Brusa,² Caroline Bouzin,³ Aure' lie Timmermans,⁴ Luc Bertrand,⁴ and Jean-Luc Balligand¹

¹ Pole of Pharmacology and Therapeutics (FATH) and ⁴ Pole of Cardiovascular Research (CARD), Institute of Experimental and Clinical Research (IREC), Universite' Catholique de Louvain (UCLouvain) and Cliniques Universitaires Saint-Luc, Brussels, Belgium.

² Flow Cytometry Platform and ³ I2P Imaging Platform, Institute of Clinical and Experimental Research (IREC), Universite' Catholique de Louvain (UCLouvain), Brussels, Belgium.

出处: *J. Biol. Chem.* 2015 Oct 09;290(41). DOI: 10.1074/jbc.M115.667246

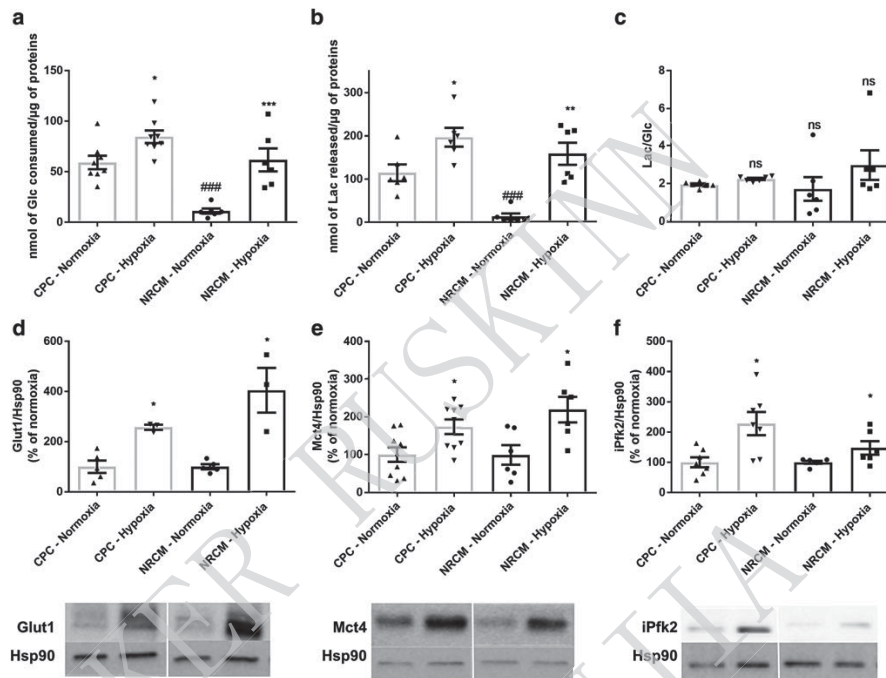
Ruskinn 工作使用情况: Ruskinn Workstation; O₂ 浓度: 1%

Abstract

Cardiac progenitor cells (CPCs) in the adult mammalian heart, as well as exogenous CPCs injected at the border zone of infarcted tissue, display very low differentiation rate into cardiac myocytes and marginal repair capacity in the injured heart. Emerging evidence supports an obligatory metabolic shift from glycolysis to oxidative phosphorylation (OXPHOS) during stem cells differentiation, suggesting that pharmacological modulation of metabolism may improve CPC differentiation and, potentially, healing properties. In this study, we investigated the metabolic transition underlying CPC differentiation toward cardiac myocytes. In addition, we tested whether activators of adenosine monophosphate-activated protein kinase (AMPK), known to promote mitochondrial biogenesis in other cell types would also improve CPC differentiation. Stem cell antigen 1 (Sca1⁺) CPCs were isolated from adult mouse hearts and their phenotype compared with more mature neonatal rat cardiac myocytes (NRCMs). Under normoxia, glucose consumption and lactate release were significantly higher in CPCs than in NRCMs. Both parameters were increased in hypoxia together with increased abundance of Glut1 (glucose transporter), of the monocarboxylic transporter Mct4 (lactate efflux mediator) and of Pfkfb3 (key regulator of glycolytic rate). CPC proliferation was critically dependent on glucose and glutamine availability in the media. Oxygen consumption analysis indicates that, compared with NRCMs, CPCs exhibited lower basal and maximal respirations with lower Tomm20 protein expression and mitochondrial DNA content. This CPC metabolic phenotype profoundly changed upon in vitro differentiation, with a decrease of glucose consumption and lactate release together with increased abundance of Tnnt2, Pgc-1a, Tomm20, and mitochondrial DNA content. Proliferative CPCs express both alpha1 and -2 catalytic subunits of AMPK that is activated by A769662. However,

A769662 or resveratrol (an activator of Pgc-1 α and AMPK) did not promote either mitochondrial biogenesis or CPC maturation during their differentiation. We conclude that although CPC differentiation is accompanied with an increase of mitochondrial oxidative metabolism, this is not potentiated by activation of AMPK in these cells.

Keywords: cardiac progenitors, differentiation, metabolism



Effect of hypoxia on the glycolytic metabolism of CPCs compared with NRCMs. Supernatants of CPCs and of NRCMs were analyzed after 48 h of incubation in normoxia or in hypoxia

(a) Glucose consumption and (b) lactate release were measured and then normalized using protein quantification; (c) lactate/glucose ratios were calculated from (a) and (b). The expression of (d) Glut1, (e) Mct4, and (f) iPfk2 were analyzed by western blotting (normalized to Hsp90) in CPCs and in NRCMs after 72 h of incubation in normoxia and in hypoxia. Within a cell type, the expression of proteins in hypoxia was compared with the expression in normoxic conditions. Representative blots for each immunoblotted protein are shown at the bottom of each bar graph. ANOVA, analysis of variance; CPCs, cardiac progenitor cells; NRCMs, neonatal rat cardiac myocytes; SEM, standard error of the mean

The Histone Demethylase KDM3A, Increased in Human Pancreatic Tumors, Regulates Expression of DCLK1 and Promotes Tumorigenesis in Mice

Prasad Dandawate,¹ Chandrayee Ghosh,¹ Kanagaraj Palaniyandi,¹ Santanu Paul,¹ Sonia Rawal,¹ Rohan Pradhan,² Afreen Asif Ali Sayed,¹ Sonali Choudhury,¹ David Standing,¹ Dharmalingam Subramaniam,¹ Subhash Padhye,^{1,2} Sumedha Gunewardena,³ Sufi M. Thomas,⁴ Moura O'Neil,⁵ Ossama Tawfik,⁵ Danny R. Welch,¹ Roy A. Jensen,⁵ Sally Maliski,⁶ Scott Weir,¹ Tomoo Iwakuma,¹ Shrikant Anant,¹ and Animesh Dhar¹

¹ Department of Cancer Biology, University of Kansas Medical Center, Kansas City, Kansas; ² Interdisciplinary Science and Technology Research Academy, Abeda Inamdar Senior College, Camp, Pune, India; ³ Department of Molecular and Integrative Physiology, University of Kansas Medical Center, Kansas City, Kansas; ⁴ Department of Otolaryngology, University of Kansas Medical Center, Kansas City, Kansas; ⁵ Department of Pathology and Laboratory Medicine, University of Kansas Medical Center, Kansas City, Kansas; and ⁶ School of Nursing, University of Kansas Medical Center, Kansas City, Kansas

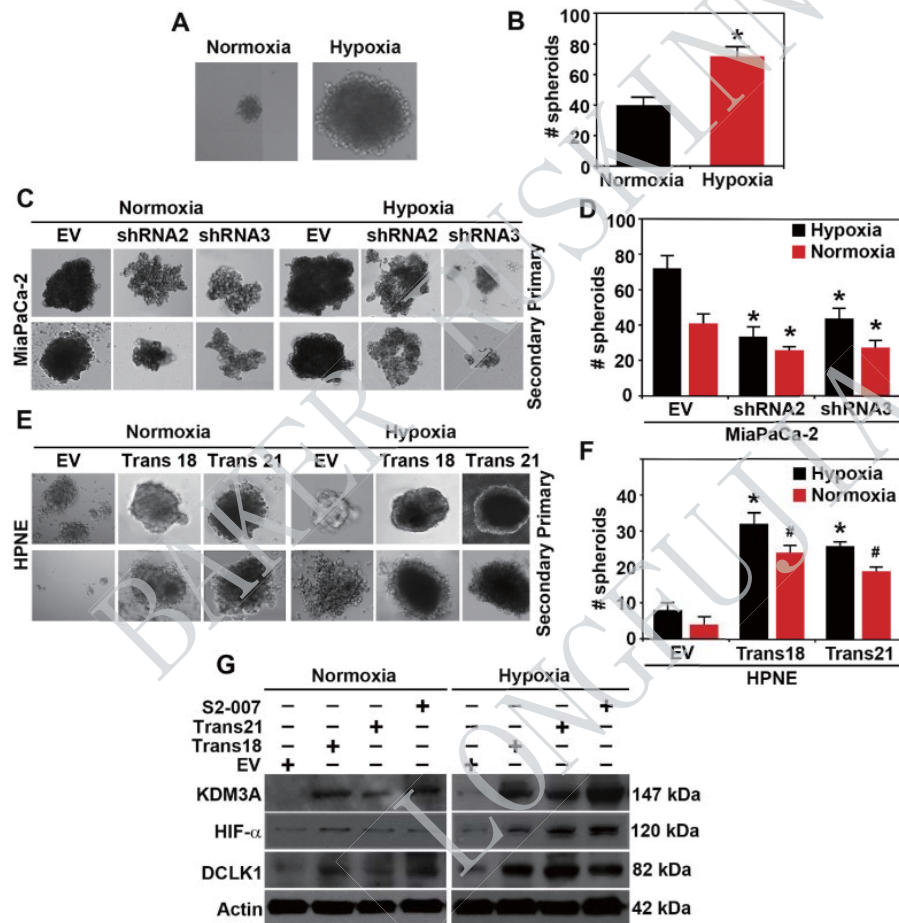
出处: *Gastroenterology* 2019 Dec; 157(6): 1646–1659, DOI: 10.1053/j.gastro.2019.08.018
Ruskinn 工作使用情况: Invivo₂ 400; O₂ 浓度: 0.5- 2%

Background&Aims

The histone lysine demethylase 3A (KDM3A) demethylates H3K⁹me¹ and H3K⁹Me² to increase gene transcription and is upregulated in tumors, including pancreatic tumors. We investigated its activities in pancreatic cancer cell lines and its regulation of the gene encoding doublecortin calmodulin-like kinase 1 (DCLK1), a marker of cancer stem cells. METHODS: We knocked down KDM3A in MiaPaCa-2 and S2-007 pancreatic cancer cell lines and overexpressed KDM3A in HPNE cells (a human pancreatic cell line); we evaluated cell migration, invasion, and spheroid formation under hypoxic and normoxic conditions. Nude mice were given orthotopic injections of S2-007 cells, with or without (control) knockdown of KDM3A, and HPNE cells, with or without (control) overexpression of KDM3A; tumor growth was assessed. We analyzed pancreatic tumor tissues from mice and pancreatic cancer cell lines by immunohistochemistry and immunoblotting. We performed RNA-sequencing analysis of MiaPaCa-2 and S2-007 cells with knockdown of KDM3A and evaluated localization of DCLK1 and KDM3A by immunofluorescence. We analyzed the cancer genome atlas for levels of KDM3A and DCLK1 messenger RNA in human pancreatic ductal adenocarcinoma (PDAC) tissues and association with patient survival time. RESULTS: Levels of KDM3A were increased in human pancreatic tumor tissues and cell lines, compared with adjacent nontumor pancreatic tissues, such as islet and acinar cells. Knockdown of KDM3A in S2-007 cells significantly reduced colony formation, invasion, migration, and spheroid formation, compared with control cells, and slowed growth of orthotopic tumors in mice. We identified KDM3A-binding sites in the DCLK1 promoter; S2-007 cells with knockdown of KDM3A had reduced levels of DCLK1. HPNE cells that overexpressed KDM3A formed foci and spheres in culture and formed tumors and metastases in mice, whereas control HPNE cells did not. Hypoxia induced sphere formation and increased levels of KDM3A in S2-007 cells and in HPNE

cells that overexpressed DCLK1, but not control HPNE cells. Levels of KDM3A and DCLK1 messenger RNA were higher in human PDAC than nontumor pancreatic tissues and correlated with shorter survival times of patients. CONCLUSIONS: We found human PDAC samples and pancreatic cancer cell lines to overexpress KDM3A. KDM3A increases expression of DCLK1, and levels of both proteins are increased in human PDAC samples. Knockdown of KDM3A in pancreatic cancer cell lines reduced their invasive and sphereforming activities in culture and formation of orthotopic tumors in mice. Hypoxia increased expression of KDM3A in pancreatic cancer cells. Strategies to disrupt this pathway might be developed for treatment of pancreatic cancer.

Keywords: Epigenetics; Gene Regulation; Oncogene; Repression.



Hypoxia induces pancosphere formation and increased KDM3A in PDAC and transformed HPNE cells.

(A, B) Pancosphere formation (size and number) is significantly increased during hypoxic conditions ($p < .05$). (C, D) Primary and secondary spheroid formation (size and number) is significantly inhibited by silencing of KDM3A (shRNA2 and shRNA3) in hypoxic and normoxic conditions in MiaPaCa2 PDAC cells ($p < .05$). (E, F) Overexpression of KDM3A in HPNE noncancerous cell (Trans18 and Trans21 transformed clones) showed a significant increase in size and number of spheroids ($p < .05$) in both normoxic and hypoxic conditions in comparison with empty vectors (EV). (G) Western blot analysis of KDM3A, HIF- α and DCLK1 in S2-007, Trans18 and Trans21 HPNE in comparison with EV during normoxic and hypoxic condition demonstrating hypoxia increased the expressions of those proteins.

Multi-dimensional histone methylations for coordinated regulation of gene expression under hypoxia

Seongyeol Lee^{1,†}, Jieon Lee^{2,†}, Sehyun Chae^{3,†}, Yunwon Moon^{1,†}, Ho-Youl Lee¹, Bongju Park¹, Eun Gyeong Yang⁴, Daehee Hwang^{2,3,} and Hyunsung Park^{1,*}*

¹Department of Life Science, University of Seoul, Seoul 02504, Republic of Korea,

²Department of Chemical Engineering, POSTECH, Pohang 37673, Republic of Korea,

³Department of New Biology and Center for Plant Aging Research, Institute of Basic Science, DGIST, Daegu 42988, Republic of Korea and

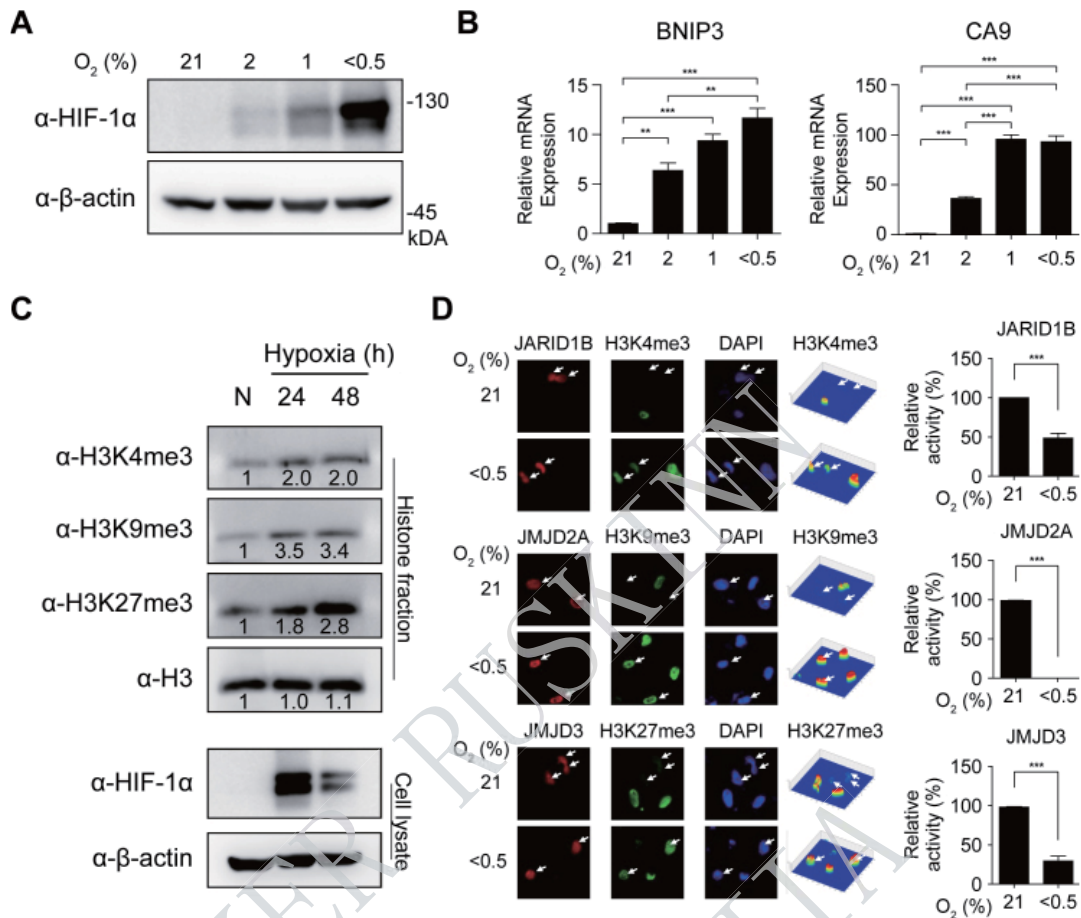
⁴Biomedical Research Institute, Korea Institute of Science and Technology, Seoul 02792, Republic of Korea

出处: *Nucleic Acids Res.* 2017 Nov 16;45(20). DOI: [10.1093/nar/gkx747](https://doi.org/10.1093/nar/gkx747)

Ruskinn 工作使用情况: Invivo₂ 200; O₂ 浓度: 2%, 1%, <0.5%

Abstract

Hypoxia increases both active and repressive histone methylation levels via decreased activity of histone demethylases. However, how such increases coordinately regulate induction or repression of hypoxia-responsive genes is largely unknown. Here, we profiled active and repressive histone tri-methylations (H3K4me₃, H3K9me₃, and H3K27me₃) and analyzed gene expression profiles in human adipocyte-derived stem cells under hypoxia. We identified differentially expressed genes (DEGs) and differentially methylated genes (DMGs) by hypoxia and clustered the DEGs and DMGs into four major groups. We found that each group of DEGs was predominantly associated with alterations in only one type among the three histone tri-methylations. Moreover, the four groups of DEGs were associated with different TFs and localization patterns of their predominant types of H3K4me₃, H3K9me₃ and H3K27me₃. Our results suggest that the association of altered gene expression with prominent singletype histone tri-methylations characterized by different localization patterns and with different sets of TFs contributes to regulation of particular sets of genes, which can serve as a model for coordinated epigenetic regulation of gene expression under hypoxia.



Increased histone tri-methylations through decreased activities of JMJDs in hypoxia.

(A) Western blot analyses of HeLa cells treated with hypoxia (21, 2, 1 and <0.5%) for 24 h using indicated antibodies. β -actin was detected as a loading control. (B) Quantitative RT-PCR for two target genes (BNIP3 and CA9) in hypoxia for 16 hours. The data were normalized using levels of 18s rRNA and shown as mean with standard error of means (SEM). * $p < 0.05$, ** $p < 0.01$ and *** $p < 0.001$ by one-way ANOVA with Turkey's correction. (C) Increased levels of H3K4me3, H3K9me3 and H3K27me3 at 24 and 48 h after decreasing oxygen concentration (<0.5%) in hADSC. The numbers under the bands represent relative band intensities. The amounts of HIF-1 and histone 3 (H3) were also shown. H3 was used as a loading control for quantification of methylated histones in histone fractions (Supplementary Materials and Methods). β -Actin was used as a loading control for quantification of HIF-1, a marker protein of hypoxia, in cell lysates. (D) Hypoxic effects on catalytic activities of histone demethylases. HeLa cells were transfected with Myc-tagged JARID1B (H3K4me3), HA-tagged JMJD2A (H3K9me3) and Myc-tagged JMJD3 (H3K27me3) by using calcium phosphate precipitation method as previously described (37). The transfected cells were treated with hypoxia (O₂% <0.5) for 16 hours and then immunostained using corresponding tag-antibodies (red) and indicated histone antibodies (green). The nuclei were stained with DAPI (blue). Arrows denote cells transfected with indicated histone demethylases. Using a Pseudo-Color 3D confocal fluorescence microscope, fluorescence intensities of H3K4me3, H3K9me3, and H3K27me3 were estimated as shown in contour maps (right columns). For each histone demethylase, catalytic activity was defined as the difference in estimated fluorescence intensities of its corresponding tri-methylated histones between untransfected and transfected cells. The catalytic activity under hypoxia was normalized by that under normoxia. Data represent the average and standard deviations of the estimated activities of histone demethylases from 6 to 38 transfected cells.

其他文章:

- 1.Sortilin inhibition limits secretion-induced progranulin-dependent breast cancer progression and cancer stem cell expansion
期刊: Breast Cancer Res. ; 发表年份: 2019; Ruskinn 工作站使用情况: Sci-tive N
- 2.Hypoxia-induced secretion stimulates breast cancer stem cell regulatory signalling pathways
期刊: Mol Oncol.; 发表年份: 2019; Ruskinn 工作站使用情况: Sci-tive N
- 3.BRCA1 regulates the cancer stem cell fate of breast cancer cells in the context of hypoxia and histone deacetylase inhibitors
期刊: Sci Rep.; 发表年份: 2019; Ruskinn 工作站使用情况: Invivo₂ 400
- 4.Hypoxia induced Sonic Hedgehog signaling regulates cancer stemness, epithelial-to-mesenchymal transition and invasion in cholangiocarcinoma
期刊: experimental cell research 发表年份: 2019; Ruskinn 工作站使用情况: Invivo₂ 300
- 5.Mutations in an Innate Immunity Pathway Are Associated with Poor Overall Survival Outcomes and Hypoxic Signaling in Cancer
期刊: Cell reports 发表年份: 2018; Ruskinn 工作站使用情况: Invivo₂ 400
- 6.Stem cells from human apical papilla decrease neuro-inflammation and stimulate oligodendrocyte progenitor differentiation via activin-A secretion
期刊: Cell. Mol. Life Sci. ; 发表年份: 2018; Ruskinn 工作站使用情况: Invivo₂ 400
- 7.Androgen receptor (AR)/miR-520f-3p/SOX9 signaling is involved in the altering hepatocellularcarcinoma (HCC) cell sensitivity to the Sorafenib therapy under hypoxia via increasing cancerstem cells phenotype.
期刊: Cancer letters; 发表年份: 2018; Ruskinn 工作站使用情况: Ruskinn Workstation
- 8.Up-regulation of miR-210 induced by a hypoxic microenvironment promotes breast cancer stem cells metastasis, proliferation, and self-renewal by targeting E-cadherin
期刊: FASEB J.; 发表年份: 2018; Ruskinn 工作站使用情况: Invivo₂ 400
- 9.Nodal induced by hypoxia exposure contributes to dacarbazine resistance and the maintenance of stemness in melanoma cancer stem- like cells.
期刊: Oncol Rep. ; 发表年份: 2018; Ruskinn 工作站使用情况: Invivo₂ 400
- 10.Targeting the Wnt Pathway and Cancer Stem Cells with Anti-progastrin Humanized Antibodies: A Major Breakthrough for K-RAS-Mutated Colorectal Cancer Treatment.
期刊: Clin Cancer Res.; 发表年份: 2018 Ruskinn; 工作站使用情况: Sci-tive U

Inducing cancer indolence by targeting mitochondrial Complex I is potentiated by blocking acrophage-mediated adaptive responses

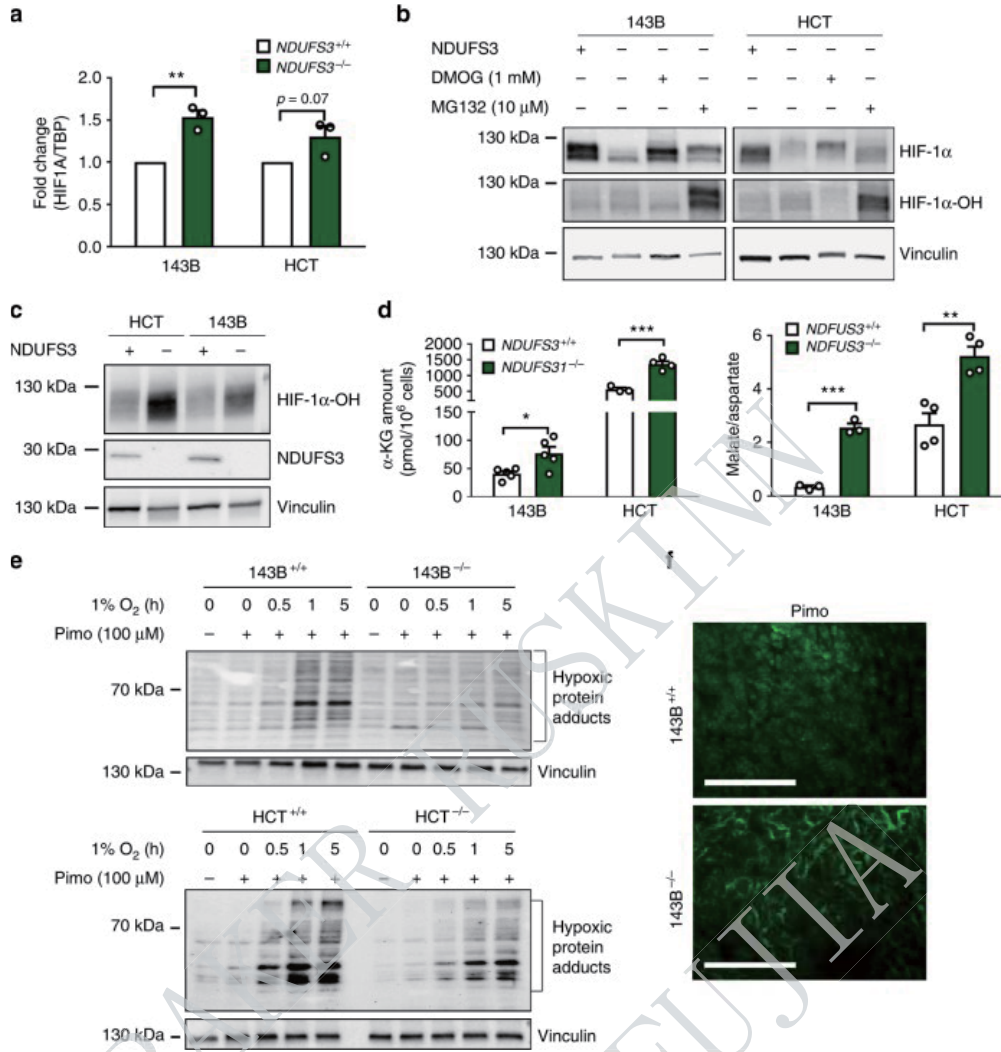
vana Kurelac^{1,2}, Luisa Iommarini³, Renaud Vatrinet^{1,3}, Laura Benedetta Amato¹, Monica De Luise¹, Giulia Leone³, Giulia Girolimetti¹, Nikkitha Umesh Ganesh¹, Victoria Louise Bridgeman², Luigi Ombrato², Marta Columbaro⁴, Moira Ragazzi⁵, Lara Gibellini⁶, Manuela Sollazzo³, Rene Gunther Feichtinger⁷, Silvia Vidali⁷, Maurizio Baldassarre¹, Sarah Foriel^{8,9}, Michele Vidone¹, Andrea Cossarizza⁶, Daniela Grifoni³, Barbara Kofler⁷, Ilaria Malanchi², Anna Maria Porcelli^{3,10} & Giuseppe Gasparre^{1,11}

¹Dipartimento di Scienze Mediche e Chirurgiche, Università di Bologna, Via Massarenti 9, 40138 Bologna, Italy. ²Tumor-Host Interaction Lab, The Francis Crick Institute, 1 Midland Rd, NW1 1AT London, UK. ³Dipartimento di Farmacia e Biotecnologie, Università di Bologna, Via Selmi 3, 40126 Bologna, Italy. ⁴Laboratory of Musculoskeletal Cell Biology, IRCCS Istituto Ortopedico Rizzoli, Via Giulio Cesare Pupilli 1, 40136 Bologna, Italy. ⁵Anatomia Patologica, Azienda Ospedaliera S. Maria Nuova di Reggio Emilia, Viale Risorgimento 80, 42123 Reggio Emilia, Italy. ⁶Dipartimento di Scienze Mediche e Chirurgiche materno infantili e dell'adulto, Università degli Studi di Modena e Reggio Emilia, Via del Pozzo 71, 41124 Modena, Italy. ⁷Research Program for Receptor Biochemistry and Tumor Metabolism, Department of Pediatrics, University Hospital of the Paracelsus Medical University, Muellner Hauptstraße 48, 5020 Salzburg, Austria. ⁸Khondrion BV, Philips van Leydenlaan 15, 6525 EX Nijmegen, The Netherlands. ⁹Radboud Center for Mitochondrial Medicine (RCMM) at the Department of Pediatrics, Radboud University Medical Center, Geert Grooteplein Zuid 10, 6500 HB Nijmegen, The Netherlands. ¹⁰Centro Interdipartimentale di Ricerca Industriale Scienze della Vita e Tecnologie per la Salute, Università di Bologna, Via Tolara di Sopra 41/E, 40064 Ozzano dell'Emilia, Italy. ¹¹Centro di Ricerca Biomedica Applicata (CRBA), Università di Bologna, Via Massarenti 9, 40138 Bologna, Italy

出处: *Nat Commun* 2019 02 22;10(1). DOI: 10.1038/s41467-019-08839-1
Ruskinn 工作情况: Invivo₂ 400; O₂ 浓度: 1%

Abstract

Converting carcinomas in benign oncocytomas has been suggested as a potential anti-cancer strategy. One of the oncocytoma hallmarks is the lack of respiratory complex I (CI). Here we use genetic ablation of this enzyme to induce indolence in two cancer types, and show this is reversed by allowing the stabilization of Hypoxia Inducible Factor-1 alpha (HIF-1 α). We further show that on the long run CI-deficient tumors re-adapt to their inability to respond to hypoxia, concordantly with the persistence of human oncocytomas. We demonstrate that CI-deficient tumors survive and carry out angiogenesis, despite their inability to stabilize HIF-1 α . Such adaptive response is mediated by tumor associated macrophages, whose blockage improves the effect of CI ablation. Additionally, the simultaneous pharmacological inhibition of CI function through metformin and macrophage infiltration through PLX-3397 impairs tumor growth in vivo in a synergistic manner, setting the basis for an efficient combinatorial adjuvant therapy in clinical trials.



CI deficiency induces HIF-1α destabilization via increased PHD activity.

a HIF1A expression level evaluated by qRT-PCR in 143B (n = 3, df = 4, t = 5.2) and HCT (n = 3, df = 4, t = 3.1) cells cultured for 5 h in 1% O₂.

b HIF-1α and HIF-1α-OH western blot analysis in 143B and HCT cells exposed to hypoxia (1% O₂ for 5 h) and treated with DMOG (1 mM for 3 h) or MG132 (10 μM for 3 h). Vinculin was used as loading control.

c HIF-1α-OH and NDUF3 western blot analysis in 143B and HCT cells exposed to hypoxia (1% O₂ for 5 h) and treated with MG132 (10 μM for 3 h). Vinculin was used as loading control.

d α-KG amount and malate/aspartate ratio in 143B [n(α-KG) = 2; n(malate/aspartate) = 3, df(malate/aspartate) = 4, t(malate/aspartate) = 14.3] and HCT [n = 4, df = 6, t(α-KG) = 6.8, t(malate/aspartate) = 4.8] cells measured under basal conditions.

e Protein adducts western blot analysis in cells incubated with pimonidazole (Pimo) (100 μM for 1 h). Vinculin was used as loading control.

f Representative images of pimonidazole (Pimo) immunofluorescent staining in 143B xenografts. Scale bars: 100 μm. In each panel, statistical significance is specified with asterisks (**p < 0.01, ***p < 0.001)

An experimental strategy unveiling exosomal microRNAs 486-5p, 181a-5p and 30d-5p from hypoxic tumour cells as circulating indicators of high-risk rectal cancer

Tonje Bjørnetro,^{a,b} Kathrine Røe Redalen,^{a,c} Sebastian Meltzer,^{a,b} Nirujah Sivarajah Thusyanthan,^a Rampradeep Samiappan,^d Caroline Jegerschöld,^d Karianne Risberg Handeland,^{a,*} and Anne Hansen Reea,^{b,*}

^aDepartment of Oncology, Akershus University Hospital, Lørenskog, Norway

^bInstitute of Clinical Medicine, University of Oslo, Oslo, Norway

^cDepartment of Physics, Norwegian University of Science and Technology, Trondheim, Norway

^dDepartment of Bioscience and Nutrition, Karolinska Institutet, Huddinge, Sweden

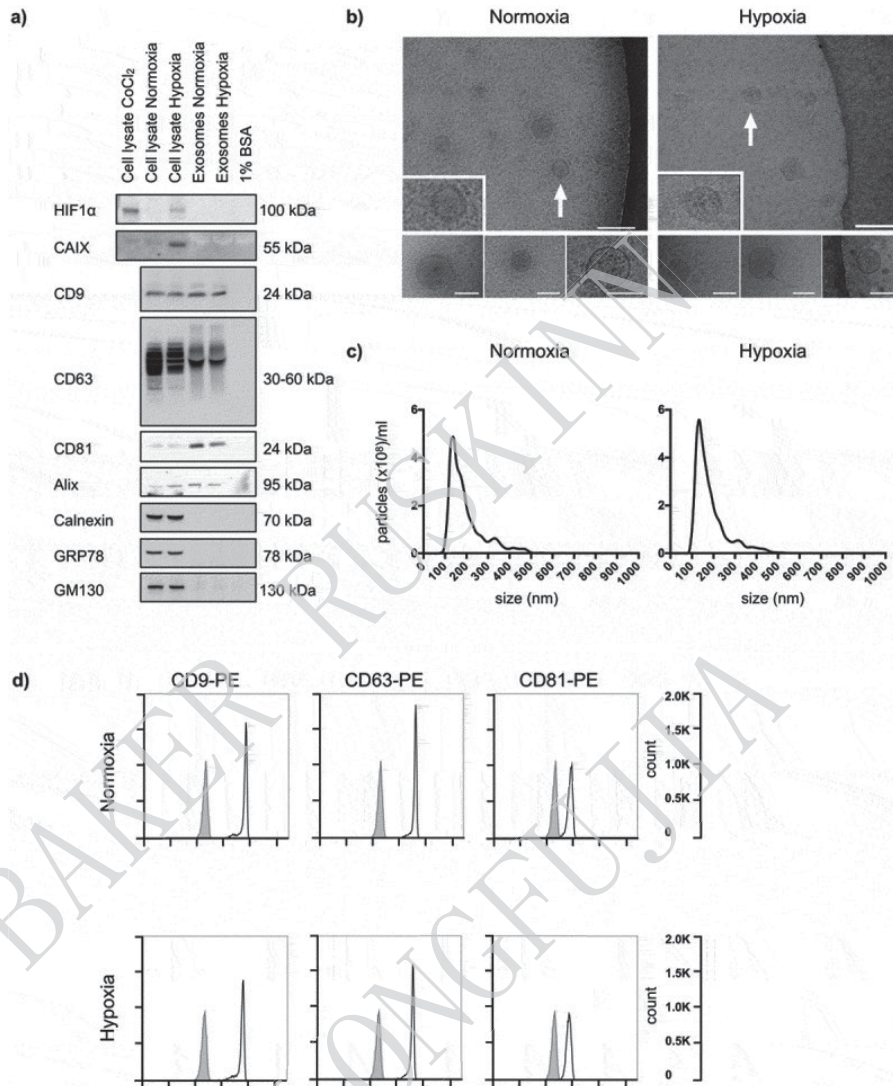
出处: *J Extracell Vesicles* 2019;8(1). DOI: 10.1080/20013073.2019.1567219

Ruskinn 工作使用情况: Invivo₂ 300; O₂ 浓度: 0.2%

Abstract

Tumour hypoxia contributes to poor treatment outcome in locally advanced rectal cancer (LARC) and circulating extracellular vesicles (EVs) as potential biomarkers of tumour hypoxia and adverse prognosis have not been fully explored. We examined EV miRNAs from hypoxic colorectal cancer cell lines as template for relevant miRNAs in LARC patients participating in a prospective biomarker study ([NCT01816607](#)). Five cell lines were cultured under normoxia (21% O₂) or hypoxia (0.2% O₂) for 24 h, and exosomes were isolated by differential ultracentrifugation. Using a commercial kit, exosomes were precipitated from 24 patient plasma samples collected at the time of diagnosis. Exosome size distribution and protein cargo were determined by cryo-electron microscopy, nanoparticle tracking analysis, immunoblotting and flow cytometry. The vesicles harboured strong cell line-specific miRNA profiles with 35 unique miRNAs differentially expressed between hypoxic and normoxic cells. Six of these miRNAs were considered candidate-circulating markers of tumour hypoxia in the patients based on the frequency or magnitude of variance in hypoxic versus normoxic cell line experiments and prevalence in patient plasma. Of these, low plasma levels of exosomal miR-486-5p and miR-181a-5p were associated with organ-invasive primary tumour ($p = 0.029$) and lymph node metastases ($p = 0.024$), respectively, both attributes of adverse LARC prognosis. In line with this, the plasma level of exosomal miR-30d-5p was elevated in patients who experienced metastatic progression ($p = 0.036$). Our strategy confirmed that EVs from colorectal cancer cell lines were exosomes containing the oxygen-sensitive miRNAs 486-5p, 181a-5p and 30d-5p, which were retrieved as circulating markers of high-risk LARC.

Keywords: Colorectal cancer, extracellular vesicles, hypoxia, miRNA, plasma, rectal cancer, exosomes



Characteristics of normoxic and hypoxic exosomes released by HCT116 cells.

Cells were incubated in medium supplemented with BSA under normoxia or hypoxia for 24 h, and whole cell lysates and extracellular vesicles (EVs) isolated by ultracentrifugation were characterised. For each set of experiments, three biological set-ups were done.

(a) Immunoblot images of hypoxia-inducible factor type-1 α (HIF1 α), carbonic anhydrase IX (CAIX), CD9, CD63, CD81, Alix, Calnexin, GRP78 and GM130 expression. CoCl₂ (100 μ M for 4 h in normoxia) was positive control for cellular HIF1 α expression; culture medium containing 1% BSA was negative control for EVs. 10 μ g proteins were loaded in each gel lane. (b) Cryo-electron microscopy images (50,000 \times , 80,000 \times and 100,000 \times magnifications) of EVs. The positions of the zoomed-in panels within the wide-field views are indicated by arrows; scale bars are 100 nm. The lower panels are independent representative high-magnification images; scale bars are 75 nm. (c) NanoSight tracking histograms of EVs. Mean values from three biological set-ups are shown. (d) Flow-cytometry histograms of EVs stained with Phycoerythrin (PE)-labelled exosome-enriched markers (open traces) or isotype control (filled traces).

其他文章:

1.Repression of Human Papillomavirus Oncogene Expression under Hypoxia Is Mediated by PI3K/mTORC2/AKT Signaling.

期刊: MBIO; 发表年份: 2019 ; Ruskinn 工作站使用情况: Invivo₂ 300

2.Nitroimidazole derivative incorporated liposomes for hypoxia-triggered drug delivery and enhanced therapeutic efficacy in patient-derived tumor xenografts.

期刊: Acta Biomater .; 发表年份: 2019; Ruskinn 工作站使用情况: Invivo₂ 400

3.Hypoxia-induced secretion stimulates breast cancer stem cell regulatory signalling pathways.

期刊: Mol Oncol .; 发表年份: 2019; Ruskinn 工作站使用情况: Sci-tive N

4.Lactic Acid Accumulation in the Tumor Microenvironment Suppresses F-FDG Uptake.

期刊: Cancer Res. ; 发表年份: 2018 ; Ruskinn 工作站使用情况: Ruskinn Workstation

5.Pyruvate Dehydrogenase PDH-E1 β Controls Tumor Progression by Altering the Metabolic Status of Cancer Cells.

期刊: Cancer Res. ; 发表年份: 2018 ; Ruskinn 工作站使用情况: Invivo₂

6.HIF-1 α -derived cell-penetrating peptides inhibit ERK-dependent activation of HIF-1 and trigger apoptosis of cancer cells under hypoxia.

期刊: Cell. Mol. Life Sci. ; 发表年份: 2018; Ruskinn 工作站使用情况: Invivo₂ 200

7.SUMOylation regulates LKB1 localization and its oncogenic activity in liver cancer.

期刊: EBioMedicine; 发表年份: 2018; Ruskinn 工作站使用情况: Invivo₂ 400

8.Sortilin inhibition limits secretion-induced progranulin-dependent breast cancer progression and cancer stem cell expansion.

期刊: Breast Cancer Res.; 发表年份: 2018; Ruskinn 工作站使用情况: Sci-tive N

9.Hypoxia-induced mobilization of NHE6 to the plasma membrane triggers endosome hyperacidification and chemoresistance.

期刊: Nat Commun.; 发表年份: 2017; Ruskinn 工作站使用情况: Invivo₂ 400

10.CBF1 is clinically prognostic and serves as a target to block cellular invasion and chemoresistance of EMT-like glioblastoma cells.

期刊: Br. J. Cancer.; 表年份: 2017; Ruskinn 工作站使用情况: Invivo₂ 200

PPAR γ Interaction with UBR5/ATMIN Promotes DNA Repair to Maintain Endothelial Homeostasis.

Caiyun G. Li,¹ Cathal Mahon,^{2,3} Nathaly M. Sweeney,^{1,7} Erik Verschuere,² Vivek Kantamani,¹ Dan Li,¹ Jan K. Hennigs,¹ David P. Marciano,⁴ Isabel Diebold,¹ Ossama Abu-Halawa,¹ Matthew Elliott,¹ Silin Sa,¹ Feng Guo,⁵ Lingli Wang,¹ Aiqin Cao,¹ Christophe Guignabert,¹ Julie Sollier,⁶ Nils P. Nickel,¹ Mark Kaschwich,¹ Karlene A. Cimprich,⁶ and Marlene Rabinovitch^{1,8,}*

¹The Vera Moulton Wall Center for Pulmonary Vascular Disease, Department of Pediatrics and Cardiovascular Institute, Stanford School of Medicine, Stanford, CA 94305, USA

²California Institute for Quantitative Biosciences, Department of Cellular and Molecular Pharmacology, University of California-San Francisco, San Francisco, CA 94158, USA

³Department of Pharmaceutical Chemistry, University of California-San Francisco, San Francisco, CA 94158, USA

⁴Department of Genetics, Stanford School of Medicine, Stanford, CA 94305, USA

⁵Department of Medicine, Stanford School of Medicine, Stanford, CA 94305, USA

⁶Department of Chemical and Systems Biology, Stanford School of Medicine, Stanford, CA 94305, USA

⁷Present address: Department of Pediatrics University of California-San Diego, San Diego, CA 92103, USA

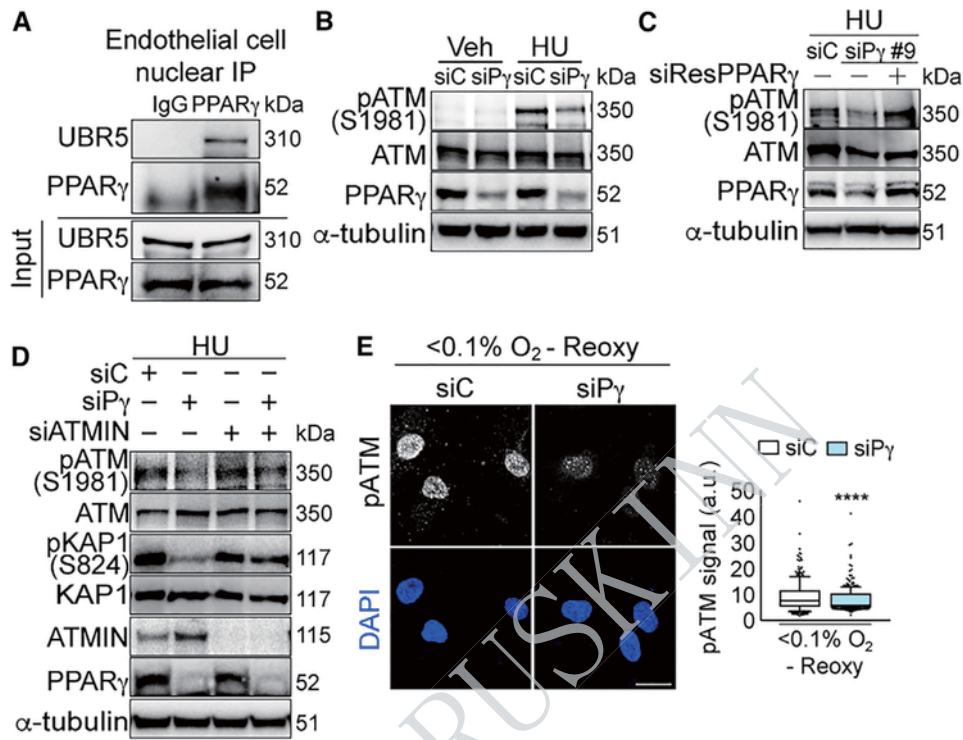
⁸Lead Contact

出处: *Cell rep.* 2019 Jan 29; 26(5): 1333–1343. DOI: 10.1016/j.celrep.2019.01.013

Ruskin 工作使用情况: Invivo₂ 300; O₂ 浓度: <0.1 %

Abstract

Using proteomic approaches, we uncovered a DNA damage response (DDR) function for peroxisome proliferator activated receptor γ (PPAR γ) through its interaction with the DNA damage sensor MRE11-RAD50-NBS1 (MRN) and the E3 ubiquitin ligase UBR5. We show that PPAR γ promotes ATM signaling and is essential for UBR5 activity targeting ATM interactor (ATMIN). PPAR γ depletion increases ATMIN protein independent of transcription and suppresses DDR-induced ATM signaling. Blocking ATMIN in this context restores ATM activation and DNA repair. We illustrate the physiological relevance of PPAR γ DDR functions by using pulmonary arterial hypertension (PAH) as a model that has impaired PPAR γ signaling related to endothelial cell (EC) dysfunction and unresolved DNA damage. In pulmonary arterial ECs (PAECs) from PAH patients, we observed disrupted PPAR γ -UBR5 interaction, heightened ATMIN expression, and DNA lesions. Blocking ATMIN in PAH PAEC restores ATM activation. Thus, impaired PPAR γ DDR functions may explain the genomic instability and loss of endothelial homeostasis in PAH.



PPAR γ -ATMIN Regulation of ATM Signaling Is Conserved in Primary Human Endothelial Cells

(A) Representative immunoblots of endogenous nuclear PPAR γ interaction with UBR5 in primary pulmonary arterial endothelial cells (PAECs) isolated from controls (Table S5).

(B) Representative immunoblots of HU-induced pATM expression with PPAR γ depletion in PAECs.

(C) Representative immunoblots of restoration of HU-induced pATM expression with siRNA (siPPAR γ #9)-resistant PPAR γ overexpression in human umbilical venous ECs (HUVECs).

(D) Representative immunoblots of HU-induced pATM and pKAP1 with PPAR γ or/and ATMIN depletions in PAECs.

(E) Confocal microscopy of PAECs shows effects of PPAR γ depletion on pATM foci with hypoxia (<0.1% O $_2$, 24 h) and reoxygenation (10 min). The line in the box of the box and whisker plots marks the median and whiskers correspond to the 10th to 90th percentiles. Unpaired Student t test was used. *****p* < 0.0001. Scale bars, 20 μ m. siC, siControl; siP γ , siPPAR γ .

Modeling of LMNA-Related Dilated Cardiomyopathy Using Human Induced Pluripotent Stem Cells

Disheet Shah^{1,*,\dagger}, *Laura Virtanen*^{2,3,\dagger}, *Chandra Prajapati*¹, *Mostafa Kiamehr*¹, *Josef Gullmets*², *Gun West*², *Joose Kreutzer*⁴, *Mari Pekkanen-Mattila*¹, *Tiina Heliö*⁵, *Pasi Kallio*⁴, *Pekka Taimen*^{2,6,\ddagger} and *Katriina Aalto-Setälä*^{1,7,8,\ddagger}

¹ BioMediTech, Faculty of Medicine and Health Technology; Tampere University, 33520 Tampere, Finland;

² Institute of Biomedicine, University of Turku, 20520 Turku, Finland;

³ Turku Doctoral Programme of Molecular Medicine, University of Turku, 20520 Turku, Finland ⁴ Micro-and Nanosystems Research Group, BioMediTech, Faculty of Medicine and Health Technology, Tampere University, 33140 Tampere, Finland;

⁵ Helsinki University Hospital, 00029 Helsinki, Finland;

⁶ Department of Pathology, Turku University Hospital, 20520 Turku, Finland;

⁷ Medical School, University of Tampere, 33520 Tampere, Finland;

⁸Heart Hospital, Tampere University Hospital, 33520 Tampere, Finland

* Correspondence: Disheet.shah@tuni.fi; † These authors contributed equally. ‡ Shared last author.

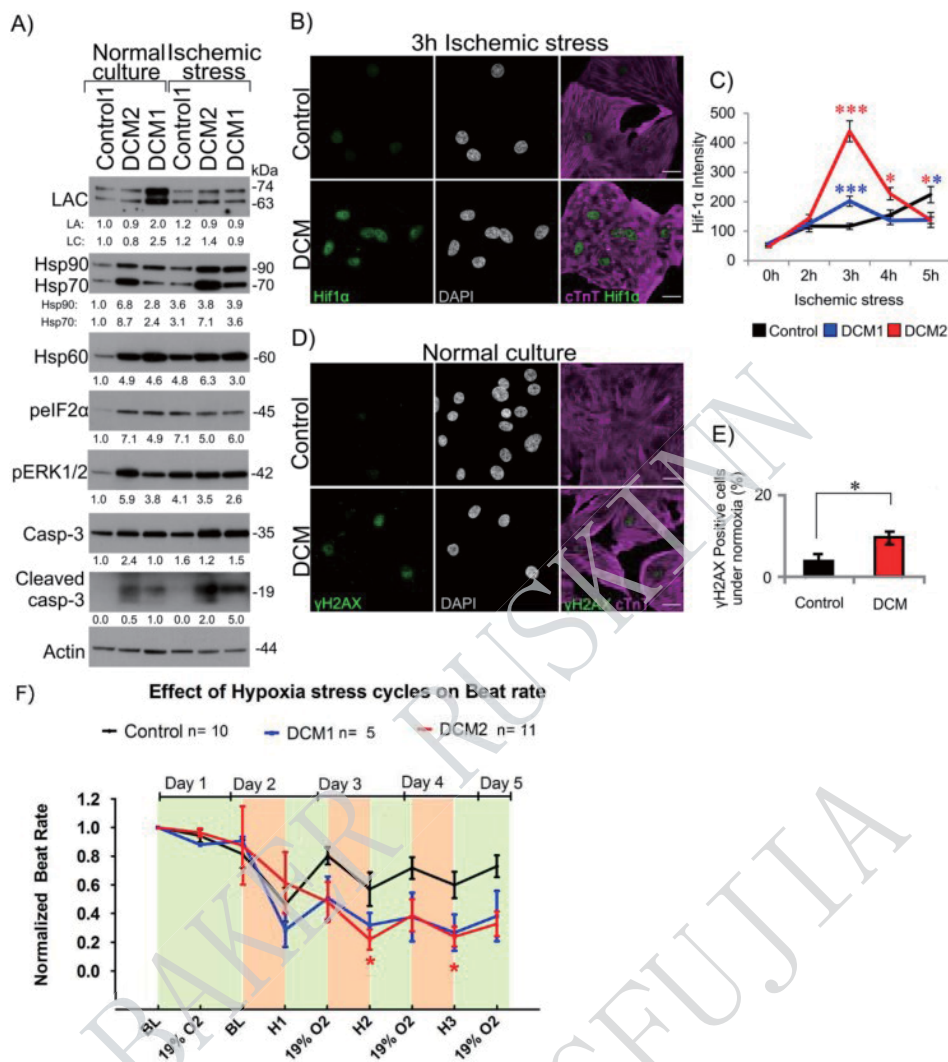
出处: **Cells** 2019 Jun; 8(6): 594. DOI: 10.3390/cells8060594

Ruskinn 工作使用情况: Invivo₂ 400; O₂ 浓度: 1%, 19%

Abstract

Dilated cardiomyopathy (DCM) is one of the leading causes of heart failure and heart transplantation. A portion of familial DCM is due to mutations in the LMNA gene encoding the nuclear lamina proteins lamin A and C and without adequate treatment these patients have a poor prognosis. To get better insights into pathobiology behind this disease, we focused on modeling LMNA-related DCM using human induced pluripotent stem cell derived cardiomyocytes (hiPSC-CM). Primary skin fibroblasts from DCM patients carrying the most prevalent Finnish founder mutation (p.S143P) in LMNA were reprogrammed into hiPSCs and further differentiated into cardiomyocytes (CMs). The cellular structure, functionality as well as gene and protein expression were assessed in detail. While mutant hiPSC-CMs presented virtually normal sarcomere structure under normoxia, dramatic sarcomere damage and an increased sensitivity to cellular stress was observed after hypoxia. A detailed electrophysiological evaluation revealed bradyarrhythmia and increased occurrence of arrhythmias in mutant hiPSC-CMs on β -adrenergic stimulation. Mutant hiPSC-CMs also showed increased sensitivity to hypoxia on microelectrode array and altered Ca²⁺ dynamics. Taken together, p.S143P hiPSC-CM model mimics hallmarks of LMNA-related DCM and provides a useful tool to study the underlying cellular mechanisms of accelerated cardiac degeneration in this disease.

Keywords: dilated cardiomyopathy; LMNA; Lamin A/C; induced pluripotent stem cell; hypoxia; microelectrode array and calcium imaging



DCM hiPSC-CMs show increased elevated cellular stress

(A) Western blot analysis of laminin A/C, phospho-eIF2 α (peIF2 α), Hsp90, Hsp70, Hsp60, phospho-ERK1/2 (pERK1/2) and cleaved caspase-3 under normal culture conditions and after exposure to ischemic stress for 3 h. Actin was used as a loading control. The average numerical values of signal intensities relative to the loading control (actin) are shown below each blot. n = 2 individual experiments. Control2 hiPSC-CMs were not qualified for analysis due to lower differentiation efficiency compared to other lines. (B) Confocal microscopy analysis of Hif-1 α intensity. Control1, DCM1 and DCM2 hiPSC-CMs were cultured either in normal culture conditions or exposed to ischemic stress for 2 h, 3 h, 4 h and 5 h, fixed and stained for Hif-1 α , cardiac marker cTnT and DNA (DAPI). A 3 h time point is shown. Scale bar 20 μ m. (C) The fluorescence intensities of Hif-1 α were determined from all the confocal sections of >15 randomly selected cells at different time points and the average normalized signals were plotted. (D) Control1 and DCM2 hiPSC-CMs were cultured under normal culture conditions, fixed and stained for γ H2AX, cTnT and DNA (DAPI). (E) γ H2AX positive cells from control1 and DCM2 were counted and plotted (n = 500). (F) Effect of three repeated 3 h cycles of hypoxia (1% O₂) shown as H1, H2 and H3 and overnight re-oxygenation (19% O₂) on beat rate of hiPSC-CMs recorded on MEA. Control data presented in F is combined from Control1 and 2. Data is expressed as mean \pm s.e.m., (*) p < 0.05, (**) p < 0.01 and (***) p < 0.001.

其他文章:

1.Pluripotent HSCs Augment α -Adrenergic Receptor Mediated Contraction of Pulmonary Artery and Contribute to the Pathogenesis of Pulmonary Hypertension

期刊: Am. J. Physiol. Lung Cell Mol. Physiol. ; 发表年份: 2020; Ruskinn 工作站使用情况: Invivo₂ 300

2.Redox regulation of nitrosyl-hemoglobin in human erythrocytes

期刊: Redox Biology; 发表年份: 2019; Ruskinn 工作站使用情况: Invivo₂ 400

3.Nogo-B Receptor Directs Mitochondria-Associated Membranes to Regulate Vacuolar Smooth Muscle Cell Proliferation

期刊: Int J Mol Sci ; 发表年份: 2019; Ruskinn 工作站使用情况: Invivo₂

4.The neuronal oxygen sensing pathway controls postnatal vascularization of the murine brain

期刊: FASEB J; 发表年份: 2019; Ruskinn 工作站使用情况: Invivo₂

5.Multinucleated polyploid cardiomyocytes undergo an enhanced adaptability to hypoxia via mitophagy

期刊: J. Mol. Cell. Cardiol. ; 发表年份: 2019; Ruskinn 工作站使用情况: Invivo₂ 1000

6.Re-enforcing hypoxia-induced polyploid cardiomyocytes enter cytokinesis through activation of β -catenin

期刊: Sci Rep 发表年份: 2019; Ruskinn 工作站使用情况: Invivo₂ 1000

7.Propofol improved hypoxia-impaired integrity of blood-brain barrier via modulating the expression and phosphorylation of zonula occludens-1

期刊: CNS Neurosci Ther ; 发表年份: 2019; Ruskinn 工作站使用情况: Ruskinn Workstation

8.Changes of Metabolic Phenotype of Cardiac Progenitor Cells During Differentiation: Neutral Effect of Stimulation of AMP-Activated Protein Kinase

期刊: Stem Cells Dev. 发表年份: 2019; Ruskinn 工作站使用情况: Ruskinn Workstation

Angiopoietin-Like Protein 4 (ANGPTL4) Induces Retinal Pigment Epithelial Barrier Breakdown by Activating Signal Transducer and Activator of Transcription 3 (STAT3): Evidence from ARPE-19 Cells Under Hypoxic Condition and Diabetic Rats

Xinyue Yang, Jinfeng Cao, Yang Du, Qiaoyun Gong, Yan Cheng, Guanfang Su

Department of Ophthalmology, The Second Hospital of Jilin University, Changchun, Jilin, China

出处: *Med Sci Monit* 2019; 25:6742-6754. DOI: 10.12659/MSM.915748

Ruskinn 工作使用情况: Ruskinn Workstation; O₂ 浓度: 1 %

Abstract:

Background

Diabetic retinopathy is a primary contributor of visual impairment in adult diabetes mellitus patients. Diabetic retinopathy causes breakdown of blood retinal barrier (BRB), and leads to diabetic macular edema. Previous studies have demonstrated angiopoietin-like protein 4 (ANGPTL4) as an effective diabetic retinopathy therapeutic target, however, its role in maintaining the outer BRB in diabetic retinopathy has yet not elucidated.

Material/Methods

We established an in vivo diabetic rat model with the use of streptozotocin injections and cultured ARPE-19 cells under (hypoxia, 1%) condition. We first investigated the expression of hypoxia induced factor-1 α (HIF-1 α) and ANGPTL4 in vivo and subsequently studied the transcriptional regulation and underlying molecular mechanisms in ARPE-19 cells under oxygen-deprived situations.

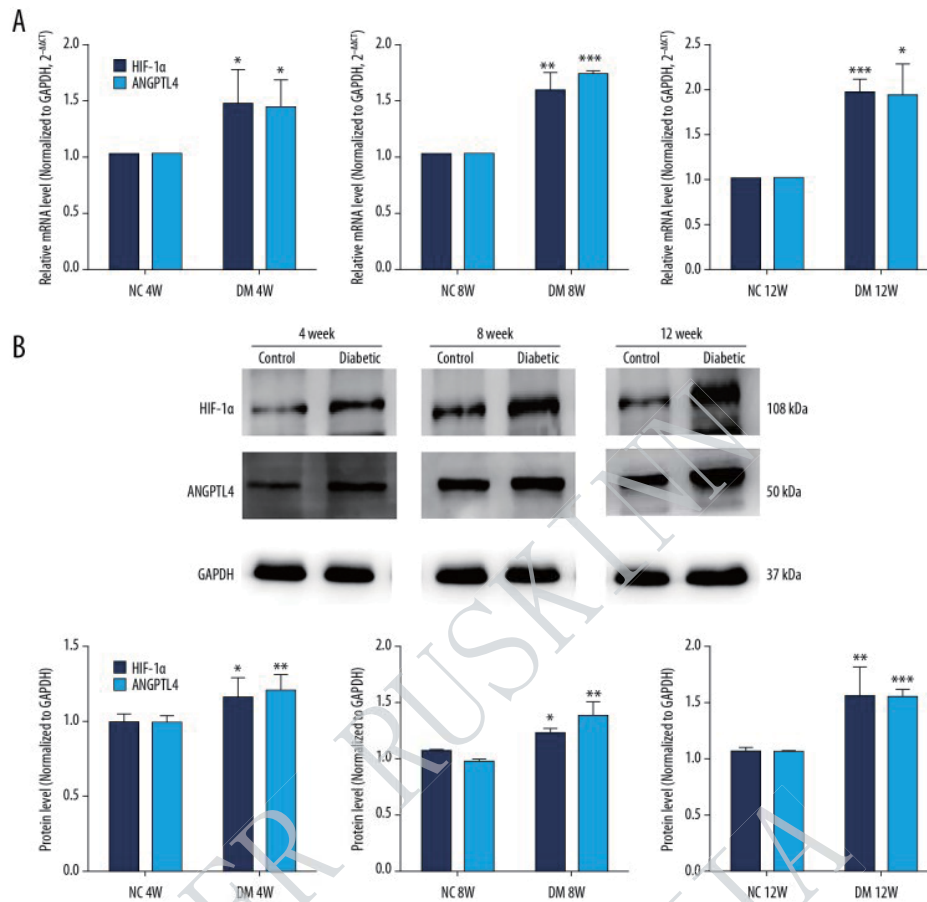
Results

The expression of HIF-1 α and ANGPTL4 was increased with diabetic retinopathy progression both in vivo and in vitro. Depletion of HIF-1 α by siRNA inhibited hypoxia-induced ANGPTL4 expression. Repressing the HIF-1 α /ANGPTL4 signaling effectively alleviated the migration and cellular permeability induced by hypoxia in ARPE-19 cells. Depletion of ANGPTL4 by siRNA significantly alleviated signal transducer and activator of transcription 3 (STAT3) activity in vitro, thereby attenuating the decrease of tight junction proteins occludin and zona occludens-1 (ZO-1) under hypoxia in ARPE-19 cells.

Conclusions

Our results suggest that ANGPTL4 partially modulates STAT3 and could serve as an effective diabetic retinopathy treatment strategy.

Keywords: Angiopoietins, Diabetic Retinopathy, STAT3 Transcription Factor



HIF-1α and ANGPTL4 expressions are upregulated in parallel during the progression of diabetic retinopathy in the retinas of diabetes mellitus rats.

(A) HIF-1α and ANGPTL4 mRNA levels were quantified via RT-qPCR. Subsequent results were calculated based on the delta-delta Ct method. GAPDH served as our reference gene.

(B) HIF-1α and ANGPTL4 protein levels were quantified via western blot analysis with densitometric analysis was based on endogenous GAPDH expression. * $p < 0.05$; ** $p < 0.01$; *** $p < 0.001$, in contrast to the negative control. HIF-1α – hypoxia induced factor-1α; ANGPTL4 – angiopoietin-like protein 4; RT-qPCR – real-time quantitative polymerase chain reaction.

Data shown is depicted as the mean ± standard deviation.

Hypoxic stabilization of mRNA is HIF independent but requires mtROS

Grey W Fortenbery,¹ Brinda Sarathy,² Kristen R Carraway,² and Kyle D Mansfield²

¹Brody School of Medicine, East Carolina University, Greenville, NC 27834 USA

²Biochemistry and Molecular Biology, Brody School of Medicine, East Carolina University, Greenville, NC 27834 USA

出处: *Cell Mol Biol Lett.* 2018; 23: 48. DOI: 10.1186/s11658-018-0112-2

Ruskinn 工作使用情况: Invivo₂ 400 ; O₂ 浓度: 1 %

Abstract

Background

Tissue ischemia can arise in response to numerous physiologic and pathologic conditions. The cellular response to decreased perfusion, most notably a decrease in glucose and oxygen, is important for cellular survival. In response to oxygen deprivation or hypoxia, one of the key response elements is hypoxia inducible factor (HIF) and a key protein induced by hypoxia is vascular endothelial growth factor (VEGF). Under hypoxia, we and others have reported an increase in the half-life of VEGF and other hypoxia related mRNAs including MYC and CYR61; however, the mediator of this response has yet to be identified. For this study, we sought to determine if HIF-mediated transcriptional activity is involved in the mRNA stabilization induced by hypoxia.

Methods

HEK293T or C6 cells were cultured in either normoxic or hypoxic (1% oxygen) conditions in the presence of 1 g/L glucose for all experiments. Pharmacological treatments were used to mimic hypoxia (desferrioxamine, dimethyloxaloglutamate, CoCl₂), inhibit mitochondrial respiration (rotenone, myxothiazol), scavenge reactive oxygen species (ROS; ebselen), or generate mitochondrial ROS (antimycin A). siRNAs were used to knock down components of the HIF transcriptional apparatus. mRNA half-life was determined via actinomycin D decay and real time PCR and western blotting was used to determine mRNA and protein levels respectively.

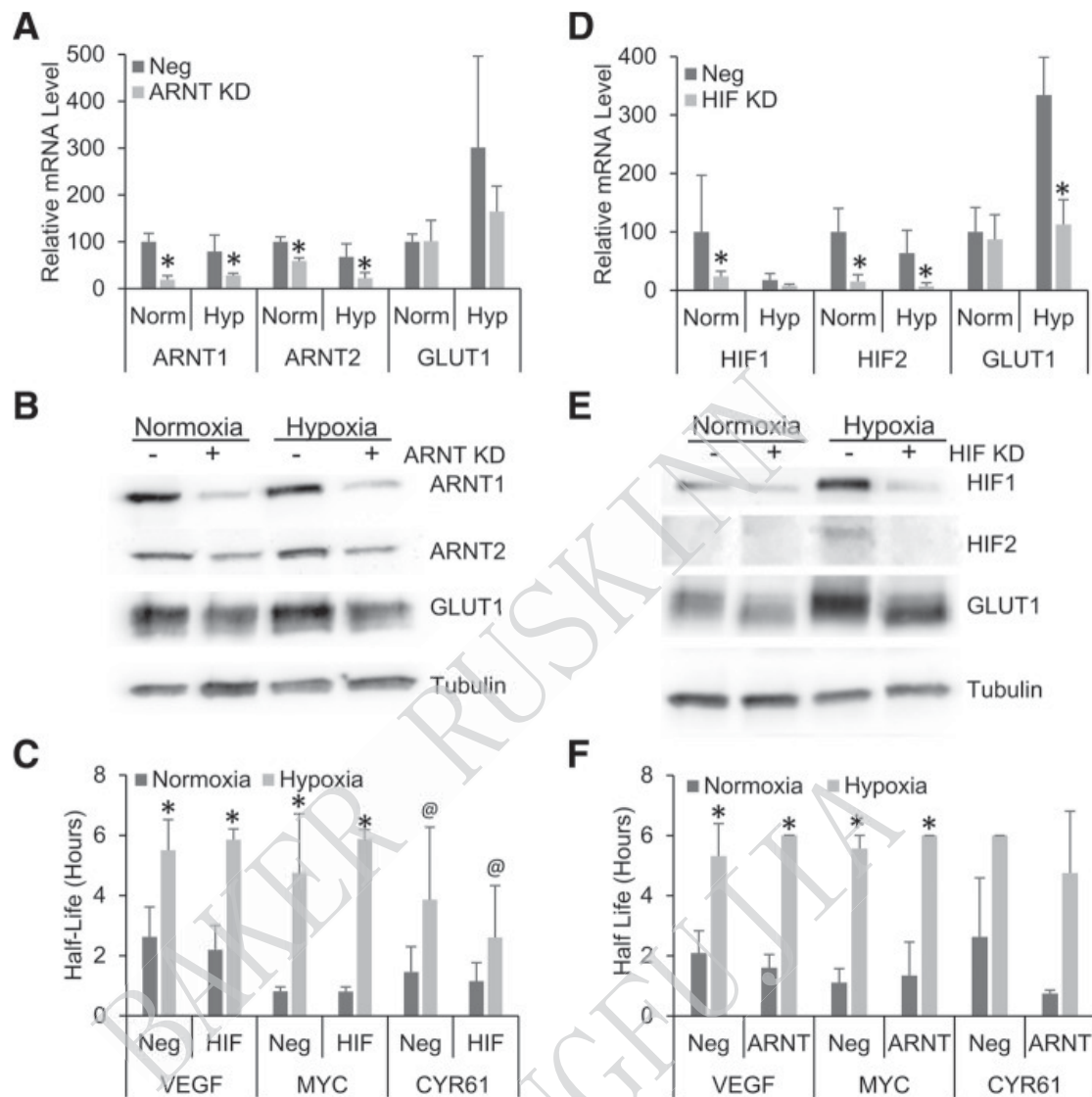
Results

Treatment of HEK293T or C6 cells with hypoxic mimetics, desferrioxamine, dimethyloxaloglutamate, or CoCl₂ showed similar induction of HIF compared to hypoxia treatment, however, in contrast to hypoxia, the mimetics caused no significant increase in VEGF, MYC or CYR61 mRNA half-life. Knockdown of HIF- α or ARNT via siRNA also had no effect on hypoxic mRNA stabilization. Interestingly, treatment of HEK293T cells with the mitochondrial inhibitors rotenone and myxothiazol, or the glutathione peroxidase mimetic ebselen did prevent the hypoxic stabilization of VEGF, MYC, and CYR61, suggesting a role for mtROS in the process. Additionally, treatment with antimycin A, which has been shown to generate mtROS, was able to drive the normoxic stabilization of these mRNAs.

Conclusion

Overall these data suggest that hypoxic mRNA stabilization is independent of HIF transcriptional activity but requires mtROS.

Keywords: Hypoxia, Hypoglycemia, HIF, Mitochondrial reactive oxygen species, mRNA stability



Hypoxic mRNA stability does not require HIF transcriptional activity

HEK293T cells were simultaneously transfected with siRNAs targeting ARNT1 and 2 (ARNT KD), HIF-1 α and 2 α (HIF KD) or negative control siRNA (Neg) for 48 h before being exposed to 24 h of Normoxia or Hypoxia (1% O₂) in the presence of 1 g/L glucose. Cells were treated with actinomycin D for 0, 1 or 2 h. RT-PCR (a, d) and western blotting (b, e) of 0 h time point were used to assess effectiveness of knockdown. c, f mRNA levels of VEGF, MYC and CYR61 were determined via qPCR, normalized to GAPDH and 0 h time point and half-lives determined. Data represents average of N = 3 \pm SD for each condition. * $p \leq 0.05$; @ $p \leq 0.1$ from respective control

Hif1 α is required for osteoclast activation and bone loss in male osteoporosis

Toshimi Tando^{a,1}, *Yuiko Sato*^{a,b,1}, *Kana Miyamoto*^{a,1}, *Mayu Morita*^{c,1}, *Tami Kobayashi*^a, *Atsushi Funayama*^a, *Arihiko Kanaji*^a, *Wu Hao*^a, *Ryuichi Watanabe*^a, *Takatsugu Oike*^a, *Masaya Nakamura*^a, *Morio Matsumoto*^a, *Yoshiaki Toyama*^a, *Takeshi Miyamoto*^{a,*}

^a Department of Orthopedic Surgery, 35 Shinano-machi, Shinjuku-ku, Tokyo 160-8582, Japan

^b Department of Musculoskeletal Reconstruction and Regeneration Surgery, 35 Shinano-machi, Shinjuku-ku, Tokyo 160-8582, Japan

^c Department of Dentistry and Oral Surgery, Keio University School of Medicine, 35 Shinano-machi, Shinjuku-ku, Tokyo 160-8582, Japan

出处: **Biochem. Biophys. Res. Commun.**, 2016 Feb 5;470(2):391-396. DOI: 10.1016/j.bbrc

Ruskinn 工作使用情况: Invivo₂ 400; O₂ 浓度: 1%, 5%

Abstract

The number of osteoporosis patients is increasing not only in women but in men. Male osteoporosis occurs due to aging or androgen depletion therapies, leading to fractures. However, molecular mechanisms underlying male osteoporosis remain unidentified. Here, we show that hypoxia inducible factor 1 alpha (Hif1 α) is required for development of testosterone deficiency-induced male osteoporosis. We found that in mice Hif1 α protein accumulates in osteoclasts following orchidectomy (ORX) in vivo. In vitro, Hif1 α protein accumulated in osteoclasts cultured in hypoxic conditions, but Hif1 α protein rather than mRNA levels were suppressed by testosterone treatment, even in hypoxia. Administration of a Hif1 α inhibitor to ORX mice abrogated testosterone deficiency-induced osteoclast activation and bone loss but did not alter osteoclast activities or bone phenotypes in sham-operated, testosterone-sufficient animals. We conclude that Hif1 α protein accumulation due to testosterone-deficiency promotes development of male osteoporosis. Thus Hif1 α protein could be targeted to inhibit pathologically-activated osteoclasts under testosterone-deficient conditions to treat male osteoporosis patients.

The Vitamin D Analogue ED71 but Not 1,25(OH)2D3 Targets HIF1 α Protein in Osteoclasts

Yuiko Sato^{1,2}, Yoshiteru Miyauchi¹, Shigeyuki Yoshida³, Mayu Morita³, Tami Kobayashi^{1,4}, Hiroya Kanagawa¹, Eri Katsuyama¹, Atsuhiko Fujie¹, Wu Hao¹, Toshimi Tando¹, Ryuichi Watanabe¹, Kana Miyamoto¹, Hideo Morioka¹, Morio Matsumoto¹, Yoshiaki Toyama¹, Takeshi Miyamoto^{1,4*}

¹ Department of Orthopedic Surgery, Keio University School of Medicine, Shinjuku-ku, Tokyo, Japan,

² Department of Musculoskeletal Reconstruction and Regeneration Surgery, Keio University School of Medicine, Shinjuku-ku, Tokyo, Japan,

³ Department of Dentistry and Oral Surgery, Keio University School of Medicine, Shinjuku-ku, Tokyo, Japan, ⁴Department of Integrated Bone Metabolism and Immunology, Keio University School of Medicine, Shinjuku-ku, Tokyo, Japan

出处: PLoS ONE, 2014, 9(11):e111845. DOI:org/10.1371/journal.pone.0111845

Ruskinn 工作使用情况: Invivo₂; O₂浓度: 5%

Abstract

Although both an active form of the vitamin D metabolite, 1,25(OH)2D3, and the vitamin D analogue, ED71 have been used to treat osteoporosis, anti-bone resorbing activity is reportedly seen only in ED71- but not in 1,25(OH)2D3 -treated patients. In addition, how ED71 inhibits osteoclast activity in patients has not been fully characterized. Recently, HIF1 α expression in osteoclasts was demonstrated to be required for development of post-menopausal osteoporosis. Here we show that ED71 but not 1,25(OH)2D3, suppress HIF1 α protein expression in osteoclasts *in vitro*. We found that 1,25(OH)2D3 or ED71 function in osteoclasts requires the vitamin D receptor (VDR). ED71 was significantly less effective in inhibiting M-CSF and RANKL-stimulated osteoclastogenesis than was 1,25(OH)2D3 *in vitro*. Downregulation of c-Fos protein and induction of *Ifn β* mRNA in osteoclasts, both of which reportedly block osteoclastogenesis induced by 1,25(OH)2D3 *in vitro*, were both significantly higher following treatment with 1,25(OH)2D3 than with ED71. Thus, suppression of HIF1 α protein activity in osteoclasts *in vitro*, which is more efficiently achieved by ED71 rather than by 1,25(OH)2D3, could be a reliable read-out in either developing or screening reagents targeting osteoporosis.

The organic solute transporters alpha and beta are induced by hypoxia in human hepatocytes

Carlos A. Schaffner*; Jessica Mwinyi*, Zhibo Gai*, Wolfgang E. Thasler†, Jyrki J. Eloranta and Gerd A. Kullak-Ublick*

*Department of Clinical Pharmacology and Toxicology, University Hospital Zurich, 8091 Zurich, Switzerland † Department of Surgery, Klinikum Grosshadern, 81377 Munich, Germany

出处: *Liver Int.* 2015 Apr; 35(4): 1152–1161. DOI: 10.1111/liv.12558

Ruskinn 工作使用情况: Invivo₂ 400; O₂ 浓度: 0.2%

Abstract

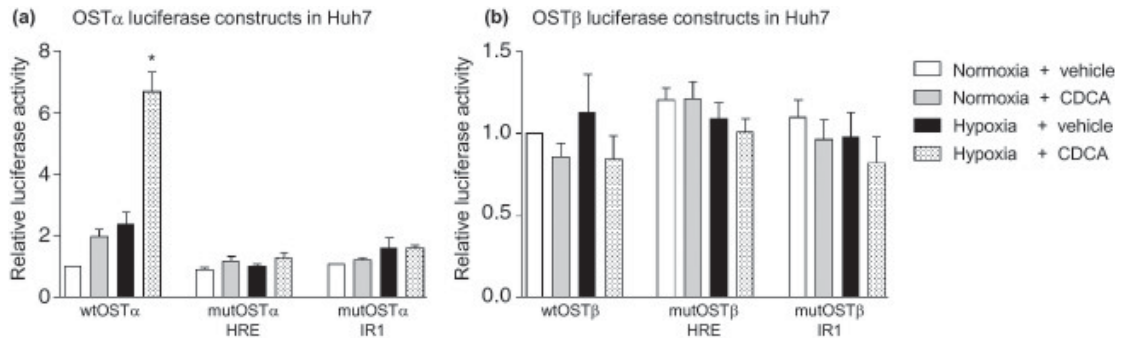
Background&Aims: OATP1B1 is a heterodimeric transporter located at the basolateral membrane of intestinal epithelial cells and hepatocytes. Liver injury caused by ischaemia-reperfusion, cancer, inflammation or cholestasis can induce a state of hypoxia in hepatocytes. Here, we studied the effect of hypoxia on the expression of OATP1B1-OATP1B2.

Methods: OATP1B1-OATP1B2 expression was measured in Huh7 cells and primary human hepatocytes (PHH) exposed to chenodeoxycholic acid (CDCA), hypoxia or both. OATP1B1-OATP1B2 promoter activity was analysed in luciferase reporter gene assays. Binding of hypoxia-inducible factor-1 alpha (HIF-1 α) to the OATP1B1-OATP1B2 gene promoters was studied in electrophoretic mobility shift assays (EMSA).

Results: Expression of OATP1B1 and OATP1B2 increased in PHH under conditions of hypoxia. Exposure of Huh7 cells or PHH to CDCA (50 μ M) enhanced the effect of hypoxia on OATP1B1 mRNA levels. In luciferase assays and EMSA, the inducing effect of low oxygen could be assigned to HIF-1 α , which binds to hypoxia responsive elements (HRE) in the OATP1B1 and OATP1B2 gene promoters. Site-directed mutagenesis of either the predicted HRE or the bile acid responsive FXR binding site abolished inducibility of the OATP1B1 promoter, indicating that both elements need to be intact for induction by hypoxia and CDCA. In a rat model of chronic renal failure, the known increase in hepatic OATP1B1 expression was associated with an increase in HIF-1 α protein levels.

Conclusion: OATP1B1-OATP1B2 expression is induced by hypoxia. FXR and HIF-1 α bind in close proximity to the OATP1B1 gene promoter and produce synergistic effects on OATP1B1 expression.

Keywords: organic anion transport, bile acid transport, nuclear receptor, ligand, gene regulation, chronic renal failure, nephrectomy, rat liver



Hypoxia induces luciferase activity in promoter constructs of OST α , an effect that is dependent on the newly identified hypoxia responsive element

Dual luciferase assays with OST α and OST β promoter constructs transfected into Huh7 cells are represented as relative luciferase activity, normalized to the pcDNA3.1 empty vector backbone. Plasmids containing either the wild-type (wt) promoter or promoters with HRE or IR1 in mutated form (mut) were transfected into cells that were treated for 18 h with 50 μ M CDCA or DMSO and exposed to either normoxia or hypoxia.

(a) A significant increase (* $P < 0.05$) in promoter activity of wt OST α was seen in cells treated with hypoxia and CDCA together. A non-significant trend was observed for single treatments. The inducing effects were markedly reduced when either the HRE or the IR1 were mutated.

(b) Luciferase activity of the OST β promoter construct was not significantly changed by any of the treatment conditions applied. Mutation of either the HRE or IR1 site did not significantly affect the basal activity.

Systemic inactivation of hypoxia-inducible factor prolyl 4-hydroxylase 2 in mice protects from alcohol-induced fatty liver disease

Anna Laitakari,^a Teemu Ollonen,^a Thomas Kietzmann,^b Gail Walkinshaw,^c Daniela Mennerich,^b Valerio Izzi,^a Kirsi-Maria Haapasaari,^d Johanna Myllyharju,^a Raisa Serpi,^a Elitsa Y. Dimova,^a and Peppi Koivunen^a, □

^a Biocenter Oulu, Faculty of Biochemistry and Molecular Medicine, Oulu Center for Cell-Matrix Research, University of Oulu, Oulu, Finland

^b Faculty of Biochemistry and Molecular Medicine, University of Oulu, Oulu, Finland

^c FibroGen Inc., San Francisco, CA, USA

^d Department of Pathology, Medical Research Center Oulu, Oulu University Hospital and University of Oulu, Oulu, Finland

出处: *Redox Biol.* 2019 Apr; 22: 101145. DOI: 10.1016/j.redox.2019.101145

Ruskinn 工作使用情况: Invivo2 400; O₂ 浓度: 1%

Abstract

Alcoholic fatty liver disease (AFLD) is a growing health problem for which no targeted therapy is available. We set out to study whether systemic inactivation of the main hypoxia-inducible factor prolyl 4-hydroxylase, HIF-P4H-2 (PHD2/Egln1), whose inactivation has been associated with protection against metabolic dysfunction, could ameliorate it. HIF-P4H-2-deficient and wild-type (WT) mice or HIF-P4H inhibitor-treated WT mice were subjected to an ethanol diet for 3–4 weeks and their metabolic health, liver and white adipose tissue (WAT) were analyzed. Primary hepatocytes from the mice were used to study cellular ethanol metabolism. The HIF-P4H-2-deficient mice retained a healthier metabolic profile, including less adiposity, better lipoprotein profile and restored insulin sensitivity, while on the ethanol diet than the WT. They also demonstrated protection from alcohol-induced steatosis and liver damage and had less WAT inflammation. In liver and WAT the expression of the key lipogenic and adipocytokine mRNAs, such as Fas and Ccl₂, were downregulated, respectively. The upregulation of metabolic and antioxidant hypoxia-inducible factor (HIF) target genes, such as Slc16a1 and 16a3 and Gclc, respectively, and a higher catalytic activity of ALDH2 in the HIF-P4H-2-deficient hepatocytes improved handling of the toxic ethanol metabolites and oxidative stress. Pharmacological HIF-P4H inhibition in the WT mice phenocopied the protection against AFLD. Our data show that global genetic inactivation of HIF-P4H-2 and pharmacological HIF-P4H inhibition can protect mice from alcohol-induced steatosis and liver injury, suggesting that HIF-P4H inhibitors, now in clinical trials for renal anemia, could also be studied in randomized clinical trials for treatment of AFLD.

Keywords: HIF, Hypoxia response, Inflammation, Metabolism, Oxidative stress

Response of human mature adipocytes to hypoxia-reoxygenation

SEOK JONG HONG, EUGENE PARK, WEI XU, SHENGXIAN JIA, ROBERT D. GALIANO & THOMAS A. MUSTOE

Laboratory for Wound Repair and Regenerative Medicine, Department of Surgery/Plastic Surgery Division, Northwestern University, Feinberg School of Medicine, Chicago, Illinois, USA

出处: *Cytotherapy*, 2014; 16: 1656-1665. DOI: 10.1016/j.jcyt.2014.07.008

Ruskinn 工作使用情况: Invivo₂ 1000; O₂ 浓度: 1%

Abstract

Background aims: Adipocytes are metabolically active cells and have endocrine functions, such as cytokine secretion. Notably, adipocytes are found underneath skin and are thought to be involved in the body's response to ischemia-reperfusion (I-R). I-R injury is an important factor in the pathogenesis of chronic skin wounds. In this study, we investigated the response of human adipocytes to hypoxia-reoxygenation (H-R), the *in vitro* equivalent of I-R.

Methods: We cultured human mature adipocytes by enclosing them in hydrogel composed of hyaluronan and collagen and analyzed their proliferation and response to H-R. Results. The average diameter of mature adipocytes isolated from abdominal subcutaneous fat tissue was between 60 and 109 μ m, and a positive correlation was found between adipocyte size and body mass index. Hydrogel-enclosed human adipocytes displayed viability in *in vitro* culture and were capable of expressing foreign genes for at least 1 month. Proliferation analysis revealed 5-bromo-2'-deoxy-uridine labeling and positive Ki67 signaling. vascular endothelial growth factor expression was differentially altered in adipocytes in response to hypoxia and H-R. Adipocyte messenger RNA expression of pro-inflammatory cytokines, such as interleukin-1, interleukin-8 and tumor necrosis factor- α , was upregulated in response to H-R. In addition, the expression of heat shock protein 70, a cytoprotective gene, and inducible nitric oxide synthase, a proapoptotic gene, were both increased in H-R. Survival of hydrogel-enclosed adipocytes was found at 2 months after delivery into athymic mice.

Conclusions: These and previous results from our group show that mature adipocytes can be cultured *in vitro* within a matrix and that they are functionally active cells that respond to environmental changes.

Keywords: cytokine, hydrogel, hypoxia-reoxygenation, mature adipocytes, proliferation

Stem cells from human apical papilla decrease neuro-inflammation and stimulate oligodendrocyte progenitor differentiation via activin-A secretion

Pauline De Berdt¹, Pauline Bottemanne², John Bianco¹, Mireille Alhouayek², Anibal Diogenes³, Amy Llyod⁴, Jose Gerardo-Nava⁵, Gary A. Brook⁵, Véronique Miron⁴, Giulio G. Muccioli², Anne des Rieux^{1,□}

¹Louvain Drug Research Institute (LDRI), Advanced Drug Delivery and Biomaterials (ADDB), Université Catholique de Louvain, Avenue E. Mounier 73, B1 73.12, 1200 Brussels, Belgium

²Louvain Drug Research Institute, Bioanalysis and Pharmacology of Bioactive Lipids Research Group (BPBL), Université Catholique de Louvain, Avenue E. Mounier 7B1 72.01, 1200 Brussels, Belgium

³ Department of Endodontics, University of Texas Health Science Center at San Antonio, San Antonio, Texas, USA

⁴ MRC Center for Reproductive Health, The Queen's Medical Research Institute, The University of Edinburgh, Edinburgh, UK

⁵ Institute of Neuropathology, Uniklinik RWTH Aachen, Pauwelsstraße 30, 52074 Aachen, Germany

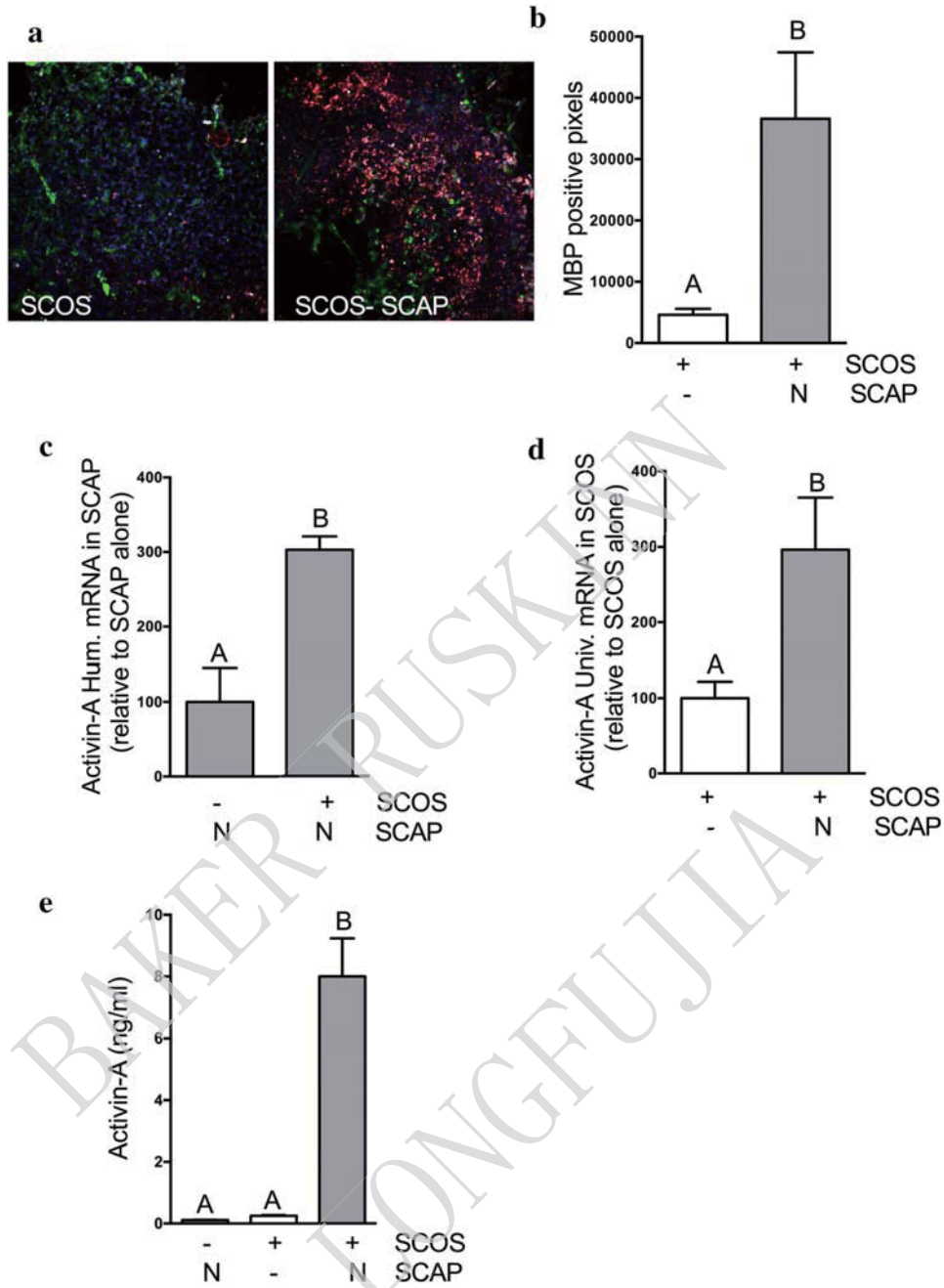
出处: *Cell. Mol. Life Sci.* 2018 08;75(15). DOI: 10.1007/s00018-018-2764-5

Ruskinn 工作使用情况: Invivo₂ 400; O₂ 浓度: 1%

Abstract

Secondary damage following spinal cord injury leads to non-reversible lesions and hampering of the reparative process. The local production of pro-inflammatory cytokines such as TNF- α can exacerbate these events. Oligodendrocyte death also occurs, followed by progressive demyelination leading to significant tissue degeneration. Dental stem cells from human apical papilla (SCAP) can be easily obtained at the removal of an adult immature tooth. This offers a minimally invasive approach to re-use this tissue as a source of stem cells, as compared to biopsying neural tissue from a patient with a spinal cord injury. We assessed the potential of SCAP to exert neuroprotective effects by investigating two possible modes of action: modulation of neuro-inflammation and oligodendrocyte progenitor cell (OPC) differentiation. SCAP were co-cultured with LPS-activated microglia, LPS-activated rat spinal cord organotypic sections (SCOS), and LPS-activated co-cultures of SCOS and spinal cord adult OPC. We showed for the first time that SCAP can induce a reduction of TNF- α expression and secretion in inflamed spinal cord tissues and can stimulate OPC differentiation via activin-A secretion. This work underlines the potential therapeutic benefits of SCAP for spinal cord injury repair.

Keywords: Spinal cord, Dental stem cell, Inflammation, Oligodendrocyte progenitor cells, Differentiation



SCOS–SCAP co-culture increased the expression of MBP in SCOS and induces activin-A secretion

a OPC were identified in SCOS by immunofluorescence using NG2 (green) staining and oligodendrocytes were identified using MBP (red) and CC1 (white) staining. b MBP positive pixels were quantified in SCOS cultured with and without SCAP (N = 2, n = 3). c Activin-A gene in SCAP 48 h after incubation with SCOS (N = 2, n = 3). d Activin-A gene expression in SCOS 48 h after incubation with SCAP (N = 2, n = 3). e Activin-A quantification in culture media using ELISA (N = 3, n = 3). Conditions not related by the same letter are significantly different. Groups without SCAP are presented in white, groups with SCAP grown in normoxia (N) in light grey and groups with SCAP grown in hypoxia (H) in dark grey

The response of five intestinal cell lines to anoxic conditions in vitro

Hanne Vissenaekens*, Charlotte Grootaert*, Andreja Rajkovic*, Tom Van De Wiele^{†1} and Marta Calatayud^{†1}

*Department of Food technology, Safety and Health, Faculty of Bioscience Engineering, Ghent University, Ghent 9000, Belgium and [†]Center for Microbial Ecology and Technology (CMET), Faculty of Bioscience Engineering, Ghent University, Ghent 9000, Belgium

出处: *Biol. Cell* 2019 Sep;111(9)DOI: 10.1111/boc.201800076

Ruskinn 工作使用情况: Ruskinn Workstation; O₂ 浓度: <0.1%

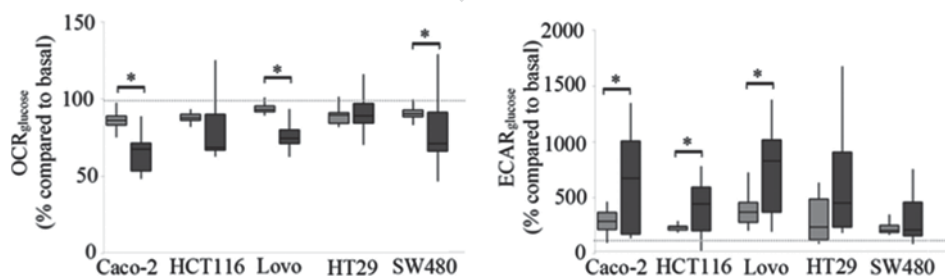
Abstract

Background information. In vivo oxygen levels in tissues range from 1% to 15%, while mechanistic cell culture studies employ an atmospheric oxygen level of 21% to grow cells. These oxygen concentrations are therefore not representative for conditions where the cell response is dependent on oxygen partial pressure. In pathological situation, such as (colon) cancer or chronic inflammation, tissue oxygenation is severely affected, and even under physiological conditions a steep oxygen gradient is present in the large intestine, where epithelial cells co-exist with microbial species, resulting in almost anoxia at the midpoint of the lumen. In these situations, a better characterisation of the essential cellular behaviour under hypoxia or anoxia is required.

Results. We have characterised the cellular response of commonly used cell cultures for the study of intestinal epithelial processes and colon cancer development (Caco-2, HT-29, SW480, HCT 116 and LoVo) under conventional normoxic conditions (21% O₂) and in an anoxic (<0.1% O₂) environment generated in an anaerobic chamber. In general, anoxic conditions led to lower levels of oxidative stress, a reduction in reduced glutathione/oxidised glutathione (GSH/GSSG) ratio, the shift of the redox status to oxidised glutathione levels, reduced cell proliferation, decreased barrier function and higher glycolysis rates at the expense of oxidative respiration. **Conclusions.**

Continuous exposure to anoxic conditions, such as occurring at the host–microbe interface in the intestine, may create an adaptive metabolic cellular response of the cells. **Significance.**

Considering adequate oxygen levels is essential for creating more physiologically relevant models for the study of host–microbe interactions and colon cancer development.



Cell response to glucose under aerobic and anoxic conditions Oxygen consumption rate (OCR, left panel) and extracellular acidification rate (ECAR, right panel) of the different cell lines cultivated under aerobic (light grey bars) and anoxic (dark grey bars). Results are expressed as per cent difference after glucose addition (25 mM) compared to the basal (glucose-free) levels (100%, indicated by light grey dotted line). Significantly different results ($P < 0.05$) between normoxic and anoxic conditions are indicated by an asterisk ($n = 6$).

IGF1R Dental Pulp Stem Cells Enhanced Neuroplasticity in Hypoxia-Ischemia Model

Hsiao-Yu Chiu^{1,2} & *Chen-Huan Lin*³ & *Chung Y. Hsu*⁴ & *John Yu*^{5,6} & *Chia-Hung Hsieh*⁴ & *Woei-Cherng Shyu*^{3,4}

¹ Children's Hospital, China Medical University and Hospital, Taichung, Taiwan

² Translational Medicine Doctoral Degree Program, China Medical University, Taichung, Taiwan ³ Translational Research Center, and Department of Neurology, China Medical University Hospital, Taichung, Taiwan 40440

⁴ Graduate Institute of Biomedical Sciences, China Medical University, Taichung, Taiwan

⁵ Institute of Stem Cell and Translational Cancer Research, Chang Gung Memorial Hospital at Linkou, Taoyuan, Taiwan

⁶ Institute of Cellular and Organismic Biology, Academia Sinica, Taipei, Taiwan

出处: *Mol. Neurobiol.* 2017 12;54(10)DOI: 10.1007/s12035-016-0210-y

Ruskinn 工作使用情况: BugBox

Abstract

Until now, the surface markers of multipotent mesenchymal stem cells (MSCs) had not been fully identified. Here, we found that the IGF1 receptor (IGF1R), regarded as a pluripotent marker of embryonic stem cells (ESCs), was also expressed in human dental pulp derived mesenchymal stem cells (hDSCs), which displayed a potential for both self-renewal and multipotency. hDSCs secreted IGF1 interacted with IGF1R through an autocrine signaling pathway to maintain this self-renewal and proliferation potential. Stereotaxic implantation of immunosorted IGF1R+ hDSCs in rats with neonatal hypoxia-ischemia (NHI) promoted neuroplasticity, improving the neurological outcome by increasing expression of the anti-apoptotic protein Bcl-2, which enhanced both neurogenesis and angiogenesis. In addition, treatment with IGF1R+ hDSCs significantly modulated neurite regeneration and anti-inflammation in vivo in NHI rats and in vitro in primary cortical cultures under oxygen/ glucose deprivation. Autocrine regulatory expression of IGF1R contributed to maintaining the self-renewal capacity of hDSCs. Furthermore, implantation of IGF1R+ hDSCs increased neuroplasticity with neurite regeneration and immunomodulation in and the NHI rat model.

Keywords: Human dental pulp mesenchymal stem cells (hDSCs); Insulin-like growth factor 1 (IGF1); Insulin-like growth factor 1 receptor (IGF1R); Neonatal hypoxia-ischemia model; Neuroplasticity

Protease-Mediated Suppression of DRG Neuron Excitability by Commensal Bacteria

Jessica L. Sessenwein,¹ Corey C. Baker,¹ Sabindra Pradhananga,¹ Megan E. Maitland,¹ e O. Petrof,¹ Emma Allen-Vercoe,² Curtis Noordhof,¹ David E. Reed,¹ Stephen J. Vanner,¹ and Alan E. Lomax¹

¹Gastrointestinal Disease Research Unit, Queen's University, Kingston, Ontario K7L 2V7, Canada, and²Department of Molecular and Cellular Biology, University of Guelph, Guelph, Ontario N1G 2W1, Canada

出处: *J. Neurosci.* 2017 11 29;37(48). DOI: 10.1523/JNEUROSCI.1672-17.2017

Ruskinn 工作使用情况: BugBox

Abstract

Peripheral pain signaling reflects a balance of pronociceptive and antinociceptive influences; the contribution by the gastrointestinal microbiota to this balance has received little attention. Disorders, such as inflammatory bowel disease and irritable bowel syndrome, are associated with exaggerated visceral nociceptive actions that may involve altered microbial signaling, particularly given the evidence for bacterial dysbiosis. Thus, we tested whether a community of commensal gastrointestinal bacteria derived from a healthy human donor (microbial ecosystem therapeutics; MET-1) can affect the excitability of male mouse DRG neurons. MET-1 reduced the excitability of DRG neurons by significantly increasing rheobase, decreasing responses to capsaicin (2 M) and reducing action potential discharge from colonic afferent nerves. The increase in rheobase was accompanied by an increase in the amplitude of voltage-gated K currents. A mixture of bacterial protease inhibitors abrogated the effect of MET-1 effects on DRG neuron rheobase. A serine protease inhibitor but not inhibitors of cysteine proteases, acid proteases, metalloproteases, or aminopeptidases abolished the effects of MET-1. The serine protease cathepsin G recapitulated the effects of MET-1 on DRG neurons. Inhibition of protease-activated receptor-4 (PAR-4), but not PAR-2, blocked the effects of MET-1. Furthermore, *Faecalibacterium prausnitzii* recapitulated the effects of MET-1 on excitability of DRG neurons. We conclude that serine proteases derived from commensal bacteria can directly impact the excitability of DRG neurons, through PAR-4 activation. The ability of microbiota-neuronal interactions to modulate afferent signaling suggests that therapies that induce or correct microbial dysbiosis may impact visceral pain.

Keywords: electrophysiology; inflammatory bowel disease; intestinal bacteria; nerve-gut interactions; neurogastroenterology

24-Hydroxycholesterol participates in pancreatic neuroendocrine tumor development

Matias Soncini^{a,1,2}, Gianfranca Corna^{a,1}, Marta Moresco^a, Nadia Coltella^b, Umberto Restuccia^c, Daniela Maggioni^a, Laura Raccosta^a, Chin-Yo Lin^d, Francesca Invernizzi^e, Roberto Crocchiolo^f, Claudio Doglioni^{g,s}, Catia Traversari^f, Angela Bachi^c, Rosa Bernardi^b, Claudio Bordignon^{f,s,2}, Jan-Åke Gustafsson^{d,2}, and Vincenzo Russo^{a,2}

^a Immuno-Biotherapy of Melanoma and Solid Tumors Unit, Division of Experimental Oncology, Istituto di Ricerca e Cura a Carattere Scientifico (IRCCS) Ospedale San Raffaele, Milan 20132, Italy;

^b Division of Experimental Oncology, IRCCS Scientific Institute San Raffaele, Milan 20132, Italy;

^c Functional Proteomics Program, Istituto FIRC di Oncologia Molecolare (IFOM), Milan 20132, Italy;

^d Center for Nuclear Receptors and Cell Signaling, Department of Biology and Biochemistry, University of Houston, Houston, TX 77004;

^e Department of Pathology, Scientific Institute San Raffaele, Milan 20132, Italy;

^f MolMed S.p.A., Milan 20132, Italy; and ^g Università Vita-Salute San Raffaele, Milan 20132, Italy

出处: *Proc. Natl. Acad. Sci. U.S.A.* 2016 10 11;113(41) DOI: 10.1073/pnas.1613332113

Ruskinn 工作使用情况: Invivo2 300

Abstract

Cells in the tumor microenvironment may be reprogrammed by tumor-derived metabolites. Cholesterol-oxidized products, namely oxysterols, have been shown to favor tumor growth directly by promoting tumor cell growth and indirectly by dampening antitumor immune responses. However, the cellular and molecular mechanisms governing oxysterol generation within tumor microenvironments remain elusive. We recently showed that tumor-derived oxysterols recruit neutrophils endowed with protumoral activities, such as neoangiogenesis. Here, we show that hypoxia inducible factor-1 α (HIF-1 α) controls the overexpression of the enzyme Cyp46a1, which generates the oxysterol 24-hydroxycholesterol (24S-HC) in a pancreatic neuroendocrine tumor (pNET) model commonly used to study neoangiogenesis. The activation of the HIF-1 α –24S-HC axis ultimately leads to the induction of the angiogenic switch through the positioning of proangiogenic neutrophils in proximity to Cyp46a1+ islets. Pharmacologic blockade or genetic inactivation of oxysterols controls pNET tumorigenesis by dampening the 24S-HC–neutrophil axis. Finally, we show that in some human pNET samples Cyp46a1 transcripts are overexpressed, which correlate with the HIF-1 α target VEGF and with tumor diameter. This study reveals a layer in the angiogenic switch of pNETs and identifies a therapeutic target for pNET patients.

Keywords: oxysterols, HIF-1 α , pancreatic neuroendocrine tumors, angiogenic switch, neutrophils

其他文章:

1. MicroRNA-21 attenuates oxygen and glucose deprivation induced apoptotic death in human neural stem cells with inhibition of JNK and p38 MAPK signaling.
期刊: Neurosci Lett.; 发表年份: 2018; Ruskinn 工作站使用情况: BugBox
2. Background levels of neomorphic 2-hydroxyglutarate facilitate proliferation of primary fibroblasts.
期刊: Physiol Res.; 发表年份: 2017; Ruskinn 工作站使用情况: Sci-tive N
3. STAT1 drives M1 microglia activation and neuroinflammation under hypoxia
期刊: Arch Biochem Biophys.; 发表年份: 2019; Ruskinn 工作站使用情况: Concept 300
4. Endothelial Progenitor Cells Conditioned Medium Supports Number of GABAergic Neurons and Exerts Neuroprotection in Cultured Striatal Neuronal Progenitor Cells
期刊: Cell Transplant.; 发表年份: 2019; Ruskinn 工作站使用情况: Invivo₂ 400
5. Propofol improved hypoxia-impaired integrity of blood-brain barrier via modulating the expression and phosphorylation of zonula occludens-1
期刊: CNS Neurosci Ther.; 发表年份: 2019; Ruskinn 工作站使用情况: Ruskinn Workstation
6. Ghrelin protects adult rat hippocampal neural stem cells from excessive autophagy during oxygen-glucose deprivation.
期刊: Endocr J.; 发表年份: 2018; Ruskinn 工作站使用情况: Ruskinn Workstation
7. THE SHC PROTEIN RAI PROMOTES AN ADAPTIVE CELL SURVIVAL PROGRAM IN HYPOXIC NEUROBLASTOMA CELLS.
期刊: J Cell Physiol.; 发表年份: 2017; Ruskinn 工作站使用情况: Invivo₂ 400
8. Hypoxia stimulates neural stem cell proliferation by increasing HIF-1 α expression and activating Wnt/ β -catenin signaling
期刊: Cell Mol Biol (Noisy-le-grand); 发表年份: 2017; Ruskinn 工作站使用情况: BugBox M
9. Temporal Rac1 - HIF-1 crosstalk modulates hypoxic survival of aged neurons.
期刊: Brain Res.; 发表年份: 2016; Ruskinn 工作站使用情况: Invivo₂ 400
10. CX3CL1/CX3CR1 Axis Plays a Key Role in Ischemia-Induced Oligodendrocyte Injury via p38MAPK Signaling Pathway.
期刊: Mol Neurobiol.; 发表年份: 2015; Ruskinn 工作站使用情况: Invivo₂

Cancer Lipid Metabolism Confers Antiangiogenic Drug Resistance

Hideki Iwamoto,^{1,2,8} Mitsuhiro Abe,^{1,2,8} Yunlong Yang,^{3,8} Dongmei Cui,⁴ Takahiro Seki,¹ Masaki Nakamura,¹ Kayoko Hosaka,¹ Sharon Lim,¹ Jieyu Wu,¹ Xingkang He,¹ Xiaoting Sun,^{1,7} Yongtian Lu,⁵ Qingjun Zhou,⁶ Weiyun Shi,⁶ Takuji Torimura,² Guohui Nie,^{5,*} Qi Li,^{7,*} and Yihai Cao^{1,9,*}

¹Department of Microbiology, Tumor and Cell Biology, Karolinska Institutet, Stockholm 171 77, Sweden

²Division of Gastroenterology, Department of Medicine, Kurume University School of Medicine, Kurume, Fukuoka, Japan

³Department of Cellular and Genetic Medicine, School of Basic Medical Sciences, Fudan University, Shanghai 200032, P.R. China

⁴Zhongshan Ophthalmic Center, State Key Laboratory of Ophthalmology, Sun Yat-sen University, Guangzhou, China

⁵Key Laboratory of International Collaborations, Second People's Hospital of Shenzhen, First Affiliated Hospital of Shenzhen University, Shenzhen 518035, China

⁶State Key Laboratory Cultivation Base, Shandong Provincial Key Laboratory of Ophthalmology, Shandong Eye Institute, Shandong Academy of Medical Sciences, Yanerdao Road, Qingdao 266071, China

⁷Department of Medical Oncology, Shuguang Hospital, Shanghai University of Traditional Chinese Medicine, Shanghai, P.R. China

⁸These authors contributed equally ⁹Lead Contact

出处: *Cell Metab.* 2018 Jul 03;28(1). DOI:10.1016/j.cmet.2018.05.005

Ruskinn 工作情况: Invivo₂ 300; O₂ 浓度: 3%

Abstract

Intrinsic and evasive antiangiogenic drug (AAD) resistance is frequently developed in cancer patients, and molecular mechanisms underlying AAD resistance remain largely unknown. Here we describe AAD-triggered, lipid-dependent metabolic reprogramming as an alternative mechanism of AAD resistance. Unexpectedly, tumor angiogenesis in adipose and non-adipose environments is equally sensitive to AAD treatment. AAD-treated tumors in adipose environment show accelerated growth rates in the presence of a minimal number of microvessels. Mechanistically, AAD-induced tumor hypoxia initiates the fatty acid oxidation metabolic reprogramming and increases uptake of free fatty acid (FFA) that stimulates cancer cell proliferation. Inhibition of carnitine palmitoyl transferase 1A (CPT1) significantly compromises the FFA-induced cell proliferation. Genetic and pharmacological loss of CPT1 function sensitizes AAD therapeutic efficacy and enhances its anti-tumor effects. Together, we propose an effective cancer therapy concept by combining drugs that target angiogenesis and lipid metabolism.

Synthetic lethality between BRCA1 deficiency and poly(ADP-ribose) polymerase inhibition is modulated by processing of endogenous oxidative DNA damage

Sara Giovannini,^{1,2,3} Marie-Christine Weller,² Simone Reppmann,² Holger Moch,⁴ and Josef Jiricny^{1,2,3}

¹ Institute of Molecular Life Sciences of the University of Zurich, Winterthurerstrasse 190, CH-8057 Zurich, Switzerland

² Institute of Molecular Cancer Research of the University of Zurich, Winterthurerstrasse 190, CH-8057 Zurich, Switzerland

³ Institute of Biochemistry of the Swiss Federal Institute of Technology, Otto-Stern-Weg 3, CH-8093 Zurich, Switzerland

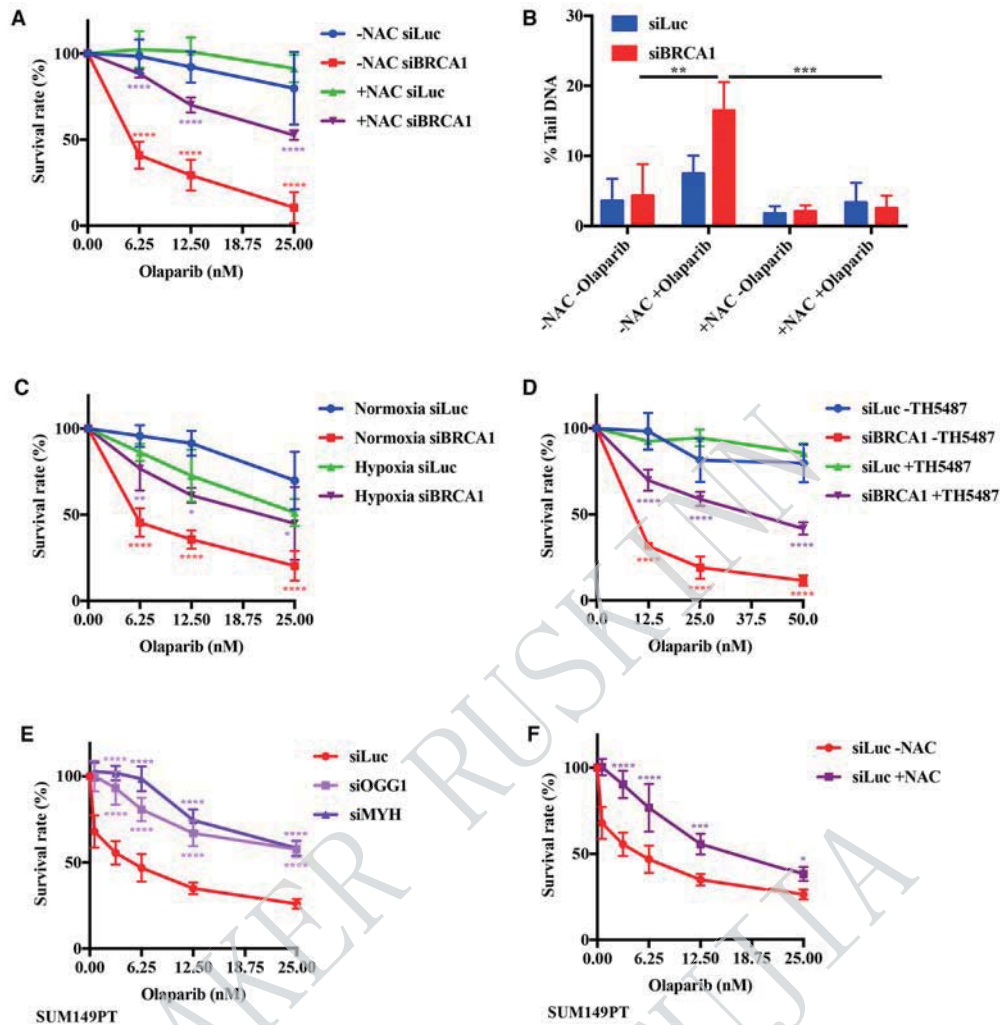
⁴ Institute of Pathology and Molecular Pathology, University Hospital Zurich, Schmelzbergstrasse 12, CH-8091 Zurich, Switzerland

出处: *Nucleic Acids Res.* 2019 Sep 26; 47(17): 9132–9143. DOI: 10.1093/nar/gkz624

Ruskinn 工作使用情况: Sci-tive; O₂ 浓度: 1%

Abstract

Poly(ADP-ribose) polymerases (PARPs) facilitate the repair of DNA single-strand breaks (SSBs). When PARPs are inhibited, unrepaired SSBs colliding with replication forks give rise to cytotoxic double-strand breaks. These are normally rescued by homologous recombination (HR), but, in cells with suboptimal HR, PARP inhibition leads to genomic instability and cell death, a phenomenon currently exploited in the therapy of ovarian cancers in *BRCA1/2* mutation carriers. In spite of their promise, resistance to PARP inhibitors (PARPi) has already emerged. In order to identify the possible underlying causes of the resistance, we set out to identify the endogenous source of DNA damage that activates PARPs. We argued that if the toxicity of PARPi is indeed caused by unrepaired SSBs, these breaks must arise spontaneously, because PARPi are used as single agents. We now show that a significant contributor to PARPi toxicity is oxygen metabolism. While *BRCA1*-depleted or -mutated cells were hypersensitive to the clinically approved PARPi olaparib, its toxicity was significantly attenuated by depletion of OGG1 or MYH DNA glycosylases, as well as by treatment with reactive oxygen species scavengers, growth under hypoxic conditions or chemical OGG1 inhibition. Thus, clinical resistance to PARPi therapy may emerge simply through reduced efficiency of oxidative damage repair.



The synthetic lethality of PARP inhibition and BRCA1 deficiency is attenuated by the antioxidant NAC, by hypoxia or by OGG1 inhibition.

(A) The hypersensitivity of BRCA1-depleted human ovarian carcinoma cell line A2780 to olaparib as measured by clonogenic assays is partially rescued by a treatment with the antioxidant NAC. Significance: (-NAC) siLuc - (-NAC) siBRCA1; (-NAC) siBRCA1 - (+NAC) siBRCA1. (B) NAC treatment attenuates the genotoxicity of olaparib in BRCA1-depleted cells measured by alkaline comet assays. Significance: (-NAC, -olaparib) siBRCA1 - (-NAC, +olaparib) siBRCA1; (-NAC, +olaparib) siBRCA1 - (+NAC, +olaparib) siBRCA1. (C) BRCA1-depleted human ovarian carcinoma cell line A2780 grown in hypoxic environment (Supplementary Figure S4A) is desensitized to olaparib, as measured by clonogenic assays. Significance: Normox siLuc - Normox siBRCA1; Normox siBRCA1 - Hypox siBRCA1; (D) The hypersensitivity of BRCA1-depleted human ovarian carcinoma cell line A2780 to olaparib as measured by clonogenic assays is partially rescued by a treatment with the OGG1 inhibitor TH5487. Significance: siLuc (-TH5487) - siBRCA1 (-TH5487); siBRCA1 (-TH5487) - siBRCA1 (+TH5487). (E) The hypersensitivity of triple-negative BRCA1-mutated SUM149PT cells to olaparib as measured by clonogenic assays is partially rescued by pre-treatment with OGG1- or MYH siRNAs (Supplementary Figure S4B). Significance: siLuc - siOGG1; siLuc - siMYH. (F) The hypersensitivity of triple-negative BRCA1-mutated SUM149PT cells to olaparib as measured by clonogenic assays is partially rescued by pre-treatment with NAC. Significance: (-NAC) siLuc - (+NAC) siLuc. The results in A-F are means of at least three independent experiments, each carried out in triplicate \pm s.d.. Asterisks indicate levels of statistical significance, calculated by Two-Way ANOVA test (p -value < 0.05 *, < 0.01 **, < 0.001 ***, < 0.0001 ****).

Nitroimidazole derivative incorporated liposomes for hypoxia-triggered drug delivery and enhanced therapeutic efficacy in patient-derived tumor xenografts

Yi Li^{1,†}, Ailing Lu^{1,†}, Mengmeng Long¹, Lei Cui³, Zhongping Chen^{1,2,*}, Li Zhu^{1,*}

¹ Institute for Nautical Medicine, Nantong University, Nantong, People's Republic of China

² Pharmaceutical Sciences Division, School of Pharmacy, University of Wisconsin-Madison, United States

³ Department of Radiology, Second Affiliated Hospital of Nantong University, Nantong, People's Republic of China

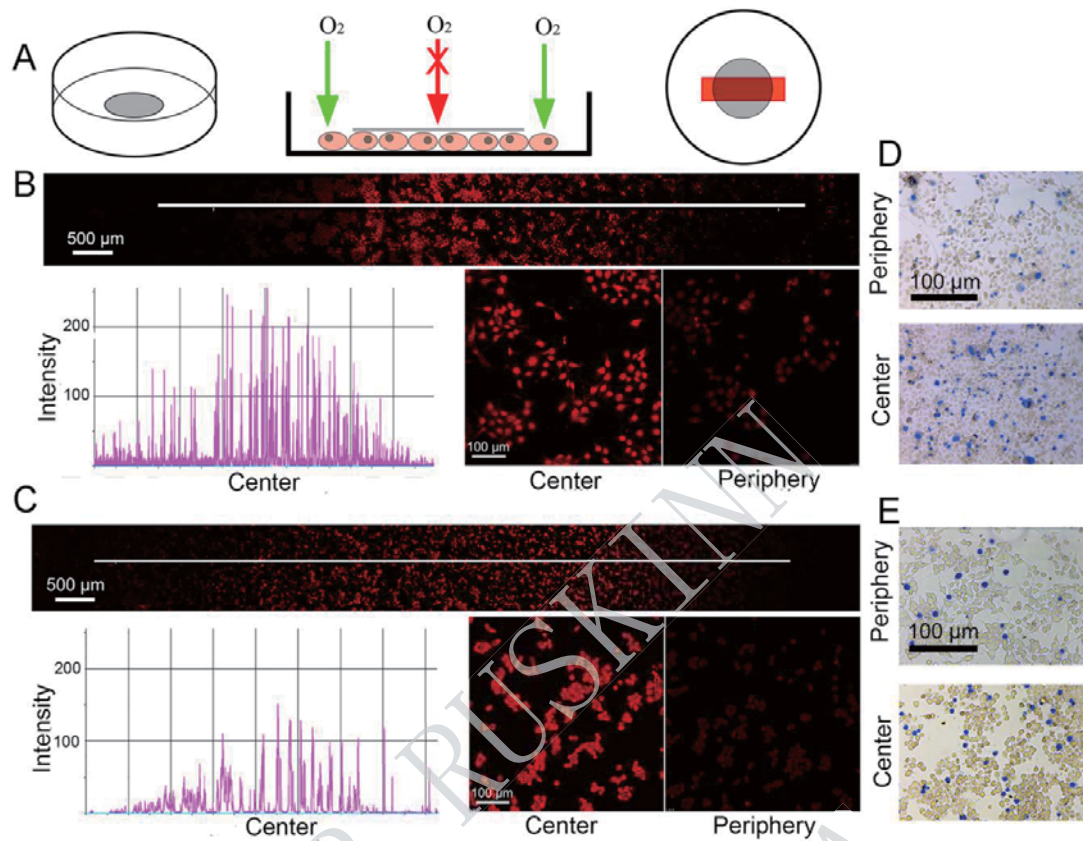
出处: *Acta Biomater* 2019 01 01;83DOI: 10.1016/j.actbio.2018.10.029

Ruskinn 工作使用情况: Invivo₂ 400; O₂ 浓度: 10, 5, 1%

Abstract

Hypoxia is not merely a tumor microenvironment byproduct, but rather an active participant in tumor development, invasion, and metastasis. Hypoxia contributes to poor outcomes in tumor treatment and has currently emerged as an important therapeutic target. In this work, a facile hypoxia-responsive liposomal drug delivery system was developed by incorporating derivatized nitroimidazole into liposome membranes. Under hypoxic conditions, hypoxia-induced reductive metabolism of the nitroimidazole derivative facilitated disassembly of the liposomes for triggered drug release. The liposomes showed high sensitivity to hypoxia, even at the cellular level, and could release payload in an oxygen-dependent manner, leading to high cytotoxicity in hypoxic conditions. *In vivo* fluorescence imaging revealed that there was a selective release of the liposomes at the hypoxic tumor site. As a result, the liposomes exhibited enhanced therapeutic efficacy in treating a hypoxic tumor in both cell line-derived and clinically relevant patient-derived xenograft models. Thus, hypoxia-responsive liposomes are a promising drug delivery system for hypoxia targeted tumor therapy.

Keywords: Nitroimidazole; liposomes; hypoxia; targeted delivery; triggered release; patient-derived xenograft



Hypoxia-triggered intracellular drug release of DOX-HR-LPs

(A) Oxygen gradient created by placing a glass cover on cultured cells. Oxygen-dependent DOX release of DOX-HR-LPs in (B) FaDu and (C) RM-1 cells observed by CLSM, showing high fluorescence intensity in the hypoxic center and relatively low fluorescence intensity in the normoxic periphery of glass cover. Trypan staining of (D) FaDu and (E) RM-1 cells treated with DOX-HR-LPs after CLSM observation. More dead cells were found in the hypoxic center.

Androgen receptor (AR)/miR-520f-3p/SOX9 signaling is involved in altering hepatocellular carcinoma (HCC) cell sensitivity to the Sorafenib therapy under hypoxia via increasing cancer stem cells phenotype

Yao Xiao^{1, 2}, Yin Sun^{2*}, Guodong Liu^{1, 2}, Jie Zhao², Yuan Gao², Shuyuan Yeh², Liansheng Gong^{1, #} and Chawnsang Chang^{2, 3, #}*

¹Department of Hepatobiliary and Pancreatic Surgery, Xiangya Hospital, Central South University, Changsha, 410008, China

²George Whipple Lab for Cancer Research, Departments of Pathology, Urology, Radiation Oncology and The Wilmot Cancer Center, University of Rochester Medical Center, Rochester, NY, USA

³Sex Hormone Research Center, China Medical University/Hospital, Taichung 404, Taiwan

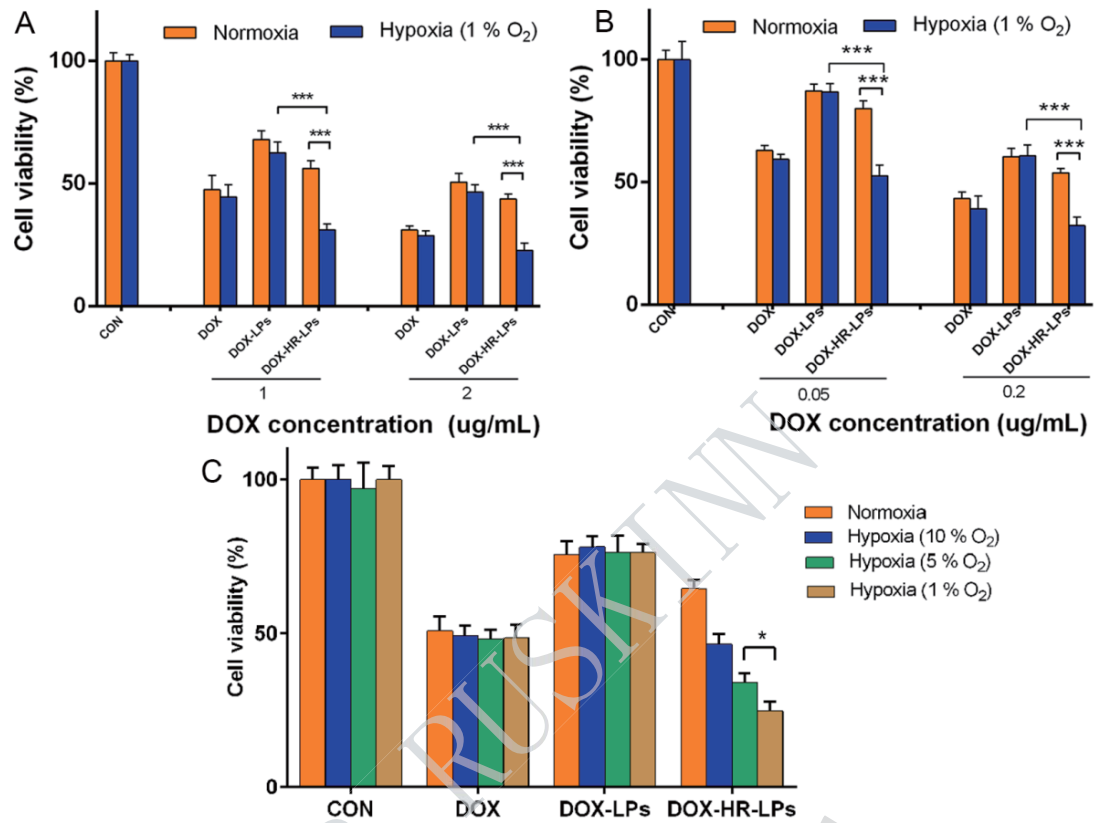
出处: **Cancer Lett. 2019 03 01;444. DOI: 10.1016/j.canlet.2018.11.004**

Ruskinn 工作使用情况: Ruskinn Workstation; O₂浓度: 1%

Abstract

Early studies indicated that the androgen receptor (AR) might play key roles to impact hepatocellular carcinoma (HCC) progression at different stages. Its linkage to hypoxia, a condition that occurs frequently during the HCC progression, however, remains unclear. Here we found that AR/miR-520f-3p/SOX9 signaling is involved in the altering HCC cells sensitivity to the Sorafenib therapy under hypoxia via increasing the cancer stem cells (CSCs) population. Mechanism dissection revealed that AR might alter the miR-520f-3p/SOX9 signaling through transcriptional regulation via binding to the androgen-response-elements (AREs) on the promoter region of miR-520f, which could then suppress SOX9 mRNA translation via targeting its 3' untranslated region (3'UTR). The in vivo mouse model with orthotopic xenografts of HCC cells also validated the in vitro data, and a human HCC sample survey confirmed the positive linkage of AR/miR-520f-3p/SOX9 signaling to the CSCs population during HCC progression. Together, these preclinical findings suggest that hypoxia may increase the HCC CSCs population via altering the AR/miR-520f-3p/SOX9 signaling, and targeting this newly identified signaling with small molecule of miR-520f-3p may help in the development of the novel therapy to better suppress the HCC progression.

Keywords: liver cancer, androgen receptor, microRNAs, drug sensitivity, CSCs



***In vitro* cytotoxicity by MTT assay**

MTT assay of DOX, DOX-LPs, and DOX-HR-LPs against (A) FaDu and (B) RM-1 cells under normoxic (20% O₂) and hypoxic (1% O₂) conditions after 48 h incubation. DOX concentrations were 1 or 2 µg/mL for FaDu cells and 0.05 or 0.2 µg/mL for RM-1 cells, respectively. (C) MTT assay of DOX, DOX-LPs, and DOX-HR-LPs against FaDu under normoxic (20% O₂) and different hypoxic (10, 5, and 1% O₂) conditions after 48 h incubation. DOX concentration was 1 µg/mL.

Optimized acriflavine-loaded lipid nanocapsules as a safe and effective delivery system to treat breast cancer

Yoann Montigaud^{a,b}, Bernard Ucakar^a, Balaji Krishnamachary^c, Zaver M Bhujwalla^{c,d}, Olivier Feron^e, Véronique Prémat^a, Fabienne Danhier^a, Bernard Gallez^{b*}, Pierre Danhier^f

^a Université catholique de Louvain, Louvain Drug Research Institute, Advanced Drug Delivery and Biomaterials, Avenue Mounier 73, B1.73.12, 1200 Brussels, Belgium

^b Université catholique de Louvain, Louvain Drug Research Institute, Biomedical Magnetic Resonance Research Group platform, Avenue Mounier 73, B1.73.08, 1200 Brussels, Belgium

^c Division of Cancer Imaging Research, In Vivo Cellular and Molecular Imaging Center, The Russell H. Morgan Department of Radiology and Radiological Science, The Johns Hopkins University School of Medicine, Baltimore, MD, USA

^d Sidney Kimmel Comprehensive Cancer Center, The Johns Hopkins University School of Medicine, Baltimore, MD, USA

^e Université catholique de Louvain, Pole of Pharmacology and Therapeutics (FATH), Institut de Recherche Expérimentale et Clinique (IREC), Avenue Mounier 53, B1.53.09, 1200 Brussels, Belgium

^f Université catholique de Louvain, Louvain Drug Research Institute, Nuclear and Electron Spin Technologies (NEST) Platform, Avenue Mounier 73, B1.73.07, 1200 Brussels, Belgium

出处: *Int J Pharm* 2018 Nov 15;551. DOI: 10.1016/j.ijpharm.2018.09.034

Ruskinn 工作使用情况: Invivo2 400; O₂ 浓度: 1%

Abstract

Acriflavine (ACF) hydrochloride is currently repurposed as multimodal drug, inhibiting hypoxia-inducible factors (HIF) pathways and exerting cytotoxic properties. The aim of this study was to encapsulate ACF in reverse micelles and to incorporate this suspension in lipid nanocapsules (LNC). Designs of experiments were used to work under quality by design conditions. LNC were formulated using a phase-inversion temperature method, leading to an encapsulation efficiency around 80%. *In vitro*, the encapsulated drug presented similar cytotoxic activity and decrease in HIF activity in 4T1 cells compared to the free drug. *In vivo*, ACF-loaded nanoparticles (ACF dose of 5 mg/kg) demonstrated a higher antitumor efficacy compared to free ACF on an orthotopic model of murine breast cancer (4T1 cells). Moreover, the use of LNC allowed to drastically decrease the number of administrations compared to the free drug (2 versus 12 injections), suppressing the ACF-induced toxicity. Keywords Lipid nanocapsules, drug delivery system, breast cancer, acriflavine, 4T1 cells, design of experiments (DoE)

其他文章:

1.The Antiproliferative and Colony-suppressive Activities of STAT3 Inhibitors in Human Cancer Cells Is Compromised Under Hypoxic Conditions.

期刊: Anticancer Res.; 发表年份: 2018; Ruskinn 工作站使用情况: Invivo₂ 300

2.Robotic Mammosphere Assay for High-Throughput Screening in Triple-Negative Breast Cancer.

期刊: SLAS Discov.; 发表年份: 2017 Ruskinn 工作站使用情况: Sci-tive N

3.Hypoxia-induced Changes in SUMO Conjugation Affect Transcriptional Regulation Under Low Oxygen.

期刊: Mol Cell Proteomics.; 发表年份: 2019; Ruskinn 工作站使用情况: Invivo₂ 200

4.The unidirectional hypoxia-activated prodrug OCT1002 inhibits growth and vascular development in castrate-resistant prostate tumors.

期刊: Prostate. ; 发表年份: 2017; Ruskinn 工作站使用情况: Invivo₂

5.Drug susceptibility testing in microaerophilic parasites: Cysteine strongly affects the effectivities of metronidazole and auranofin, a novel and promising antimicrobial.

期刊: Int J Parasitol Drugs Drug Resist.; 发表年份: 2017; Ruskinn 工作站使用情况: BugBox

6.HIF-1 α inhibition by diethylstilbestrol and its polyacetal conjugate in hypoxic prostate tumour cells: Insights from NMR metabolomics.

期刊: Neurosci Lett.; 发表年份: 2018; Ruskinn 工作站使用情况: BugBox

7.Identification of Small Molecule PHD2 Zinc Finger Inhibitors that Activate Hypoxia Inducible Factor.

期刊: Chembiochem.; 发表年份: 2017; Ruskinn 工作站使用情况: Invivo₂

8.Targeting and Treatment of Tumor Hypoxia by Newly Designed Prodrug Possessing High Permeability in Solid Tumors.

期刊: Mol Pharm.; 发表年份: 2016; Ruskinn 工作站使用情况: Invivo₂ 400

Lypd8 promotes the segregation of flagellated microbiota and colonic epithelia.

Ryu Okumura^{1,2}, Takashi Kurakawa¹, Takashi Nakano³, Hisako Kayama^{1,2}, Makoto Kinoshita^{1,2}, Daisuke Motooka⁴, Kazuyoshi Gotoh^{4,5}, Taishi Kimura¹, Naganori Kamiyama¹, Takashi Kusu¹, Yoshiyasu Ueda¹, Hong Wu³, Hideki Iijima⁶, Soumik Barman^{1,2}, Hideki Osawa⁷, Hiroshi Matsuno⁷, Junichi Nishimura⁷, Yusuke Ohba⁸, Shota Nakamura⁴, Tetsuya Iida^{4,9}, Masahiro Yamamoto¹⁰, Eiji Umemoto^{1,2}, Koichi Sano³ & Kiyoshi Takeda^{1,2}

¹Laboratory of Immune Regulation, Department of Microbiology and Immunology, Graduate School of Medicine, WPI Immunology Frontier Research Center, Osaka University, Suita, Osaka 565-0871, Japan. ²Core Research for Evolutional Science and Technology, Japan Agency for Medical Research and Development, Tokyo 100-0004, Japan. ³Department of Microbiology and Infection Control, Osaka Medical College, Takatsuki, Osaka 569-8686, Japan. ⁴Department of Infection Metagenomics, Genome Information Research Center, Research Institute for Microbial Diseases, Osaka University, Suita, Osaka 565-0871, Japan. ⁵Department of Bacteriology, Okayama University Graduate School of Medicine, Okayama 700-8558, Japan. ⁶Department of Gastroenterology and Hepatology, Graduate School of Medicine, Osaka University, Osaka 565-0871, Japan. ⁷Department of Gastroenterological Surgery, Graduate School of Medicine, Osaka University, Osaka 565-0871, Japan. ⁸Department of Cell Physiology, Hokkaido University Graduate School of Medicine, Sapporo 060-8638, Japan. ⁹Department of Bacterial Infections, Research Institute for Microbial Diseases, Osaka University, Suita, Osaka 565-0871, Japan. ¹⁰Laboratory of Immunoparasitology, Research Institute for Microbial Diseases, WPI Immunology Frontier Research Center, Osaka University, Suita, Osaka 565-0871, Japan.

出处: **Nature 2016 Apr; 07;532(7597). DOI: 10.1038/nature17406**

Ruskinn 工作使用情况: **Bugbox Plus**

Abstract

Colonic epithelial cells are covered by thick inner and outer mucus layers. The inner mucus layer is free of commensal microbiota, which contributes to the maintenance of gut homeostasis. In the small intestine, molecules critical for prevention of bacterial invasion into epithelia such as Paneth-cell-derived anti-microbial peptides and regenerating islet-derived 3 (RegIII) family proteins have been identified. Although there are mucus layers providing physical barriers against the large number of microbiota present in the large intestine, the mechanisms that separate bacteria and colonic epithelia are not fully elucidated. Here we show that Ly6/PLAUR domain containing 8 (Lypd8) protein prevents flagellated microbiota invading the colonic epithelia in mice. Lypd8, selectively expressed in epithelial cells at the uppermost layer of the large intestinal gland, was secreted into the lumen and bound flagellated bacteria including *Proteus mirabilis*. In the absence of Lypd8, bacteria were present in the inner mucus layer and many flagellated bacteria invaded epithelia. Lypd8(-/-) mice were highly sensitive to intestinal inflammation induced by dextran sulfate sodium (DSS). Antibiotic elimination of Gram-negative flagellated bacteria restored the bacterial-free state of the inner mucus layer and ameliorated DSS-induced intestinal inflammation in Lypd8(-/-) mice. Lypd8 bound to flagella and suppressed motility of flagellated bacteria.

Thus, Lypd8 mediates segregation of intestinal bacteria and epithelial cells in the colon to preserve intestinal homeostasis.

Gut-derived *Enterococcus faecium* from ulcerative colitis patients promotes colitis in a genetically susceptible mouse host

Jun Seishima,^{#1} Noriho Iida,^{#1} Kazuya Kitamura,¹ Masahiro Yutani,² Ziyu Wang,¹ Akihiro Seki,¹ Taro Yamashita,¹ Yoshio Sakai,¹ Masao Honda,³ Tatsuya Yamashita,¹ Takashi Kagaya,¹ Yukihiro Shiota,¹ Yukako Fujinaga,² Eishiro Mizukoshi,¹ and Shuichi Kaneko¹

¹Department of Gastroenterology, Graduate School of Medical Sciences, Kanazawa University, Kanazawa, Ishikawa 920-8641 Japan

²Department of Bacteriology, Graduate School of Medicinal Sciences, Kanazawa University, Kanazawa, Ishikawa Japan

³Department of Advanced Medical Technology, Graduate School of Health Medicine, Kanazawa University, Kanazawa, Ishikawa Japan

出处: **Genome Biol. 2019; 20: 252. DOI: 10.1186/s13059-019-1879-9**

Ruskinn 工作使用情况: **Ruskinn Workstation**

Background

Recent metagenomic analyses have revealed dysbiosis of the gut microbiota of ulcerative colitis (UC) patients. However, the impacts of this dysbiosis are not fully understood, particularly at the strain level.

Results

We perform whole-genome shotgun sequencing of fecal DNA extracts from 13 healthy donors and 16 UC and 8 Crohn's disease (CD) patients. The microbiota of UC and CD patients is taxonomically and functionally divergent from that of healthy donors, with *E. faecium* being the most differentially abundant species between the two microbial communities. Transplantation of feces from UC or CD patients into Il10^{-/-} mice promotes pathological inflammation and cytokine expression in the mouse colon, although distinct cytokine expression profiles are observed between UC and CD. Unlike isolates derived from healthy donors, *E. faecium* isolates from the feces of UC patients, along with *E. faecium* strain ATCC 19434, promotes colitis and colonic cytokine expression. Inflammatory *E. faecium* strains, including ATCC 19434 and a UC-derived strain, cluster separately from commercially available probiotic strains based on whole-genome shotgun sequencing analysis. The presence of *E. faecium* in fecal samples is associated with large disease extent and the need for multiple medications in UC patients.

Conclusions

E. faecium strains derived from UC patients display an inflammatory genotype that causes colitis.

Keywords: Inflammatory bowel disease, Crohn's disease, Microbiota, Metagenome

Assessing the viability of transplanted gut microbiota by sequential tagging with D-amino acid-based metabolic probes.

Wei Wang,^{1,2} Liyuan Lin,^{1,3} Yahui Du,³ Yanling Song,¹ Xiaoman Peng,¹ Xing Chen,² and Chaoyong James Yang^{1,3}

¹Institute of Molecular Medicine, Renji Hospital, Shanghai Jiao Tong University School of Medicine, Shanghai, 200127 China

²College of Chemistry and Molecular Engineering, Peking-Tsinghua Center for Life Sciences, Synthetic and Functional Biomolecules Center, and Key Laboratory of Bioorganic Chemistry and Molecular Engineering of Ministry of Education, Peking University, Beijing, 100871 China

³Collaborative Innovation Center of Chemistry for Energy Materials, The MOE Key Laboratory of Spectrochemical Analysis and Instrumentation, State Key Laboratory of Physical Chemistry of Solid Surfaces, Department of Chemical Biology, College of Chemistry and Chemical Engineering, Xiamen University, Xiamen, 361005 China

出处: *Nat Commun* 2019 03 21;10(1)DOI: 10.1038/s41467-019-09267-x

Ruskinn 工作使用情况: Concept 400

Abstract

Currently, there are more than 200 fecal microbiota transplantation (FMT) clinical trials worldwide. However, our knowledge of this microbial therapy is still limited. Here we develop a strategy using sequential tagging with D-amino acid-based metabolic probes (STAMP) for assessing the viabilities of transplanted microbiotas. A fluorescent D-amino acid (FDAA) is first administered to donor mice to metabolically label the gut microbiotas in vivo. The labeled microbiotas are transplanted to recipient mice, which receive a second FDAA with a different color. The surviving transplants should incorporate both FDAAs and can be readily distinguished by presenting two colors simultaneously. Isolation of surviving bacteria and 16S rDNA sequencing identify several enriched genera, suggesting the importance of specific bacteria in FMT. In addition, using STAMP, we evaluate the effects on transplant survival of pre-treating recipients using different antibiotics. We propose STAMP as a versatile tool for deciphering the complex biology of FMT, and potentially improving its treatment efficacy.

Conventional culture methods with commercially available media unveil the presence of novel culturable bacteria

Tamaki Ito, Tsuyoshi Sekizuka, Norimi Kishi, Akifumi Yamashita, and Makoto Kuroda

Laboratory of Genomics, Pathogen Genomics Center, National Institute of Infectious Diseases, Tokyo, Japan

出处: *Gut Microbes*. 2019; 10(1): 77–91. doi: 10.1080/19490976.2018.1491265

Ruskinn 工作使用情况: Bugbox Plus

Abstract

Recent metagenomic analysis has revealed that our gut microbiota plays an important role in not only the maintenance of our health but also various diseases such as obesity, diabetes, inflammatory bowel disease, and allergy. However, most intestinal bacteria are considered ‘unculturable’ bacteria, and their functions remain unknown. Although culture-independent genomic approaches have enabled us to gain insight into their potential roles, culture-based approaches are still required to understand their characteristic features and phenotypes. To date, various culturing methods have been attempted to obtain these ‘unculturable’ bacteria, but most such methods require advanced techniques. Here, we have tried to isolate possible unculturable bacteria from a healthy Japanese individual by using commercially available media. A 16S rRNA (ribosomal RNA) gene metagenomic analysis revealed that each culture medium showed bacterial growth depending on its selective features and a possibility of the presence of novel bacterial species. Whole genome sequencing of these candidate strains suggested the isolation of 8 novel bacterial species classified in the Actinobacteria and Firmicutes phyla. Our approach indicates that a number of intestinal bacteria hitherto considered unculturable are potentially culturable and can be cultured on commercially available media. We have obtained novel gut bacteria from a healthy Japanese individual using a combination of comprehensive genomics and conventional culturing methods. We would expect that the discovery of such novel bacteria could illuminate pivotal roles for the gut microbiota in association with human health.

KEYWORDS: Human gut microbiota, commercially available media, 16S rRNA gene metagenomic sequencing, whole genome sequencing, novel bacteria, unculturable bacteria

Protease-Mediated Suppression of DRG Neuron Excitability by Commensal Bacteria

Jessica L. Sessenwein,¹ Corey C. Baker,¹ Sabindra Pradhananga,¹ Megan E. Maitland,¹ Elaine O. Petrof,¹ Emma Allen-Vercoe,² Curtis Noordhof,¹ David E. Reed,¹ Stephen J. Vanner,¹ and Alan E. Lomax¹

¹Gastrointestinal Disease Research Unit, Queen's University, Kingston, Ontario K7L 2V7, Canada, and

²Department of Molecular and Cellular Biology, University of Guelph, Guelph, Ontario N1G 2W1, Canada

出处: *J. Neurosci.* 2017 11 29;37(48)DOI: 10.1523/JNEUROSCI.1672-17.2017

Ruskinn 工作使用情况: Bugbox

Abstract

Peripheral pain signaling reflects a balance of pronociceptive and antinociceptive influences; the contribution by the gastrointestinal microbiota to this balance has received little attention. Disorders, such as inflammatory bowel disease and irritable bowel syndrome, are associated with exaggerated visceral nociceptive actions that may involve altered microbial signaling, particularly given the evidence for bacterial dysbiosis. Thus, we tested whether a community of commensal gastrointestinal bacteria derived from a healthy human donor (microbial ecosystem therapeutics; MET-1) can affect the excitability of male mouse DRG neurons. MET-1 reduced the excitability of DRG neurons by significantly increasing rheobase, decreasing responses to capsaicin (2 μ m) and reducing action potential discharge from colonic afferent nerves. The increase in rheobase was accompanied by an increase in the amplitude of voltage-gated K⁺ currents. A mixture of bacterial protease inhibitors abrogated the effect of MET-1 effects on DRG neuron rheobase. A serine protease inhibitor but not inhibitors of cysteine proteases, acid proteases, metalloproteases, or aminopeptidases abolished the effects of MET-1. The serine protease cathepsin G recapitulated the effects of MET-1 on DRG neurons. Inhibition of protease-activated receptor-4 (PAR-4), but not PAR-2, blocked the effects of MET-1. Furthermore, *Faecalibacterium prausnitzii* recapitulated the effects of MET-1 on excitability of DRG neurons. We conclude that serine proteases derived from commensal bacteria can directly impact the excitability of DRG neurons, through PAR-4 activation. The ability of microbiota-neuronal interactions to modulate afferent signaling suggests that therapies that induce or correct microbial dysbiosis may impact visceral pain.

Keywords: electrophysiology, inflammatory bowel disease, intestinal bacteria, nerve-gut interactions, neurogastroenterology

Live *Faecalibacterium prausnitzii* induces greater TLR2 and TLR2/6 activation than the dead bacterium in an apical anaerobic co-culture system.

Eva Maier^{1,2}, *Rachel C. Anderson*^{1,2}, *Eric Altermann*^{2,3}, *Nicole C. Roy*^{1,2,4}

¹ Food Nutrition & Health Team, Food & Bio - based Products Group, AgResearch Grasslands, Palmerston North, New Zealand

²Riddet Institute, Massey University, Palmerston North, New Zealand

³Rumen Microbiology Team, Animal Science Group, AgResearch Grasslands, Palmerston North, New Zealand

⁴High - Value Nutrition National Science Challenge, Auckland, New Zealand

出处: **Cellular Microbiology. 2018;20:e12805. DOI: 10.1111/cmi.12805**

Ruskinn 工作使用情况: **Concept Plus**

Abstract

Inappropriate activation of intestinal innate immune receptors, such as toll - like receptors (TLRs), by pathogenic bacteria is linked to chronic inflammation. In contrast, a “tonic” level of TLR activation by commensal bacteria is required for intestinal homeostasis. A technical challenge when studying this activation *in vitro* is the co - culturing of oxygen - requiring mammalian cells with obligate anaerobic commensal bacteria. To overcome this, we used a novel apical anaerobic co - culture system to successfully adapt a TLR activation assay to be conducted in conditions optimised for both cell types. Live *Faecalibacterium prausnitzii*, an abundant obligate anaerobe of the colonic microbiota, induced higher TLR2 and TLR2/6 activation than the dead bacterium. This enhanced TLR induction by live *F. prausnitzii*, which until now has not previously been described, may contribute to maintenance of gastrointestinal homeostasis. This highlights the importance of using physiologically relevant co - culture systems to decipher the mechanisms of action of live obligate anaerobes.

其他文章:

- 1.Optimization of Culturomics Strategy in Human Fecal Samples.
期刊: Cell Microbiol.; 发表年份: 2019; Ruskinn 工作站使用情况: Ruskinn Workstation
- 2.Comparison of Japanese and Indian intestinal microbiota shows diet-dependent interaction between bacteria and fungi.
期刊: NPJ Biofilms Microbiomes.; 发表年份: 2019; Ruskinn 工作站使用情况: BugBox
- 3.Heterologous gene expression in the human gut bacteria *Eubacterium rectale* and *Roseburia inulinivorans* by means of conjugative plasmids
期刊: Anaerobe; 发表年份: 2019; Ruskinn 工作站 使用情况: Concept Plus
- 4.Endothelial cells cope with hypoxia-induced depletion of ATP via activation of cellular purine turnover and phosphotransfer networks
期刊: Biochim Biophys Acta. ; 发表年份: 2018; Ruskinn 工作站使用情况: Concept plus
- 5.Sharing of human milk oligosaccharides degradants within bifidobacterial communities in faecal cultures supplemented with *Bifidobacterium bifidum*.
期刊: Scientific Reports; 发表年份: 2018; Ruskinn 工作站使用情况: Invivo₂ 400
- 6.The ability of human intestinal anaerobes to metabolize different oligosaccharides: Novel means for microbiota modulation?
期刊: Anaerobe; 发表年份: 2018; Ruskinn 工作站使用情况: BugBox
- 7.Functional analysis of arginine decarboxylase gene *speA* of *Bacteroides dorei* by markerless gene deletion
期刊: FEMS Microbiol Lett 发表年份: 2018 Ruskinn 工作站使用情况: Invivo₂ 400
- 8.Analysis of polyamine biosynthetic- and transport ability of human indigenous Bifido bacterium
期刊: Biosci Biotechnol Biochem; 发表年份: 2018; Ruskinn 工作站使用情况: Invivo₂ 400
- 9.Intestinal microbiota as a tetrahydrobiopterin exogenous source in *hph-1* mice
期刊: Sci Rep.; 发表年份: 2017; Ruskinn 工作站使用情况: Concept 400
- 10.Microencapsulation of *Clostridium difficile* specific bacteriophages using microfluidic glass capillary devices for colon delivery using pH triggered release.
期刊: PLoS One.; 发表年份: 2017; Ruskinn 工作站使用情况: Ruskinn anaerobic chamber
- 11.Strong antimicrobial activity of xanthohumol and other derivatives from hops (*Humulus lupulus* L.) on gut anaerobic bacteria
期刊: APMIS; 发表年份: 2017; Ruskinn 工作站使用情况: BugBox
- 12.A human gut ecosystem protects against *C. difficile* disease by targeting TcdA.
期刊: J Gastroenterol. ; 发表年份: 2016; Ruskinn 工作站使用情况: BugBox
- 13.Live *Faecalibacterium prausnitzii* induces greater TLR2 and TLR2/6 activation than the dead bacterium in an apical anaerobic co-culture system.
期刊: Cell Microbiol.; 发表年份: 2017; Ruskinn 工作站使用情况: Concept Plus
- 14.Use of Gifu Anaerobic Medium for culturing 32 dominant species of human gut microbes and its evaluation based on short-chain fatty acids fermentation profiles.
期刊: Biosci. Biotechnol. Biochem.; 发表年份: 2017; Ruskinn 工作站使用情况: Invivo₂ 400

The Bacterial Chromatin Protein HupA Can Remodel DNA and Associates with the Nucleoid in *Clostridium difficile*

Ana M. Oliveira Paiva^{1,3}, Annemieke H. Friggen^{1,3}, Liang Qin^{2,3}, Roxanne Douwes¹, Remus T. Dame^{2,3} and Wiep Klaas Smits^{1,3}

¹ - Department of Medical Microbiology, Section Experimental Bacteriology, Leiden University Medical Center, Leiden, the Netherlands

² - Faculty of Science, Leiden Institute of Chemistry, Leiden University, Leiden, the Netherlands

³ - Center for Microbial Cell Biology, Leiden, the Netherlands

出处: J. Mol. Biol. 2019 02 15;431(4). DOI: 10.1016/j.jmb.2019.01.001

Ruskinn 工作使用情况: Concept 1000

Abstract

The maintenance and organization of the chromosome plays an important role in the development and survival of bacteria. Bacterial chromatin proteins are architectural proteins that bind DNA and modulate its conformation, and by doing so affect a variety of cellular processes. No bacterial chromatin proteins of *Clostridium difficile* have been characterized to date.

Here, we investigate aspects of the *C. difficile* HupA protein, a homologue of the histone-like HU proteins of *Escherichia coli*. HupA is a 10-kDa protein that is present as a homodimer in vitro and self-interacts in vivo. HupA co-localizes with the nucleoid of *C. difficile*. It binds to the DNA without a preference for the DNA G + C content. Upon DNA binding, HupA induces a conformational change in the substrate DNA in vitro and leads to compaction of the chromosome in vivo.

The present study is the first to characterize a bacterial chromatin protein in *C. difficile* and opens the way to study the role of chromosomal organization in DNA metabolism and on other cellular processes in this organism.

Microencapsulation of *Clostridium difficile* specific bacteriophages using microfluidic glass capillary devices for colon delivery using pH triggered release

Gurinder K. Vinner¹, Goran T. Vladisavljević^{1*}, Martha R. J. Clokie², Danish J. Malik^{1*}

¹ Chemical Engineering Department, Loughborough University, Loughborough, United Kingdom

² Department of Infection, Immunity and Inflammation, University of Leicester, Leicester, United Kingdom

出处: PLoS One. 2017; 12(10): e0186239. DOI: 10.1371/journal.pone.0186239

Ruskinn 工作使用情况: Anaerobic chamber

Abstract

The prevalence of pathogenic bacteria acquiring multidrug antibiotic resistance is a global health threat to mankind. This has motivated a renewed interest in developing alternatives to conventional antibiotics including bacteriophages (viruses) as therapeutic agents. The bacterium *Clostridium difficile* causes colon infection and is particularly difficult to treat with existing antibiotics; phage therapy may offer a viable alternative. The punitive environment within the gastrointestinal tract can inactivate orally delivered phages. *C. difficile* specific bacteriophage, myovirus CDKM9 was encapsulated in a pH responsive polymer (Eudragit® S100 with and without alginate) using a flow focussing glass microcapillary device. Highly monodispersed core-shell microparticles containing phages trapped within the particle core were produced by in situ polymer curing using 4-aminobenzoic acid dissolved in the oil phase. The size of the generated microparticles could be precisely controlled in the range 80 µm to 160 µm through design of the microfluidic device geometry and by varying flow rates of the dispersed and continuous phase. In contrast to free 'naked' phages, those encapsulated within the microparticles could withstand a 3 h exposure to simulated gastric fluid at pH 2 and then underwent a subsequent pH triggered burst release at pH 7. The significance of our research is in demonstrating that *C. difficile* specific phage can be formulated and encapsulated in highly uniform pH responsive microparticles using a microfluidic system. The microparticles were shown to afford significant protection to the encapsulated phage upon prolonged exposure to an acid solution mimicking the human stomach environment. Phage encapsulation and subsequent release kinetics revealed that the microparticles prepared using Eudragit® S100 formulations possess pH responsive characteristics with phage release triggered in an intestinal pH range suitable for therapeutic purposes. The results reported here provide proof-of-concept data supporting the suitability of our approach for colon targeted delivery of phages for therapeutic purposes.

Biocide Resistance and Transmission of *Clostridium difficile* Spores Spiked onto Clinical Surfaces from an American Health Care Facility.

Calie Dyer,^a Lee P. Hutt,^b Robert Burky,^c and Lovleen Tina Joshi^{a,b}

^aMedical Microbiology, School of Medicine, Cardiff University, Cardiff, United Kingdom

^bFaculty of Medicine & Dentistry, ITSMED, University of Plymouth, Plymouth, United Kingdom

^cAdventist Health Hospital, Yuba City, California, USA

出处: *Appl Environ Microbiol.* 2019 Sep 1; 85(17): e01090-19.

Ruskinn 工作使用情况: BugBox Plus

Abstract

Clostridium difficile is the primary cause of antibiotic-associated diarrhea globally. In unfavorable environments, the organism produces highly resistant spores which can survive microbicidal insult. Our previous research determined the ability of *C. difficile* spores to adhere to clinical surfaces, finding that spores had markedly different hydrophobic properties and adherence abilities. Investigation into the effect of the microbicide sodium dichloroisocyanurate on *C. difficile* spore transmission revealed that sublethal concentrations increased spore adherence without reducing viability. The present study examined the ability of spores to transmit across clinical surfaces and their response to an in-use disinfection concentration of 1,000 ppm of chlorine-releasing agent sodium dichloroisocyanurate. In an effort to understand if these surfaces contribute to nosocomial spore transmission, surgical isolation gowns, hospital-grade stainless steel, and floor vinyl were spiked with 1×10^6 spores/ml of two types of *C. difficile* spore preparations: crude spores and purified spores. The hydrophobicity of each spore type versus clinical surface was examined via plate transfer assay and scanning electron microscopy. The experiment was repeated, and spiked clinical surfaces were exposed to 1,000 ppm sodium dichloroisocyanurate at the recommended 10-min contact time. Results revealed that the hydrophobicity and structure of clinical surfaces can influence spore transmission and that outer spore surface structures may play a part in spore adhesion. Spores remained viable on clinical surfaces after microbicide exposure at the recommended disinfection concentration, demonstrating ineffectual sporicidal action. This study showed that *C. difficile* spores can transmit and survive between various clinical surfaces despite appropriate use of microbicides.

IMPORTANCE *Clostridium difficile* is a health care-acquired organism and the causative agent of antibiotic-associated diarrhea. Its spores are implicated in fecal to oral transmission from contaminated surfaces in the health care environment due to their adherent nature. Contaminated surfaces are cleaned using high-strength chemicals to remove and kill the spores; however, despite appropriate infection control measures, there is still high incidence of *C. difficile* infection in patients in the United States. Our research examined the effect of a high-strength biocide on spores of *C. difficile* which had been spiked onto a range of clinically relevant surfaces, including isolation gowns, stainless steel, and floor vinyl. This study found that *C. difficile* spores were able to survive exposure to appropriate concentrations of biocide, highlighting the need to examine the effectiveness of infection control measures to prevent spore transmission and to consider the prevalence of biocide resistance when decontaminating health care surfaces.

Keywords: *Clostridium difficile*, biocide, public health, spores, surfaces, survival, transmission

Sharing of human milk oligosaccharides degradants within bifidobacterial communities in faecal cultures supplemented with *Bifidobacterium bifidum*

Aina Gotoh,¹ Toshihiko Katoh,¹ Mikiyasu Sakanaka,² Yiwei Ling,³ Chihaya Yamada,¹ Sadaki Asakuma,⁴ Tadasu Urashima,⁵ Yusuke Tomabechi,² Ayako Katayama-Ikegami,² Shin Kurihara,² Kenji Yamamoto,² Gaku Harata,⁶ Fang He,⁶ Junko Hirose,⁷ Motomitsu Kitaoka,⁸ Shujiro Okuda, corresponding author³ and Takane Katayama corresponding author^{1,2}

¹Graduate School of Biostudies, Kyoto University, Sakyo-ku, Kyoto 606-8502 Japan

²Faculty of Bioresources and Environmental Sciences, Ishikawa Prefectural University, Nonoiichi, Ishikawa 921-8836 Japan

³Graduate School of Medical and Dental Sciences, Niigata University, Chuo-ku, Niigata 951-8510 Japan

⁴Hokkaido Agricultural Research Center, National Agriculture and Food Research Organization, Sapporo, Hokkaido 062-8555 Japan

⁵Obihiro University of Agriculture and Veterinary Medicine, Obihiro, Hokkaido 080-8555 Japan

⁶Takanashi Milk Products Co., Ltd., Yokohama, Kanagawa 241-0023 Japan

⁷School of Human Cultures, The University of Shiga Prefecture, Hikone, Shiga 522-8533 Japan

⁸Food Research Institute, National Agriculture and Food Research Organization, Tsukuba, Ibaraki 305-8642 Japan

出处: **Sci Rep. 2013; 8: 13958. DOI: 10.1038/s41598-018-32080-3**

Ruskinn 工作站使用情况: Invivo2 400

Abstract

Gut microbiota of breast-fed infants are generally rich in bifidobacteria. Recent studies show that infant gut-associated bifidobacteria can assimilate human milk oligosaccharides (HMOs) specifically among the gut microbes. Nonetheless, little is known about how bifidobacterial-rich communities are shaped in the gut. Interestingly, HMOs assimilation ability is not related to the dominance of each species. *Bifidobacterium longum* subsp. *longum* and *Bifidobacterium breve* are commonly found as the dominant species in infant stools; however, they show limited HMOs assimilation ability in vitro. In contrast, avid in vitro HMOs consumers, *Bifidobacterium bifidum* and *Bifidobacterium longum* subsp. *infantis*, are less abundant in infant stools. In this study, we observed altruistic behaviour by *B. bifidum* when incubated in HMOs-containing faecal cultures. Four *B. bifidum* strains, all of which contained complete sets of HMO-degrading genes, commonly left HMOs degradants unconsumed during in vitro growth. These strains stimulated the growth of other *Bifidobacterium* species when added to faecal cultures supplemented with HMOs, thereby increasing the prevalence of bifidobacteria in faecal communities. Enhanced HMOs consumption by *B. bifidum*-supplemented cultures was also observed. We also determined the complete genome sequences of *B. bifidum* strains JCM7004 and TMC3115. Our results suggest *B. bifidum*-mediated cross-feeding of HMOs degradants within bifidobacterial communities.

其他文章:

1. Analysis of polyamine biosynthetic- and transport ability of human indigenous Bifidobacterium
期刊: Biosci Biotechnol Biochem; 发表年份: 2018; Ruskinn 工作站使用情况: Ruskinn Workstation
2. Molecular Insight into Evolution of Symbiosis between Breast-Fed Infants and a Member of the Human Gut Microbiome Bifidobacterium longum.
期刊: Cell Chem Biol. ; 发表年份: 2017; Ruskinn 工作站使用情况: Invivo2 400
3. The Impact of Storage Conditions on the Stability of Lactobacillus rhamnosus GG and Bifidobacterium animalis subsp. lactis Bb12 in Human Milk.
期刊: Breastfeed Med. 发表年份: 2017; Ruskinn 工作站使用情况: Concept 400

BAKER RUSKINN
LONGFUJIA

A survey of *Fusobacterium nucleatum* genes modulated by host cell infection

Kyla Cochrane^{1,2}, *Avery V. Robinson*², *Robert A. Holt*^{3,4,5}, *Emma Allen-Vercoe*²

¹ Genome Sciences Center, BC Cancer Agency, Vancouver, British Columbia, V5Z 1L3, Canada

² Molecular and Cellular Biology, University of Guelph, Guelph, Ontario, N1G 2W1, Canada

³ Molecular Biology and Biochemistry, Simon Fraser University, Burnaby, British Columbia, Canada

⁴ Medical Genetics, University of British Columbia, Vancouver, British Columbia, Canada

⁵ Canada's Michael Smith Genome Sciences Centre, Vancouver, British Columbia, Canada

出处: *Microb Genom* 2020 Feb;6(2). DOI: 10.1099/mgen.0.000300

Ruskinn 工作站使用情况: BugBox

Abstract

Here, we report comprehensive transcriptomic profiles from *Fusobacterium nucleatum* under conditions that mimic the first stages of bacterial infection in a highly differentiated adenocarcinoma epithelial cell line. Our transcriptomic in vitro adenocarcinoma approach allows us to measure the expression dynamics and regulation of bacterial virulence and response factors in real time, and is a novel strategy for clarifying the role of *F. nucleatum* infection in colorectal cancer (CRC) progression. Our data show that: (i) infection alters metabolic and functional pathways in *F. nucleatum*, allowing the bacterium to adapt to the host-imposed milieu; (ii) infection also stimulates the expression of genes required to help induce and promote a hypoxic and inflammatory microenvironment in the host; and (iii) *F. nucleatum* invasion occurs by a haematogenous route of infection. Our study identifies novel gene targets from *F. nucleatum* that are activated during invasion and which may aid in determining how this species invades and promotes disease within the human gastrointestinal tract. These invasion-specific genes may be useful as biomarkers for CRC progression in a host and could also assist in the development of new diagnostic tools and treatments (such as vaccines or small molecule drug targets), which will be able to combat infection and inflammation in the host while circumventing the potential problem of *F. nucleatum* tolerization.

Keywords: *Fusobacterium nucleatum*, transcriptome, infection

Targeted Mass Spectrometry Analysis of *Clostridium perfringens* Toxins

*Miloslava Duracova*¹, *Jana Klimentova*^{1,*}, *Alena Myslivcova Fucikova*^{1,2}, *Lenka Zidkova*¹,
*Valeria Sheshko*¹, *Helena Rehulkova*¹, *Jiri Dresler*³ and *Zuzana Krocova*¹

¹ Faculty of Military Health Sciences, University of Defense in Brno, Třebešská 1575,

² Department of Biology, Faculty of Science, University of Hradec Kralove, Hradecká 1285,

³ Military Health Institute, Military Medical Agency, Tychonova 1, CZ-160 00 Prague 6, Czech Republic;

出处: *Toxins* 2019, 11, 177; DOI:10.3390/toxins11030177

Ruskinn 工作站使用情况: Ruskinn Workstation

Abstract

Targeted proteomics recently proved to be a technique for the detection and absolute quantification of proteins not easily accessible to classical bottom-up approaches. Due to this, it has been considered as a high fidelity tool to detect potential warfare agents in wide spread kinds of biological and environmental matrices. *Clostridium perfringens* toxins are considered to be potential biological weapons, especially the epsilon toxin which belongs to a group of the most powerful bacterial toxins. Here, the development of a target mass spectrometry method for the detection of *C. perfringens* protein toxins (alpha, beta, beta2, epsilon, iota) is described. A high-resolution mass spectrometer with a quadrupole-Orbitrap system operating in target acquisition mode (parallel reaction monitoring) was utilized. Because of the lack of commercial protein toxin standards recombinant toxins were prepared within *Escherichia coli*. The analysis was performed using proteotypic peptides as the target compounds together with their isotopically labeled synthetic analogues as internal standards. Calibration curves were calculated for each peptide in concentrations ranging from 0.635 to 1101 fmol/μL. Limits of detection and quantification were determined for each peptide in blank matrices.

Keywords: mass spectrometry; PRM; *Clostridium perfringens*; protein toxin; epsilon toxin

Antimicrobial Susceptibility, Biotypes and Phylotypes of Clinical *Cutibacterium* (Formerly *Propionibacterium*) *acnes* Strains Isolated from Acne Patients: An Observational Study

Nanxue Zhang,^{#1} Ruoyue Yuan,^{#1} Kevin Z. Xin,² Zhong Lu,^{#1} and Ying Ma^{#1}

¹Department of Dermatology, Huashan Hospital, Fudan University, Shanghai, China

²Johns Hopkins University School of Medicine, 733 N Broadway, Baltimore, MD USA

出处: *Dermatol Ther (Heidelb)*. 2019 Dec; 9(4): 735–746. DOI: 10.1007/s13555-019-00320-7

Ruskinn 工作站使用情况: Invivo2 400

Introduction

The aim of this study was to investigate the distribution of antimicrobial susceptibility, biotypes and phylotypes of clinical *Cutibacterium acnes* (*C. acnes*, formerly *Propionibacterium acnes*) isolates as well as the relationship among demographic factors, *C. acnes* biotypes and phylotypes.

Methods

Cutibacterium acnes was collected from the skin lesions of acne patients who visited the dermatologic department of Huashan Hospital in Shanghai from October 2016 to March 2017. The agar dilution method was conducted to determine the minimum inhibitory concentrations (MICs) of *C. acnes*, the fermentation test to identify biotypes and then multiplex touchdown polymerase chain reaction (PCR) to identify phylotypes.

Results

Of the 63 *C. acnes* strains we isolated, 18 (28.6%), 31 (49.2%) and 4 (6.3%) strains were resistant to clindamycin, erythromycin and moxifloxacin, respectively; no strains were resistant to tetracycline, minocycline, fusidic acid or β -lactam, while metronidazole was completely resisted; 3 strains showed multidrug resistance (MDR). Biotype III (BIII) was the major biotype (50.8%) followed by BI and BV (both 15.9%), BII (12.7%) and lastly BIV (4.8%). IA1 was the predominant phylotype (71.4%) followed by IA2 (19.0%), II (4.8%), IB (3.2%) and IC (1.6%), while III was not detected. Significant differences were observed in the severity of disease: different degrees of acne severity reflected different biotype and phylotype distributions, and the biotype distribution of mild acne was different from that of moderate acne; the phylotype distribution of moderate acne varies from that of severe acne, too. Additionally, there was no significant difference in the distribution of biotypes or phylotypes between resistant and susceptible strains.

Conclusion

Erythromycin and clindamycin resistances are the most common in clinical *C. acnes* strains; BIII is the predominant biotype and IA1 is the major phylotype of *C. acnes*, which are mainly related to disease severity.

Keywords: Acne, Antibiotic resistance, Antimicrobial susceptibility, Biotype, *Cutibacterium acnes*, Phylotype

Bioluminescence Imaging to Track *Bacteroides fragilis* Inhibition of *Vibrio parahaemolyticus* Infection in Mice

Zhengchao Li,^{1,2} Huimin Deng,^{1,2} Yazhou Zhou,² Yafang Tan,² Xiaoyi Wang,² Yanping Han,² Yangyang Liu,³ Ye Wang,³ Ruifu Yang,^{2,*} Yujing Bi,^{2,*} and Fachao Zhi^{1,*}

¹Guangdong Provincial Key Laboratory of Gastroenterology, Department of Gastroenterology, Institute of Gastroenterology of Guangdong Province, Nanfang Hospital, Southern Medical University, Guangzhou, China

²State Key Laboratory of Pathogen and Biosecurity, Beijing Institute of Microbiology and Epidemiology, Beijing, China

³Guangzhou ZhiYi Biotechnology Co. Ltd., Guangzhou, China

出处: **Front Cell Infect Microbiol. 2017; 7: 170. DOI: 10.3389/fcimb.2017.00170**

Ruskinn 工作使用情况: **BugBox**

Abstract

Bacteroides fragilis is an anaerobic, Gram-negative, commensal bacterium of the human gut. It plays an important role in promoting the maturation of the immune system, as well as suppressing abnormal inflammation. Many recent studies have focused on the relationship between *B. fragilis* and human immunity, and indicate that *B. fragilis* has many useful probiotic effects. As inhibition of intestinal pathogens is an important characteristic of probiotic strains, this study examined whether *B. fragilis* could inhibit pathogenic bacteria. Results showed that *Vibrio parahaemolyticus* was inhibited by *B. fragilis* in vitro, and that *B. fragilis* could protect both RAW 264.7 and LoVo cells from damage caused by *V. parahaemolyticus*. Using in vivo imaging, we constructed a light-emitting *V. parahaemolyticus* strain and showed that *B. fragilis* might shorten the colonization time and reduce the number of lux-expressing bacteria in a mouse model. These results provide useful information for developing *B. fragilis* into a probiotic product, and also indicate that this commensal bacterium might aid in the clinical treatment of gastroenteritis caused by *V. parahaemolyticus*.

Keywords: *Bacteroides fragilis*, *Vibrio parahaemolyticus*, real-time cell analysis, bioluminescence, in vivo imaging

其他文章:

1.Extraintestinal Clostridioides difficile Infections: Epidemiology in a University Hospital in Hungary and Review of the Literature

期刊: antibiotics 发表年份: 2020; Ruskinn 工作站使用情况: Ruskinn Workstation

2.Lipoprotein modifications by gingipains of Porphyromonas gingivalis

期刊: J. Periodont. Res. 发表年份: 2019; Ruskinn 工作站使用情况: Concept 400

3.Bacteroides fragilis Bioluminescence Imaging to Track Inhibition of Infection in Mice.

期刊: Front Cell Infect Microbiol 发表年份: 2017; Ruskinn 工作站使用情况: Bugbox

4.Propionibacterium acnes biofilm is present in intervertebral discs of patients undergoing microdiscectomy.

期刊: PLoS ONE 发表年份: 2017; Ruskinn 工作站使用情况: Concept 400

5.Emergence and evolution of an international cluster of MDR Bacteroides fragilis isolates.

期刊: J. Antimicrob. Chemother. 发表年份: 2016; Ruskinn 工作站使用情况: Concept 400

6.The relevance of anaerobic bacteria in brain abscesses: a ten-year retrospective analysis (2008-2017).

期刊: Infect Dis (Lond) 发表年份: 2019 ; Ruskinn 工作站使用情况: Ruskinn Workstation

BAKER RUSKINN
LONGFUJIA

Lipoprotein modifications by gingipains of *Porphyromonas gingivalis*

J. Lönn,^{1,2} S. Ljunggren,³ K. Klarström - Engström,⁴ I. Demirel,⁴ T. Bengtsson,⁴ and H. Karlsson³

¹ Department of Oral Biology, Institute of Odontology, Malmö University, Malmö, Sweden,

² PEAS Institute AB, Linköping, Sweden,

³ Department of Clinical and Experimental Medicine, Occupational and Environmental Medicine Center, Linköping University, Linköping, Sweden,

⁴ Department of Medical Sciences, Örebro University, Örebro, Sweden,

出处: *J Periodontol Res.* 2018 Jun; 53(3): 403–413. DOI: 10.1111/jre.12527

Ruskinn 工作站使用情况: Concept 400

Abstract

Background and Objective: Several studies have shown an association between periodontitis and cardiovascular disease (CVD). Atherosclerosis is the major cause of CVD, and a key event in the development of atherosclerosis is accumulation of lipoproteins within the arterial wall. Bacteria are the primary etiologic agents in periodontitis and *Porphyromonas gingivalis* is the major pathogen in the disease. Several studies support a role of modified low-density lipoprotein (LDL) in atherogenesis; however, the pathogenic stimuli that induce the changes and the mechanisms by which this occur are unknown. This study aims to identify alterations in plasma lipoproteins induced by the periodontopathic species of bacterium, *P. gingivalis*, in vitro. Material and Methods: Plasma lipoproteins were isolated from whole blood treated with wild-type and gingipain-mutant (lacking either the Rgp- or Kgp gingipains) *P. gingivalis* by density/gradient-ultracentrifugation and were studied using 2-dimensional gel electrophoresis followed by matrix-assisted laser desorption/ionization mass spectrometry. *Porphyromonas gingivalis*-induced lipid peroxidation and antioxidant levels were measured by thiobarbituric acid-reactive substances and antioxidant assay kits, respectively, and lumiaggregometry was used for measurement of reactive oxygen species (ROS) and aggregation. Results: *Porphyromonas gingivalis* exerted substantial proteolytic effects on the lipoproteins. The Rgp gingipains were responsible for producing 2 apoE fragments, as well as 2 apoB-100 fragments, in LDL, and the Kgp gingipain produced an unidentified fragment in high-density lipoproteins. *Porphyromonas gingivalis* and its different gingipain variants induced ROS and consumed antioxidants. Both the Rgp and Kgp gingipains were involved in inducing lipid peroxidation. Conclusion: *Porphyromonas gingivalis* has the potential to change the expression of lipoproteins in blood, which may represent a crucial link between periodontitis and CVD.

Keywords: gingipains, lipoproteins, MALDI-TOF mass spectrometry, *Porphyromonas gingivalis*, twodimensional gel electrophoresis

PKC, ERK/p38 MAP kinases and NF - κ B targeted signalling play a role in the expression and release of IL - 1 β and CXCL8 in *Porphyromonas gingivalis* - infected THP1 cells

Kartheyaene Jayaprakash Isak Demirel Sezin Gunaltay Hazem Khalaf Torbjörn Bengtsson

Department of Medical Sciences, Örebro University, Örebro, Sweden

出处: APMIS 2017 Jul;125(7). DOI: 10.1111/apm.12701

Ruskinn 工作站使用情况: Concept 400

Abstract

Porphyromonas gingivalis is a keystone pathogen in periodontitis and is gaining importance in cardiovascular pathogenesis. Protease - activated receptors (PARs), toll - like receptors (TLRs) and nucleotide - binding oligomerization domain (NOD) on monocytes recognize the structural components on *P. gingivalis*, inducing inflammatory intermediates. Here, we elucidate the modulation of PARs, TLRs, NODs, and the role of MAPK and NF - κ B in IL - 1 β and CXCL8 release. THP1 cells were stimulated with *P. gingivalis* wild - type W50 and its isogenic gingipain mutants: Rgp mutant E8 and Kgp mutant K1A. We observed modulation of PARs, TLRs, NOD, IL - 1 β and CXCL8 expression by *P. gingivalis*. Gingipains hydrolyse IL - 1 β and CXCL8, which is more evident for IL - 1 β accumulation at 24 h. Inhibition of PKC (protein kinase C), p38 and ERK (extracellular signal - regulated kinases) partially reduced *P. gingivalis* - induced IL - 1 β at 6 h, whereas PKC and ERK reduced CXCL8 at both 6 and 24 h. Following NF - κ B inhibition, *P. gingivalis* - induced IL - 1 β and CXCL8 were completely suppressed to basal levels. Overall, TLRs, PARs and NOD possibly act in synergy with PKC, MAPK ERK/p38 and NF - κ B in *P. gingivalis* - induced IL - 1 β and CXCL8 release from THP1 cells. These pro - inflammatory cytokines could affect leucocytes in circulation and exacerbate other vascular inflammatory conditions such as atherosclerosis.

其他文章:

1. The role of toll-like and protease-activated receptors and associated intracellular signaling in *Porphyromonas gingivalis*-infected gingival fibroblasts.

期刊: J. Periodont. Res.; 发表年份: 2017; Ruskinn 工作站使用情况: Concept 400

2. Dual action of bacteriocin PLNC8 α β through inhibition of *Porphyromonas gingivalis* infection and promotion of cell proliferation.

期刊: APMIS; 发表年份: 2017; Ruskinn 工作站使用情况: Concept 400

3. Transcriptional profiling of human smooth muscle cells infected with gingipain and fimbriae mutants of *Porphyromonas gingivalis*.

期刊: Sci Rep; 发表年份: 2016; Ruskinn 工作站使用情况: Concept 400

The evaluation of gamma irradiation and cold storage for the reduction of *Campylobacter jejuni* in chicken livers

Nereus W. Gunther IV^{a,□}, Aisha Abdul-Wakeela, O. Joseph Scullen^b, Christopher Sommers^b

^a U.S.

Department of Agriculture, Agricultural Research Service, Eastern Regional Research Center, Molecular Characterization of Foodborne Pathogens Research Unit, Wyndmoor, PA, 19038, USA

^b U.S.

Department of Agriculture, Agricultural Research Service, Eastern Regional Research Center, Food Safety and Intervention Technologies, Wyndmoor, PA, 19038, USA

出处: **Food Microbiol. 2019 Sep;82. DOI: 10.1016/j.fm.2019.02.014**

Ruskinn 工作站使用情况: Concept M

Abstract

Recent outbreaks of *Campylobacter* mediated disease attributed to undercooked chicken livers have highlighted a continuing need for methods to reduce *Campylobacter* numbers in these types of food products. In this study, gamma irradiation is evaluated for its effectiveness in reducing *Campylobacter jejuni* numbers in experimentally contaminated chicken livers. A wide range of radiation doses were evaluated in conjunction with cold storage parameters, before and after irradiation. Storage of chicken livers at $-20\text{ }^{\circ}\text{C}$ prior to radiation treatment, as expected, increased *C. jejuni* radiation resistance. Livers previously stored at $-20\text{ }^{\circ}\text{C}$ exhibited D10 values of 0.748 kiloGray (kGy) compared to livers without previous storage that had a significantly lower D10 value of 0.361 kGy. Cold storage conditions post-irradiation at both $4\text{ }^{\circ}\text{C}$ and $-20\text{ }^{\circ}\text{C}$ further reduced the *C. jejuni* numbers over those reduced by the initial irradiation. The largest reduction (3.8 logs) of *C. jejuni* numbers in livers produced by combining irradiation and cold storage was achieved using 0.8 kGy of radiation followed by 1 week storage at $-20\text{ }^{\circ}\text{C}$. This reduction of 3.8 logs was not determined to be significantly different from the 3.5 log reduction achieved with the same radiation dose (0.8 kGy) after only 48 h of subsequent storage at $-20\text{ }^{\circ}\text{C}$.

In Vitro Anaerobic Pharmacokinetic/ Pharmacodynamic Model to Simulate the Bactericidal Activity of Levornidazole Against *Bacteroides fragilis*

Jiali Hu, MMed^{1,2}; Jing Zhang, PhD^{1,2}; Yuancheng Chen, PhD^{1,2}; Wang Liang, PhD¹; and Shi Wu, BSc¹

¹ Institute of Antibiotics, Huashan Hospital, Fudan University, Shanghai, China;

² Key Laboratory of Clinical Pharmacology of Antibiotics, National Health and Family Planning Commission, Shanghai, China

出处: *Clin Ther.* 2017 Apr;39(4):828-836. DOI: 10.1016/j.clinthera.2017.03.003. Epub 2017 Mar 28.

Ruskinn 工作使用情况: Invivo₂ 400

Abstract

Purpose: This study was designed to correlate the pharmacokinetic/pharmacodynamic (PK/PD) parameters with PD indices of levornidazole against *Bacteroides fragilis* and to calculate the PK/PD target value for levornidazole to attain its expected maximal bactericidal effect using an in vitro anaerobic dynamic PK/PD model. **Methods:** An anaerobic dynamic PK/PD model was developed in vitro. The scheme for PK modeling was designed according to the PK parameters of levornidazole in the human body. The device of 2-compartment PK/PD model was constructed by using digital control of flow rate to simulate 4 regimens of single-dose intravenous infusion of levornidazole to determine the bactericidal activity of levornidazole against the 3 strains of *B. fragilis* within 72 hours. PD parameters such as reduction of colony count within 24 hours ($\Delta\text{Log}_{24\text{h}}$), area under bactericidal curve (AUBC), and 2-hour initial killing rate (IKR) were calculated and correlated with PK/PD parameters. Sigmoid Emax model of levornidazole was established to calculate PK/PD target values to attain corresponding PD effect. **Findings:** PK and PD validation proved the stability of the model in simulating levornidazole against *B. fragilis* and the precision and accuracy in the results of PK modeling. C_{max} and $\text{AUC}_{0-24\text{h}}$ found only -1.46% and -6.72% differences from the values in vivo. Our study found that $\Delta\text{Log}_{24\text{h}}$, AUBC, and IKR were more correlated with $\text{AUC}_{0-24\text{h}}/\text{MIC}$ and $C_{\text{max}}/\text{MIC}$ than with %T4MIC. According to $\Delta\text{Log}_{24\text{h}}$, the PK/PD target values of $\text{AUC}_{0-24\text{h}}/\text{MIC}$, $C_{\text{max}}/\text{MIC}$, and %T4MIC of levornidazole against *B. fragilis* were 157.6%, 14.1%, and 56.4%, respectively. **Implications:** Our findings are useful for optimizing the clinical dosing regimen of levornidazole sodium chloride injection to attain maximal bactericidal effect. (*Clin Ther.* 2017;:]]-]]]) & 2017 Elsevier HS Journals, Inc. All rights reserved.

Keywords: anaerobe, dynamic pharmacokinetic/ pharmacodynamic model, in vitro, levornidazole, PK/PD target value

其他文章:

1.Strong antimicrobial activity of xanthohumol and other derivatives from hops (*Humulus lupulus* L.) on gut anaerobic bacteria

期刊: APMIS; 发表年份: 2017; Ruskinn 工作站使用情况: BugBox

2.Antimicrobial susceptibility against metronidazole and carbapenem in clinical anaerobic isolates from Pakistan

期刊: Antimicrob Resist Infect Control; 发表年份: 2019; Ruskinn 工作站使用情况: Concept Plus

3.Bioluminescence Imaging to Track *Bacteroides fragilis* Inhibition of *Vibrio parahaemolyticus* Infection in Mice.

期刊: Front Cell Infect Microbiol; 发表年份: 2017; Ruskinn 工作站使用情况: BugBox

4. The influence of incubation time, sample preparation and exposure to oxygen on the quality of the MALDI-TOF MS spectrum of anaerobic bacteria.

期刊: Clin. Microbiol. Infect.; 发表年份: 2014; Ruskinn 工作站使用情况: Concept 400

BAKER RUSKINN
LONGFUJIA

Investigation of anaerobic phenanthrene biodegradation by a highly enriched co-culture, PheN9, with nitrate as an electron acceptor

Zuotao Zhang, Haijiao Guo, Jiao Sun, Hui Wang[□]

State Key Joint Laboratory of Environment Simulation and Pollution Control, School of Environment, Tsinghua University, Beijing, 100084, PR China

出处: *J. Hazard. Mater.* 2020 Feb 05;383. DOI: 10.1016/j.jhazmat.2019.121191

Ruskinn 工作使用情况: BugBox

Abstract

In this study, we developed a highly enriched phenanthrene-degrading co-culture, PheN9, which uses nitrate as an electron acceptor under anaerobic conditions, and the processes mediating biodegradation were proposed. The dominant bacteria populations included *Pseudomonas stutzeri* (91.7% relative abundance), which shared 98% 16S rRNA-sequence similarity with the naphthalene-degrading, nitrate-reducing strain NAP-3-1, and *Candidatus_Kuenenia* (2.3% relative abundance), which is a type of anammox bacteria. Enrichment transformed 54% of the added phenanthrene, reduced nitrate, and generated significant amounts of nitrite. Enrichment also result in partial consumption of the produced nitrite by the anammox bacteria. The key initial steps of anaerobic phenanthrene biodegradation by PheN9 were methylation and carboxylation, which were identified for detection of metabolic products, as well as carboxylase and methyltransferase activities. The methylation product was then oxidized to 2-naphthoic acid and then underwent sequential biodegradation steps. Then, ring-system reducing occurred, and the metabolic products were identified as dihydro-, tetrahydro-, hexahydro-, and octahydro-2-phenanthroic acid. Downstream degradation proceeded via a substituted benzene series and cyclohexane derivatives. This study employed anaerobic phenanthrene-biodegradation processes with nitrate as an electron acceptor. These findings can improve our understanding of anaerobic polycyclic aromatic hydrocarbon (PAH) biodegradation processes and guide PAH bioremediation by adding nitrate to anaerobic environments.

Keywords: Anaerobic phenanthrene biodegradation Nitrate Co-culture Bacteria population Biodegradation process